Comparative transcriptome analysis of catfish swimbladder reveals expression signatures in chamber formation and their response to low oxygen stress

by

Yujia Yang

A dissertation submitted to the Graduate Faculty of
Auburn University
in partial fulfillment of the
requirements for the Degree of
Doctor of Philosophy

Auburn, Alabama
August 4, 2018

Keywords: Swimbladder, Transcriptome, Catfish, Branching morphogenesis, Low oxygen

Approved by

Zhanjiang Liu, Chair, Professor of Fisheries, Aquaculture and Aquatic Sciences
Rex Dunham, Co-chair, Professor of Fisheries, Aquaculture and Aquatic Sciences
Ya-xiong Tao, Professor of Anatomy, Physiology and Pharmacology
Charles Y. Chen, Professor of Crop, Soil and Environmental Sciences

Abstract

The swimbladder is an internal gas-filled organ in teleosts. Its major function is to regulate buoyancy. Swimbladder exhibits great variations in size, shape, number of compartments or chambers among teleosts. However, the genomic control of swimbladder variations is unknown. Channel catfish (*Ictalurus punctatus*), blue catfish (*Ictalurus furcatus*), and their F1 hybrids of female channel catfish x male blue catfish (C×B hybrid catfish) provide a good model to investigate the swimbladder morphology, because channel catfish possess a single-chambered swimbladder whereas blue catfish possess a bi-chambered swimbladder; and C×B hybrid catfish possess a bi-chambered swimbladder but with significantly reduced posterior chamber. In Chapter 2, we determined the transcriptional profiles of swimbladder from channel catfish, blue catfish, and C×B hybrid catfish. We examined their transcriptomes at both the fingerling and adult stages. Through comparative transcriptome analysis, approximately 4,000 differentially expressed genes (DEGs) were identified. Among these DEGs, members of the Wnt signaling pathway (*wnt1*, *wnt2*, *nfatc1*, *rac2*), Hedgehog signaling pathway (*shh*), and growth factors (*fgf10, igf-1*) were identified. As these genes were known to be important for branching morphogenesis of mammalian lung and of mammary glands, their association with budding of posterior chamber primordium and progressive development of bi-chambered swimbladder in fish suggested that these branching morphogenesis related genes and their functions in branching are evolutionarily conserved across a broad spectrum of species.

Channel catfish is the leading aquaculture species in the US, and one of the reasons for its application in aquaculture is its relatively high tolerance against hypoxia. However, hypoxia can still cause huge economic losses to the catfish industry. Studies on hypoxia tolerance, therefore, are important for aquaculture. Fish swimbladder has been considered as an accessory respiration organ surrounded by a dense capillary countercurrent exchange system. In this regard, we conducted RNA-Seq analysis with swimbladder samples of catfish under hypoxic and normal conditions to determine if swimbladder was responsive to low oxygen treatment, and to reveal genes, their expression patterns and pathways involved in hypoxia responses in catfish. A total of 155 differentially expressed genes (DEGs) were identified from swimbladder of adult catfish, whereas a total of 2,127 DEGs were identified from swimbladder of fingerling catfish, under hypoxic condition as compared to untreated controls. Subsequent pathway analysis revealed that many DEGs under hypoxia were involved in HIF signaling pathway (*nos2*, *eno2*, *camk2d2*, *prkcb*, *cdkn1a*, *eno1*, and *tfrc*), MAPK signaling pathway (voltage-dependent calcium channel subunit genes), PI3K/Akt/mTOR signaling pathway (*itga6*, *g6pc*, and *cdkn1a*), Ras signaling pathway (*efna3* and *ksr2*), and signaling by VEGF (*fn1*, *wasf3*, and *hspb1*) in catfish swimbladder. This study provided insights into regulation of gene expression and their involved gene pathways in catfish swimbladder in response to low oxygen stresses.

Acknowledgments

I would like to express my sincere appreciation to my graduate committee members, friends, colleagues, and family members, who have all provided strong support for my graduate work. My deepest gratitude goes to my advisor, Dr. Zhanjiang Liu, who has provided me with the opportunity to study abroad as a PhD student in his lab. It is really an honor for both of me and my family. Throughout my four-year study in Auburn, Dr. Liu has provided strong guidance for my research, and kind encouragement and inspirations for my study. Without his guidance, help, encouragement and support, I would never have been able to finish my dissertation. Many sincere thanks go to my committee Co-chair Dr. Dunham for his advice of my research and helping me develop my background in genetics. He has always given me his valuable advice and great help with my dissertation, and encouraged me to learn more basic knowledge. I would like to thank my committee member, Dr. Ya-xiong Tao, who gave his advice to me not only for my research but also for my life. His passion in research deeply influence me on my own research. I would like to thank my committee member, Dr. Charles Chen, who has reminded me of not forgetting the basic knowledge of genetics, and encouraged me to be confident in myself. My thanks also extend to the outside reader of my dissertation, Dr. Luxin Wang for her great support and guidance.

I would like to express my thanks to Dr. Huseyin Kucuktas and Ludmilla Kaltenboeck for all the technical support. My sincere thanks also goes to Mrs. Dongya Gao, who encouraged

me to believe in myself and supported me all the time. My thanks also goes to Dr. Shikai Liu, Dr. Lisui Bao, Dr. Yang Liu, Dr. Yun Li, Dr. Chen Jiang, Dr. Jun Yao, Dr. Qifan Zeng, Dr. Sen Gao, Dr. Xiaozhu Wang, Dr. Changxu Tian, Dr. Qiang Fu, Dr. Ning Li, Dr. Tao Zhou, Dr. Zihao Yuan, Mr. Suxu Tan, Ms. Yulin Jin, Ms. Huitong Shi, and Ms. Wenwen Wang in the laboratory for their help, collaboration and friendship. I would like to say thanks to all the members in the lab who helped me a lot.

I would like to express my deepest appreciation to my loved parents, Hongsheng Yang and Chuntao Huo, for their unconditional and endless love, encouragement, and tremendous support. Finally, I would like to thank my boyfriend, Likun Yang, for his support and love all the time, and especially in Auburn.

Table of Contents

List of Tables

List of Figures

Chapter 1 Introduction

1.1 Problem statement

Catfish serve as a good model to investigate the swimbladder morphology because channel catfish (*Ictalurus punctatus*) possess a single-chambered swimbladder, whereas blue catfish (*Ictalurus furcatus*) possess a distinct bi-chambered swimbladder with the two lobes being similar in size; and their hybrids (female channel catfish x male blue catfish) possess a bi-chambered swimbladder but with significantly reduced posterior chamber, more similar to its paternal parent than the maternal parent (Dunham and Masser, 2012). Despite such a good model, the molecular basis of the difference in swimbladder morphology among channel catfish, blue catfish and C×B hybrid catfish is still unknown. To understand the mechanisms for development of single-chambered and bi-chambered swimbladder, we examined transcriptional profiles of the swimbladder from channel catfish, blue catfish, and C×B hybrid catfish at both fingerling and adult stages. Here we report a set of differentially expressed genes among these catfish, and the potential gene pathways involved in swimbladder morphology.

As an internal gas-filled organ, swimbladder contributes to various functions, including aerial respiration, buoyancy control, pressure reception, sound production, and auditory system (Alexander, 1966). Fish swimbladder has long been hypothesized as the homolog of the vertebrate lung (Owen, 1846). When comparing the transcriptomes of zebrafish swimbladder and mammalian lung, they shared significantly high resemblance in gene expression profiling (Zheng et al., 2011). Due to rich capillary network in the walls and a connection with pharynx, swimbladder has been considered as an accessory respiratory organ in teleost fish (Potter, 1927).

Here in this study, we performed RNA-Seq analysis of swimbladder in fingerlings and adults of channel catfish under normal and hypoxic conditions. We report the resemblance of genes of teleost swimbladder with those involved in oxygen homeostasis of tetrapod lung, and their involved gene pathways in responses to hypoxia.

1.2 Review of literatures

1.2.1 Fish swimbladder and their morphology

In general, fish swimbladder can be categorized into two types in terms of their morphology: physostomous (an open swimbladder system) and physoclistous (a closed swimbladder system) (Trotter et al., 2001). Physostomous fish possesses a pneumatic duct between the swimbladder and the gut, whereas physoclistous fish lacks a duct but has specialized structures associated with the respiratory and circulatory system for inflation and deflation (Trotter et al., 2001). Great variation has been reported in size, shape, and chamber number of the swimbladder among various fish species. The swimbladders of rainbow trout, northern pike and zander possess only one swimbladder chamber, whereas the swimbladders of most Ostariophysi consist of two chambers (anterior and posterior chambers), such as common carp, grass carp, and zebrafish (Grom, 2015). The anterior and posterior chambers in swimbladder also vary in size, as well as their functions. In most Cypriniformes, the anterior chamber is larger than the posterior chamber due to oxygen secreting (Hsia et al., 2013). In zebrafish, the anterior chamber possesses acoustic resonance properties, whereas the posterior chamber is used for buoyancy control (Finney et al., 2006). The great variations in swimbladder morphology among various fish species might be associated with their hydrostatic function,

the center of gravity, their behavior, and lifestyle (Horn, 1975; Whitehead and Blaxter, 1989). Additionally, the diversity of swimbladder in shape and size also has a great influence on their hearing abilities (Lechner and Ladich, 2008). Catfish is a good model to investigate the swimbladder morphology because channel catfish has a single-chambered swimbladder, whereas blue catfish possess a distinct bi-chambered swimbladder; and their hybrids (female channel catfish x male blue catfish) possesses a bi-chambered swimbladder with significantly reduced posterior chamber (Dunham and Masser, 2012).

1.2.2 Fish swimbladder and mammalian lung

Swimbladder exerts various functions with inclusion of accessory breathing, buoyancy regulation, sound and pressure reception, and sound production (Alexander, 1966). The swimbladder exists in most of teleost fish, while it is absent in cartilaginous fish. The similarities in homology, as well as their functions, of fish swimbladder and vertebrate lung have been long noted (Owen, 1846). In a previous study, a high level of resemblance in the gene expression pattern between zebrafish swimbladder and mammalian lung were identified (Zheng et al., 2011). Interestingly, Hedgehog signaling and Wnt signaling pathways both exert essential roles in the developmental process of zebrafish swimbladder (Winata et al., 2009; Yin et al., 2011) and of vertebrate lung (Bellusci et al., 1997; Okubo and Hogan, 2004; Pepicelli et al., 1998; Shu et al., 2002; Yin et al., 2010). In zebrafish swimbladder, the budding of second chamber primordium was demonstrated as a simplified form of branching morphogenesis similar to that in mammalian lung development (Winata et al., 2009). Conserved divergent elements involving *Shh/Shha* signals (Winata et al., 2009), and members in Wnt signaling

pathway (Yin et al., 2011) have been detected to exert their important functions during subsequent branching morphogenesis in the development of zebrafish swimbladder and mammalian lung.

1.2.3 Adaptive strategies of fish to low dissolved oxygen

Fish live in aquatic environments with relatively low dissolved oxygen. To face the low dissolved oxygen in water, fish have evolved various adaptive strategies to survive under hypoxic conditions, including behavioral adaptions and physiological adaptions. Fish has shifted their breathing mode from water breathing to surface breathing (Kramer and McClure, 1982) and reduced their locomotor activities (Nilsson et al., 1993). To adapt to low dissolved oxygen, their gill has extremely large surface areas for gas exchange and they can regulate their enzymatic activities and metabolic rate (Burggren and Cameron, 1980; Jensen et al., 1993). Due to rich capillary network in the walls and a connection with pharynx, fish swimbladder has been considered as an accessory respiratory organ in teleost fish (Potter, 1927).

1.2.4 Impact of low oxygen stress

Even though catfish is relative tolerant to low dissolved oxygen to other fish species, hypoxia still cause huge economic loss to catfish industry due to heavy mortalities. Hypoxia can adversely affect not only survival rate but also various performance traits. The molecular response to low dissolved oxygen is a really complicated biological process. In catfish industry, hypoxia can adversely affect the growth rate and cause relatively low yield (Burggren and Cameron, 1980; Welker et al., 2007). What is more, exposure to low dissolved oxygen has a

great influence on the immune system of catfish and increases the susceptibility to fish diseases, especially enteric septicemia of catfish (ESC) (Geng et al., 2014; Kvamme et al., 2013; Welker et al., 2007). In the previous study, after sub-lethal hypoxia exposure, channel catfish were more susceptible to *Edwardsiella ictaluri* (Welker et al., 2007). Especially when challenged with high dose of *E. ictaluri*, catfish after hypoxic exposure had significantly higher cumulative mortality (approximately 36%) than catfish in control groups (approximately 12%) (Welker et al., 2007). After hypoxia exposure, fish were more vulnerable to predation and less efficient to forage for predators (Pollock et al., 2007). Also, their reproductive activities can be adversely influenced, leading to high mortality in their eggs (Pollock et al., 2007). Even though fish survive from hypoxia exposure, the adverse effects still exist, including reduced metabolic rate (Aboagye and Allen, 2014), and feed conversion efficiency (Buentello et al., 2000).

1.2.5 Hypoxia tolerance of catfish

There are great variation on low dissolved oxygen tolerance among different catfish species, strains or lines. In general, channel catfish show more tolerant to low dissolved oxygen than blue catfish, however, the opposite results were also observed. The hybrid catfish (female channel catfish and male blue catfish) showed highest tolerance to low dissolved oxygen compared to channel catfish or blue catfish (Dunham et al., 1983). The low dissolved oxygen tolerance can be determined by the time to lose their equilibrium. In channel catfish, two strains (103KS and Marion S) had higher low dissolved oxygen tolerance than the other strains, whereas the Marion strain had the poorest low dissolved oxygen tolerance (Wang et al., 2017a). Because of genetic background in different strains, strains of parents can affect the tolerance

of hybrid catfish to low dissolved oxygen (Dunham et al., 2014). For instance, hybrid catfish sired by Rio Grande (Texas) strain of blue catfish showed higher tolerance to low dissolved oxygen than hybrid catfish sired by Alabama strains of blue catfish (Dunham et al., 2014). The superior tolerance to low dissolved oxygen were observed in hybrid catfish sired by Alabama strains at lower temperatures (Dunham et al., 2014).

1.2.6 Molecular response to low oxygen stress

In an aerobic organism, oxygen homeostasis is really important to maintain the proper biological functions and processes. To maintain the oxygen homeostasis, they can induce a series of important genes through oxygen sensing and signal transduction pathways (Wenger, 2000). This biological process is extremely complicated. When exposure to low oxygen levels, they can induce a hypoxic response centered on the hypoxia-inducible transcription factors (HIFs) (Bruick, 2003). HIFs include HIF1 and HIF2, which are important regulators in oxygen homeostasis (Semenza, 2000). In channel catfish, HIF-1α, HIF-2αa, HIF-2αb, HIF-3α, and FIH-1 genes have been identified (Geng et al., 2014). After exposure to low dissolved oxygen, they were temporally and spatially regulated, suggesting that they can be regulated at pre-translational levels (Geng et al., 2014). The mRNAs of HIF-1α were repressed at 1.5 h after hypoxia treatment but induced at 5 h (Geng et al., 2014). HIF-3α were the most dramatically regulated after hypoxia treatment (Geng et al., 2014). HIF-1α can bind with HIF-1β to activate the expression of hypoxic-induced genes (Kietzmann et al., 2016). In several studies, significantly differentially-expressed miRNAs were also identified after hypoxia treatment (Huang et al., 2015; Lau et al., 2014; Sun et al., 2017; Zhao et al., 2014). For instance, the

miRNA-462/731 cluster was induced after hypoxia treatment in *Megalobrama amblycephala* (Huang et al., 2017). Alternative splicing of specific genes were also identified to be involved in hypoxia responses, such as LDH (LvanLDH) in shrimp (Soñanez-Organis et al., 2012), and HIF prolyl hydroxylase PHD3 in *Megalobrama amblycephala* (Chen et al., 2016). Several gene families have been found to be involved in molecular response to hypoxia, such as CC and CXC chemokine families (including ligands and receptors) (Fu et al., 2017a; Fu et al., 2017b; Fu et al., 2017c), receptor tyrosine kinases (RTKs) (Tian et al., 2015), claudin genes (Sun et al., 2015), and bcl-2 genes (Yuan et al., 2016). Several signaling pathways, HIF1, MAPK, PI3K-Akt, mTOR, Ras, VEGF, and FoxO signaling pathway were observed to exert their important roles in molecular hypoxic responses (Eijkelenboom and Burgering, 2013; Koong et al., 1994; Lee et al., 2007; Mazure et al., 1997; Risau, 1997; Wang et al., 2017b).

1.2.7 QTL and candidate genes associated with hypoxia tolerance in catfish

There have been two GWAS studies on tolerance to low dissolved oxygen in channel catfish and hybrid catfish. The first GWAS analysis were made using six strains of channel catfish (Wang et al., 2017b). In total, one significant QTL on LG6 and four suggestive QTL (two QTL on LG5, one QTL on LG10 and LG12, respectively) were identified across catfish strains (Wang et al., 2017b). On LG6, 25 genes were located within the most significant SNP, including *lrrc1*, *tceb3*, *mlip*, *fam83b*, *gclc*, *fgfr2*, *plpp4*, *fbxo9*, *bmp5*, and *bag2* (Wang et al., 2017b). The annotated genes within QTL were involved in MAPK signaling pathway and PI3K/AKT/mTOR signaling pathway (Wang et al., 2017b). These signaling pathways were already identified associated with oxygen homeostasis and the expression of the hypoxia-

inducible factors (Akman et al., 2001; Shiojima and Walsh, 2002). Within catfish strains, six significant QTL and multiple suggestive QTL were identified (Wang et al., 2017b). There were almost no overlaps among these QTL across strains or within strains, this indicated that the molecular mechanisms in low dissolved oxygen tolerance are really complicated (Wang et al., 2017b).

In the GWAS study of channel catfish × blue catfish interspecific system (Zhong et al., 2000), four LGs (LG2, LG4, LG23, and LG29) were identified associated with low dissolved oxygen tolerance. On LG2, 8 genes were located within the significant SNPs associated with low dissolved oxygen tolerance, including *dmbx1a*, *pif1*, *ptger4*, *artemin*, *st3gal3a*, *kdm4a*, *ptprf*, and *pkib*. A total of 106 genes on LG23 and 9 genes on LG4 (*cyp1a1*, *ccbe1*, *syt4*, *sema7a*, *arid3a*, *fam219b*, *p2ry1*, and *rap2b*) and 3 genes on LG29 (*klhl5*, *fam114a1*, and *klf3*) were located within the significant QTL associated with low dissolved oxygen tolerance. Gene were mainly involved in VEGF signaling pathway, MAPK signaling pathway, mTOR signaling pathway, PI3K-Akt signaling pathway, P53-mediated apoptosis, and DNA damage checkpoint pathways (Zhong et al., 2000). Also, there were almost no overlaps of QTL between channel catfish and hybrid catfish (Zhong et al., 2000).

References

Aboagye, D.L., Allen, P.J., 2014. Metabolic and locomotor responses of juvenile paddlefish Polyodon spathula to hypoxia and temperature. Comp. Biochem. Physiol. A Mol. Integr. Physiol. 169, 51-59.

Akman, H.O., Zhang, H., Siddiqui, M., Solomon, W., Smith, E.L., Batuman, O.A., 2001. Response to hypoxia involves transforming growth factor-β2 and Smad proteins in human endothelial cells. Blood 98, 3324-3331.

Alexander, R., 1966. Physical aspects of swimbladder function. Biol. Rev. 41, 141-176.

Bellusci, S., Furuta, Y., Rush, M.G., Henderson, R., Winnier, G., Hogan, B., 1997. Involvement of Sonic hedgehog (Shh) in mouse embryonic lung growth and morphogenesis. Development 124, 53-63.

Bruick, R.K., 2003. Oxygen sensing in the hypoxic response pathway: regulation of the hypoxia-inducible transcription factor. Genes Dev. 17, 2614-2623.

Buentello, J.A., Gatlin III, D.M., Neill, W.H., 2000. Effects of water temperature and dissolved oxygen on daily feed consumption, feed utilization and growth of channel catfish (Ictalurus punctatus). Aquaculture 182, 339-352.

Burggren, W.W., Cameron, J.N., 1980. Anaerobic metabolism, gas exchange, and acid-base balance during hypoxic exposure in the channel catfish, Ictalurus punctatus. J. Exp. Zool. A Ecol. Genet. Physiol. 213, 405-416.

Chen, N., Huang, C.-H., Chen, B.-X., Liu, H., Wang, W.-M., Gul, Y., Wang, H.-L., 2016. Alternative splicing transcription of Megalobrama amblycephala HIF prolyl hydroxylase PHD3 and up-regulation of PHD3 by HIF-1α. Biochem. Biophys. Res. Commun. 469,

737-742.

Dunham, R.A., Masser, M.P., 2012. Production of hybrid catfish. Southern Regional Aquaculture Center.

Dunham, R.A., Ramboux, A.C., Perera, D.A., 2014. Effect of strain on tolerance of low dissolved oxygen of channel X blue catfish hybrids. Aquaculture 420, S25-S28.

Dunham, R.A., Smitherman, R.O., Webber, C., 1983. Relative tolerance of channel x blue hybrid and channel catfish to low oxygen concentrations. The Progressive Fish-Culturist 45, 55-57.

Eijkelenboom, A., Burgering, B.M., 2013. FOXOs: signalling integrators for homeostasis maintenance. Nature reviews. Nat. Rev. Mol. Cell Biol. 14, 83.

Finney, J.L., Robertson, G.N., McGee, C.A., Smith, F.M., Croll, R.P., 2006. Structure and autonomic innervation of the swim bladder in the zebrafish (Danio rerio). J. Comp. Neurol. 495, 587-606.

Fu, Q., Yang, Y., Li, C., Zeng, Q., Zhou, T., Li, N., Liu, Y., Li, Y., Wang, X., Liu, S., Li, D., Liu, Z., 2017a. The chemokinome superfamily: II. The 64 CC chemokines in channel catfish and their involvement in disease and hypoxia responses. Dev. Comp. Immunol. 73, 97-108.

Fu, Q., Yang, Y., Li, C., Zeng, Q., Zhou, T., Li, N., Liu, Y., Liu, S., Liu, Z., 2017b. The CC and CXC chemokine receptors in channel catfish (Ictalurus punctatus) and their involvement in disease and hypoxia responses. Dev. Comp. Immunol. 77, 241-251.

Fu, Q., Zeng, Q., Li, Y., Yang, Y., Li, C., Liu, S., Zhou, T., Li, N., Yao, J., Jiang, C., Li, D., Liu, Z., 2017c. The chemokinome superfamily in channel catfish: I. CXC subfamily and their

involvement in disease defense and hypoxia responses. Fish Shellfish Immunol. 60, 380-390.

Geng, X., Feng, J., Liu, S., Wang, Y., Arias, C., Liu, Z., 2014. Transcriptional regulation of hypoxia inducible factors alpha (HIF-α) and their inhibiting factor (FIH-1) of channel catfish (Ictalurus punctatus) under hypoxia. Comp. Biochem. Physiol. B Biochem. Mol. Biol. 169, 38-50.

Grom, K., 2015. Comparative anatomical study of swimbladder in different species of fish. Scientific Works. Series C. Veterinary Medicine 61, 156-160.

Horn, M.H., 1975. Swim− bladder state and structure in relation to behavior and mode of life in stromateoid fishes. Fish. Bull. 73, 95-109.

Hsia, C.C., Schmitz, A., Lambertz, M., Perry, S.F., Maina, J.N., 2013. Evolution of air breathing: oxygen homeostasis and the transitions from water to land and sky. Compr. Physiol. 3, 849-915.

Huang, C.-H., Chen, N., Huang, C.-X., Zhang, B., Wu, M., He, L., Liu, H., Tang, R., Wang, W.-M., Wang, H.-L., 2017. Involvement of the miR-462/731 cluster in hypoxia response in Megalobrama amblycephala. Fish Physiol. Biochem. 43, 863-873.

Huang, C.-X., Chen, N., Wu, X.-J., Huang, C.-H., He, Y., Tang, R., Wang, W.-M., Wang, H.-L., 2015. The zebrafish miR-462/miR-731 cluster is induced under hypoxic stress via hypoxia-inducible factor 1α and functions in cellular adaptations. FASEB J. 29, 4901-4913.

Jensen, F.B., Nikinmaa, M., Weber, R.E., 1993. Environmental perturbations of oxygen transport in teleost fishes: causes, consequences and compensations, Fish ecophysiology.

Springer, 161-179.

Kietzmann, T., Mennerich, D., Dimova, E.Y., 2016. Hypoxia-Inducible Factors (HIFs) and phosphorylation: impact on stability, localization, and transactivity. Front. Cell Dev. Biol. 4, 11.

Koong, A.C., Chen, E.Y., Mivechi, N.F., Denko, N.C., Stambrook, P., Giaccia, A.J., 1994. Hypoxic activation of nuclear factor-κB is mediated by a Ras and Raf signaling pathway and does not involve MAP kinase (ERK1 or ERK2). Cancer Res. 54, 5273-5279.

Kramer, D.L., McClure, M., 1982. Aquatic surface respiration, a widespread adaptation to hypoxia in tropical freshwater fishes. Environ. Biol. Fish. 7, 47-55.

Kvamme, B.O., Gadan, K., Finne-Fridell, F., Niklasson, L., Sundh, H., Sundell, K., Taranger, G.L., Evensen, Ø., 2013. Modulation of innate immune responses in Atlantic salmon by chronic hypoxia-induced stress. Fish Shellfish Immunol. 34, 55-65.

Lau, K., Lai, K.P., Bao, J.Y.J., Zhang, N., Tse, A., Tong, A., Li, J.W., Lok, S., Kong, R.Y.C., Lui, W.Y., 2014. Identification and expression profiling of microRNAs in the brain, liver and gonads of marine medaka (Oryzias melastigma) and in response to hypoxia. PLoS One 9, e110698.

Lechner, W., Ladich, F., 2008. Size matters: diversity in swimbladders and Weberian ossicles affects hearing in catfishes. J. Exp. Biol. 211, 1681-1689.

Lee, S., Chen, T.T., Barber, C.L., Jordan, M.C., Murdock, J., Desai, S., Ferrara, N., Nagy, A., Roos, K.P., Iruela-Arispe, M.L., 2007. Autocrine VEGF signaling is required for vascular homeostasis. Cell 130, 691-703.

Mazure, N.M., Chen, E.Y., Laderoute, K.R., Giaccia, A.J., 1997. Induction of vascular

endothelial growth factor by hypoxia is modulated by a phosphatidylinositol 3-kinase/Akt signaling pathway in Ha-ras-transformed cells through a hypoxia inducible factor-1 transcriptional element. Blood 90, 3322-3331.

Nilsson, G.E., Rosen, P., Johansson, D., 1993. Anoxic depression of spontaneous locomotor activity in crucian carp quantified by a computerized imaging technique. J. Exp. Biol. 180, 153-162.

Okubo, T., Hogan, B.L., 2004. Hyperactive Wnt signaling changes the developmental potential of embryonic lung endoderm. J. Biol. 3, 11.

Owen, R., 1846. Lectures on the Comparative Anatomy and Physiology of the Vertebrate Animals: Delivered at the Royal College of Surgeons of England, in 1844 and 1846. Longman, Brown, Green, and Longmans.

Pepicelli, C.V., Lewis, P.M., McMahon, A.P., 1998. Sonic hedgehog regulates branching morphogenesis in the mammalian lung. Curr. Biol. 8, 1083-1086.

Pollock, M., Clarke, L., Dubé, M., 2007. The effects of hypoxia on fishes: from ecological relevance to physiological effects. Environ. Rev. 15, 1-14.

Potter, G.E., 1927. Respiratory function of the swim bladder in Lepidosteus. J. Exp. Zool. A Ecol. Genet. Physiol. 49, 45-67.

Risau, W., 1997. Mechanisms of angiogenesis. Nature 386, 671.

Semenza, G.L., 2000. HIF-1: mediator of physiological and pathophysiological responses to hypoxia. J. Appl. Physiol. 88, 1474-1480.

Shiojima, I., Walsh, K., 2002. Role of Akt signaling in vascular homeostasis and angiogenesis. Circ. Res. 90, 1243-1250.

Shu, W., Jiang, Y.Q., Lu, M.M., Morrisey, E.E., 2002. Wnt7b regulates mesenchymal proliferation and vascular development in the lung. Development 129, 4831-4842.

Soñanez-Organis, J.G., Rodriguez-Armenta, M., Leal-Rubio, B., Peregrino-Uriarte, A.B., Gómez-Jiménez, S., Yepiz-Plascencia, G., 2012. Alternative splicing generates two lactate dehydrogenase subunits differentially expressed during hypoxia via HIF-1 in the shrimp Litopenaeus vannamei. Biochimie 94, 1250-1260.

Sun, L., Liu, S., Bao, L., Li, Y., Feng, J., Liu, Z., 2015. Claudin multigene family in channel catfish and their expression profiles in response to bacterial infection and hypoxia as revealed by meta-analysis of RNA-Seq datasets. Comp. Biochem. Physiol. Part D Genomics Proteomics 13, 60-69.

Sun, S., Xuan, F., Ge, X., Zhu, J., Zhang, W., 2017. Dynamic mRNA and miRNA expression analysis in response to hypoxia and reoxygenation in the blunt snout bream (Megalobrama amblycephala). Sci. Rep. 7, 12846.

Tian, Y., Yao, J., Liu, S., Jiang, C., Zhang, J., Li, Y., Feng, J., Liu, Z., 2015. Identification and expression analysis of 26 oncogenes of the receptor tyrosine kinase family in channel catfish after bacterial infection and hypoxic stress. Comp. Biochem. Physiol. Part D Genomics Proteomics 14, 16-25.

Trotter, A., Pankhurst, P., Hart, P., 2001. Swim bladder malformation in hatchery-reared striped trumpeter Latris lineata (Latridae). Aquaculture 198, 41-54.

Wang, X., Liu, S., Dunham, R., Liu, Z., 2017a. Effects of strain and body weight on low-oxygen tolerance of channel catfish (Ictalurus punctatus). Aquac. Int. 25, 1645-1652.

Wang, X., Liu, S., Jiang, C., Geng, X., Zhou, T., Li, N., Bao, L., Li, Y., Yao, J., Yang, Y., Zhong,

X., Jin, Y., Dunham, R., Liu, Z., 2017b. Multiple across-strain and within-strain QTLs suggest highly complex genetic architecture for hypoxia tolerance in channel catfish. Mol. Genet. Genomics 292, 63-76.

Welker, T.L., Mcnulty, S.T., Klesius, P.H., 2007. Effect of sublethal hypoxia on the immune response and susceptibility of channel catfish, Ictalurus punctatus, to enteric septicemia. J. World Aquacult. Soc. 38, 12-23.

Wenger, R.H., 2000. Mammalian oxygen sensing, signalling and gene regulation. J. Exp. Biol. 203, 1253-1263.

Whitehead, P., Blaxter, J., 1989. Swimbladder form in clupeoid fishes. Zool. J. Linn. Soc. 97, 299-372.

Winata, C.L., Korzh, S., Kondrychyn, I., Zheng, W., Korzh, V., Gong, Z., 2009. Development of zebrafish swimbladder: The requirement of Hedgehog signaling in specification and organization of the three tissue layers. Dev. Biol. 331, 222-236.

Yin, A., Korzh, S., Winata, C.L., Korzh, V., Gong, Z., 2011. Wnt signaling is required for early development of zebrafish swimbladder. PloS One 6, e18431.

Yin, A., Winata, C.L., Korzh, S., Korzh, V., Gong, Z., 2010. Expression of components of Wnt and Hedgehog pathways in different tissue layers during lung development in Xenopus laevis. Gene Expr. Patterns 10, 338-344.

Yuan, Z., Liu, S., Yao, J., Zeng, Q., Tan, S., Liu, Z., 2016. Expression of Bcl-2 genes in channel catfish after bacterial infection and hypoxia stress. Dev. Comp. Immunol. 65, 79-90.

Zhao, Y., Zhu, C.-D., Yan, B., Zhao, J.-L., Wang, Z.-H., 2014. miRNA-directed regulation of VEGF in tilapia under hypoxia condition. Biochem. Biophys. Res. Commun. 454, 183-

188.

Zheng, W., Wang, Z., Collins, J.E., Andrews, R.M., Stemple, D., Gong, Z., 2011. Comparative transcriptome analyses indicate molecular homology of zebrafish swimbladder and mammalian lung. PloS One 6, e24019.

Zhong, H., Chiles, K., Feldser, D., Laughner, E., Hanrahan, C., Georgescu, M.-M., Simons, J.W., Semenza, G.L., 2000. Modulation of hypoxia-inducible factor 1α expression by the epidermal growth factor/phosphatidylinositol 3-kinase/PTEN/AKT/FRAP pathway in human prostate cancer cells: implications for tumor angiogenesis and therapeutics. Cancer Res. 60, 1541-1545.

Chapter 2 Comparative transcriptome analysis reveals conserved branching morphogenesis related genes involved in chamber formation of catfish swimbladder

2.1 Abstract

The swimbladder is an internal gas-filled organ in teleosts. Its major function is to regulate buoyancy. Swimbladder exhibits great variations in size, shape, number of compartments or chambers among teleosts. However, the genomic control of swimbladder variations is unknown. Channel catfish (*Ictalurus punctatus*), blue catfish (*Ictalurus furcatus*), and their F1 hybrids of female channel catfish x male blue catfish (C×B hybrid catfish) provide a good model to investigate the swimbladder morphology, because channel catfish possess a single-chambered swimbladder whereas blue catfish possess a bi-chambered swimbladder; and C×B hybrid catfish possess a bi-chambered swimbladder but with significantly reduced posterior chamber. Here we determined the transcriptional profiles of swimbladder from channel catfish, blue catfish, and C×B hybrid catfish. We examined their transcriptomes at both the fingerling and adult stages. Through comparative transcriptome analysis, approximately 4,000 differentially expressed genes (DEGs) were identified. Among these DEGs, members of the Wnt signaling pathway (*wnt1*, *wnt2*, *nfatc1*, *rac2*), Hedgehog signaling pathway (*shh*), and growth factors (*fgf10*, *igf-1*) were identified. As these genes were known to be important for branching morphogenesis of mammalian lung and of mammary glands, their association with budding of posterior chamber primordium and progressive development of bi-chambered swimbladder in fish suggested that these branching morphogenesis related genes and their functions in branching are evolutionarily conserved across a broad spectrum of species.

2.2 Background

Swimbladder is an internal gas-filled organ in teleosts that exerts various functions with inclusion of respiration, buoyancy regulation, pressure reception, hearing and sound production (Alexander, 1966). The swimbladder exists in most teleost fish, while it is absent in cartilaginous fish. The similarities in homology, and perhaps also the functions, of fish swimbladder and vertebrate lung have been long noted (Owen, 1846). Using comparative transcriptome analysis, Zheng et al. demonstrated a high level of resemblance between zebrafish swimbladder and the mammalian lung (Zheng et al., 2011). Interestingly, Hedgehog and Wnt signaling pathways play essential roles in development of both zebrafish swimbladder (Winata et al., 2009; Yin et al., 2011) and of vertebrate lung (Bellusci et al., 1997a; Okubo and Hogan, 2004; Pepicelli et al., 1998; Shu et al., 2002; Yin et al., 2010). In the zebrafish swimbladder, the budding of second chamber primordium was demonstrated as a simplified form of branching morphogenesis similar to that in mammalian lung (Winata et al., 2009). Conserved divergent elements involving *Shh/Shha* signals (Winata et al., 2009) and Wnt signaling pathway (Yin et al., 2011) have been both detected during subsequent branching morphogenesis in the development of zebrafish swimbladder and mammalian lung.

The fish swimbladder can be divided into two main types based on their morphology: physostomous (an open swimbladder system) and physoclistous (a closed swimbladder system). Physostomous fish has a pneumatic duct between the swimbladder and the gut, whereas the physoclistous fish lacks a duct but possesses specialized structures associated with the respiratory and circulatory system for inflation and deflation (Trotter et al., 2001). Great

variation has been reported in size, shape, and the number of chambers of the swimbladder among various fish species. For example, the swimbladders of rainbow trout, northern pike and zander possess only one chamber, whereas the swimbladders of most Ostariophysi consist of two chambers (anterior and posterior chambers), such as common carp, grass carp, and zebrafish (Grom, 2015). The anterior and posterior chambers are linked and separated by a clear constriction. The anterior and posterior chambers in swimbladder varies in size, as well as their functions. In most Cypriniformes, the anterior chamber is bigger than the posterior chamber for oxygen secreting (Hsia et al., 2013). In zebrafish, the anterior chamber was demonstrated to possess acoustic resonance properties, whereas the posterior chamber is important for buoyancy control (Finney et al., 2006). It has been long noted that the great variations in morphology of the swimbladder among fish species are associated with their hydrostatic function, the variation in the center of gravity, their behavior, and lifestyle (Horn, 1975; Whitehead and Blaxter, 1989). Additionally, the diversity of swimbladder in shape and size also has a great influence on their hearing abilities (Lechner and Ladich, 2008).

Catfish serve as a good model to investigate the swimbladder morphology because channel catfish (*Ictalurus punctatus*) possess a single-chambered swimbladder, whereas blue catfish (*Ictalurus furcatus*) possess a distinct bi-chambered swimbladder with the two lobes being similar in size; and their hybrids (female channel catfish x male blue catfish) possess a bi-chambered swimbladder but with significantly reduced posterior chamber (**Figure 1**), more similar to its paternal parent than the maternal parent (Dunham and Masser, 2012).

Despite such a good model, the molecular basis of the difference in morphology among channel catfish, blue catfish and C×B hybrid catfish is still unknown. To understand the

mechanisms for development of single-chambered and bi-chambered swimbladder, we examined transcriptional profiles of the swimbladder from channel catfish, blue catfish, and C×B hybrid catfish at both fingerling and adult stages. Here we report a set of differentially expressed genes among these catfish, and the potential gene pathways involved for the control of swimbladder morphology.

Figure 1. Schematic presentation of the shape of swimbladders of channel catfish (*Ictalurus punctatus*) (A), blue catfish (*Ictalurus furcatus*) (B), and C X B hybrid catfish (C). Note that channel catfish has a single-chambered, heart-shaped swimbladder without constriction; blue catfish has a long, narrow, bi-chambered swimbladder; and the hybrid catfish has a bi-chambered swimbladder with a large, heart-shaped anterior chamber and a small attached posterior chamber. Figure adopted from (Dunham et al., 1982).

Figure 1

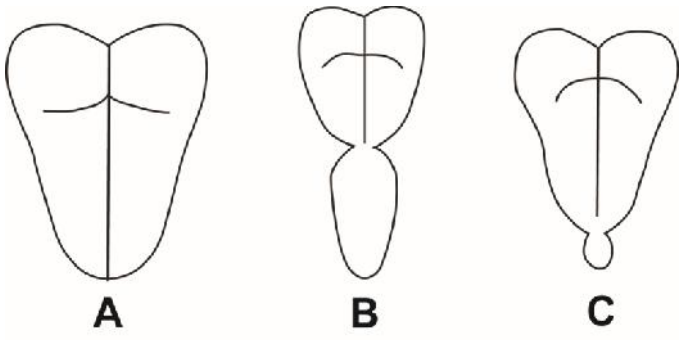

2.3 Materials and methods

2.3.1 Ethics statement

Experimental protocols of animal care and tissue collection were approved by the Auburn University Institutional Animal Care and Use Committee (AU-IACUC). All surgery was performed after euthanization with MS-222 (200 mg/L) buffered with sodium bicarbonate to

minimize suffering.

2.3.2 Tissue collection, RNA isolation, library construction and sequencing

After the catfish were euthanized with MS-222 (200 mg/L), swimbladder samples were collected from catfish at two stages (fingerlings at 4 months of age/adult fish at two years of age). At each time point, 9 fish were randomly selected from channel, blue, and C×B hybrid catfish and divided into 3 replicate pools (3 fish each). The swimbladder samples were flash-frozen in liquid nitrogen and stored in -80 until RNA extraction. For each replicate, swimbladder samples of 3 fish were homogenized in liquid nitrogen with a mortar and pestle. Total RNA was extracted using RNeasy Plus Kit (Qiagen, USA) following the manufacturer's instructions. The concentration and quality of RNA was measured on an Agilent 2100 Bioanalyzer using a RNA Nanodrop chip (NanoDrop Technologies, USA). Equal amounts of RNA from the three replicates for each sample were pooled together for RNA-Seq library preparation. The remaining replicate pools were preserved as biological replicates for qRT-PCR validation. The cDNA libraries were prepared by HudsonAlpha Genomic Services Lab (Huntsville, AL, USA) using standard protocols. Sequencing was conducted on HiSeq v4 as 100 bp paired-end reads.

2.3.3 Pre-filtering and read mapping

As channel catfish and blue catfish share an average of about 98.7% gene sequence identity (Gregory et al., 2004), the channel catfish reference genome was used as a reference for mapping short expressed reads from swimbladder samples of channel catfish, blue catfish, and C×B hybrid catfish. The simpler direct read-to-genome mapping approach where quality-

controlled short transcriptome reads are aligned directly against the closest available annotated reference sequence has been applied in previous studies (Marasco et al., 2016; Ockendon et al., 2016). Raw reads were trimmed by removing adapter sequences and ambiguous nucleotides. Reads with quality scores less than 20 and lengths below 30 bp were all removed. All the trimmed reads were mapped to the channel catfish genome assembly (Liu et al., 2016) using STAR-2.5.2b (Dobin et al., 2013). After mapping, the output BAM files were sorted by samtools-1.3.1 (http://www.htslib.org/doc/samtools.html). HTSeq-count version 0.6.1p1 (http://www-huber.embl.de/users/anders/HTSeq/doc/count.html) was used to extract the count files from the mapping files (Anders et al., 2014).

2.3.4 Differential expression analysis and gene ontology (GO) enrichment

Differential expression analysis of sequence count data in this study was performed using EdgeR (Robinson et al., 2010), and resulting *P*-values were corrected for the false discovery rate (FDR). Prior to computations for differential expression, we conducted trimmed mean of M-values (TMM) normalization of expression values between each pair of samples. Genes with FDR <0.05 were considered as DEGs. The DEGs were annotated by performing BLASTP searches against NCBI non-redundant (nr) protein database with an E-value cutoff of $1E^{-5}$. GO Ontology (GO) annotation analysis was performed using Blast2GO with a E-value cutoff of $1E^{-6}$ (Conesa et al., 2005). The annotation result was then categorized with respect to biological process, molecular function, and cellular component at level 2. To identify the overrepresented GO terms in DEG set compared with the reference assembly, we performed GO analysis and enrichment analysis via Ontologizer 2.1 by the Parent-Child-Intersection method with a Benjamini-Hochberg multiple testing correction (Bauer et al., 2008; Grossmann et al., 2007).

GO terms for each gene were obtained by utilizing uniprot annotations for the unigene set. The threshold was set as FDR corrected value < 0.05. Gene pathway analysis of significant differentially expressed genes was carried out based on GO annotation and KEGG tools (BlastKOALA and GhostKOALA) (Kanehisa et al., 2016), as well as on manual literature review.

2.3.5 Experimental validation by quantitative real time qRT-PCR

Seventeen genes revealed by functional enrichment and pathway analysis with differential expression patterns were selected for qRT-PCR validation. The specific primers of all these genes were designed by Primer3 software (Rozen and Skaletsky, 1999) and listed in **Table 1**. The specificity of primers was assessed by aligning with the channel catfish whole genome database (Liu et al., 2016) using BLASTN with E-value of $1e^{-10}$. Reverse transcription were performed using the qScriptTM cDNA Synthesis Kit (Quanta Bioscience, Gaithersburg, MD). All the cDNA products were then diluted to 250 ng/μL. The qPCR was performed using SYBR Green PCR Master Mix on a CFX96 real-time PCR detection system (Bio-Rad, USA). The cycling conditions of qPCR were denaturation, 95 °C/30 s, 40 cycles of 95 °C/5 s, 60 °C/5 s, and 72 °C/5 s. Test PCR were performed in advance to ensure all the genes were amplified with expect PCR product sizes. A no-template control was run on all plates. The *gusb* gene was used as an internal reference gene (Zeng et al., 2016). The melting curve analysis was performed to verify that each primer set amplified a single product. The relative expression was analyzed based on the cycle threshold (Ct) values using BIO-RAD CFX Manager Software. The qPCR was repeated in triplicate runs to confirm expression patterns.

Table 1. Primers used for qPCR validation.

Table 1

Gene	Gene symbol	Primers
Glucuronidase beta	gusb	F:5'GGATGGGCGCAAACTCATTC R: 5'ACCAGCTCCTTCATGACGAC
Zinc transporter ZIP10	zip10	F: 5'AGATGATGCTTCCCAGAGCG R: 5'TGTCCTTCTCCGAATGGCAG
Nuclear receptor subfamily 4 group A member 1	nr4a1	F: 5'ACAGATCACACCCAGAGACG R: 5'AGGCCGTGTCGATCTGTTAT
Collagen alpha-2(I) chain	col1a2	F: 5'ATGGACGAAAAGGAGAGGCT R: 5'GGACCAGTGTTACCATCAGC
Egl nine homolog 3	egln3	F: 5'CCTCGGTGAAGCAATTGGTC R: 5'ATGGCTTCGGATCCTCTCTC
RING finger protein 183	rnf183	F: 5'GGATAATCTGCGCCTTCTGC R: 5'TCTTTAGACTGGCCGGTTGT
CD209 antigen	cd209	F: 5'CAGAGGTGAAGCAGTGCATG R: 5'CACTCAAACTGCGGGCTATT
Cholesterol side-chain cleavage enzyme, mitochondrial	cyp11a1	F: 5'TCAGAGTGGAACCTTGGACC R: 5'CCAACCTCATCCAGCAATGG
Cyclin-dependent kinase inhibitor 1	cdkn1a	F: 5'CGGTTCAGTGGATCATGAGG R: 5'GGAACTCGAGCCTCAGGAAG
Epiplakin	eppk1	F: 5'CAGTTTACAGCCACCGTGTC R: 5'ACAAGCAGTCTAAGGCCAGT
Ferritin, middle subunit	frim	F: 5'GCCTCCTACACCTACACCTC R: 5'AACACCTTTGCTTGACGTCC
Tripartite motif-containing protein 35	trim35	F: 5'AGCGGCAGATTAAGGAGGAG R: 5'GTCTTCGGCTCTCATCTCCT
Ankyrin repeat and EF-hand domain-containing protein 1	ankef1	F: 5'GAGCTGCAAATTTACCGGCT R: 5'GGACAAGCACCATGAAGCAT
Endosialin	cd248	F:5'GACCAGAGGAAGCAGCATTG R: 5'TCCTCACGTTGCCAGTTAGT
Zona pellucida sperm-binding protein 3	zp3	F: 5'TGGTGCAGTTCAACCATGTG R: 5'GAAGCGGGAACTGGAATGTG
TRPM8 channel-associated factor homolog	tcaf	F: 5'GCTTTGCTAGCCATGCCATC R: 5'AACACACTTGCGGAACTCCT
Galanin receptor type 2	galr2	F: 5'AGAACGGTACCAGACGCAAG R: 5'GCGCAAAAGTAGCGAAAGGT

2.4 Results

2.4.1 Sequencing and mapping of short expressed reads from catfish swimbladder

As shown in **Table 2**, a total of about 1,159 million raw reads of 100 bp long were generated. Ambiguous nucleotides, low-quality sequences (quality score < 20) and short reads (length < 30bp) were removed. After trimming, a total of approximately 1,040 million clean reads were retained for subsequent analysis (**Table 2**). The short read sequences were deposited at the NCBI Sequence Read Archive (SRA) with BioProject ID PRJNA400910. All filtered reads were mapped to the channel catfish reference genome (Liu et al., 2016) using STAR-2.5.2b (Dobin et al., 2013). Principal component analysis (PCA) was conducted to identify the outliers within swimbladder transcriptomes of channel, blue, and C×B hybrid catfish (**Figure 2**). The segregation and clustering were consistent with the relevance of the data. Samples from three genetic types of catfish were separated by the first principal component (PC1) which accounted for 70% of expression variability.

Table 2. Summary of RNA-seq of swimbladder transcriptomes.

Table 2

Groups	No. of raw reads (million)	Total bases of raw data (Gb)	No. of reads after trim (million)	Average length after trim (bp)	Total bases after trim (Gb)
Channel					
Adult	139.59	13.96	123.77	97.41	12.06
Fingerling	128.48	12.85	115.06	95.68	11.01
Subtotal	268.07	26.81	238.83	-	23.07
Blue					
Adult	270.65	27.07	243.29	97.89	23.82
Fingerling	191.19	19.12	170.91	97.77	16.71
Subtotal	461.84	46.18	414.2	-	40.53
Hybrid					
Adult	256.46	25.65	232.75	97.97	22.8

Fingerling	172.83	17.28	154.77	97.99	15.17
Subtotal	429.29	42.93	387.52	-	37.97
Total	1159.2	115.92	1040.55	-	101.57

Figure 2. Sample structure identified by Principal component analysis (PCA) with the first two principal components. The coordinates are the first two principal components.

Figure 2

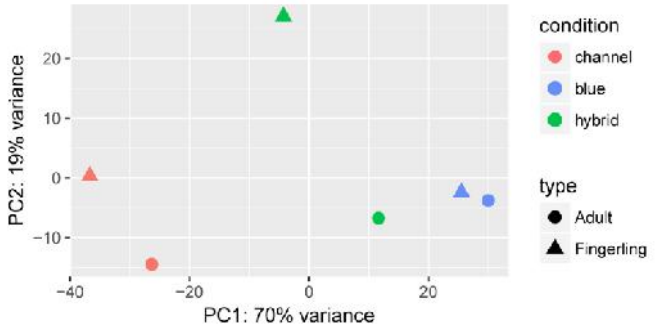

2.4.2 Analysis of differentially expressed genes

Pairwise comparisons were conducted to identify DEGs among swimbladder transcriptomes of channel, blue and C×B hybrid catfish. Overall, the number of DEGs identified in fingerlings was larger than that in the adult fish (**Table 3**). A total of 3,346 and 1,639 DEGs were identified in fingerlings and adults between channel and blue catfish, respectively. A total of 603 and 338 DEGs were identified in fingerlings and adult fish between channel and C×B hybrid catfish, respectively. A total of 239 and 270 DEGs were identified in fingerlings and adult fish between blue and C×B hybrid catfish, respectively. Notably, the largest number of DEGs was identified between channel and blue catfish. The number of DEGs identified between blue and C×B hybrid catfish was lower than the DEGs between channel catfish and C×B hybrid catfish at both in fingerlings and in adult fish, which was consistent with the morphological resemblance of swimbladder between blue catfish and C×B hybrid

catfish (Dunham et al., 1982). This might be explained by paternal predominance (Dunham et al., 1982).

Table 3. Summary of differentially expressed genes (DEG, FDR-corrected *P* value < 0.05) in the swimbladder as identified by comparing transcripts in channel catfish (*Ictalurus punctatus*), blue catfish (*Ictalurus furcatus*), and female channel catfish x male blue catfish (CxB hybrid catfish). Comparisons were made between channel catfish and blue catfish, channel catfish and CxB hybrid catfish, and blue catfish and CxB hybrid catfish.

Table 3

Comparison	DEG	In Fingerling	In Adult
Channel	**Higher in channel**	1158	862
vs	**Higher in blue**	2188	777
Blue	**Total**	3346	1639
Channel	**Higher in channel**	195	181
vs	**Higher in hybrid**	408	157
Hybrid	**Total**	603	338
Blue	**Higher in blue**	32	113
vs	**Higher in hybrid**	207	157
Hybrid	**Total**	239	270

2.4.3 Clustering, GO analysis and pathway analysis

Hierarchical clustering was performed to group DEGs according to the similarity in pattern of gene expression using DEseq2 (Love et al., 2014). A total of 9 clusters were identified according to their expression patterns. As shown on the heatmap (**Figure 3**), swimbladder samples of blue catfish were first clustered with swimbladder samples of C×B hybrid catfish, and then clustered with channel catfish. The clustering of these six samples suggested that the expression profiles between blue and C×B hybrid catfish were more similar, whereas the expression profiles of channel catfish were significantly different from that of blue catfish and C×B hybrid catfish.

The differentially expressed genes identified in catfish swimbladder transcriptomes were characterized using Gene Ontology (GO) (**Figure 4**). The level 2 GO term distribution indicated that large proportions of DEGs were involved in cellular process (GO:0009987) and single-organism process (GO:0044699) under the biological process terms, whereas binding (GO:0005488) and catalytic activity (GO:0003824) were the most common annotation terms under molecular function. Under cellular component, cell (GO:0005623) and membrane part (GO:0044425) were the most common annotation terms. The uniquely differently expressed genes were then used as inputs to perform enrichment analysis using Ontologizer 2.1. Parent-child GO term enrichment analysis was performed to detect significantly overrepresented GO terms with *p* value (FDR) <0.01. The GO term analysis for each cluster is listed in **Table 4**. In cluster 1, 2 and 9, extracellular region part (GO:0044421), collagen trimer (GO:0005581), extracellular matrix (GO:0031012), and structural molecule activity (GO:0005198) were the most common GO terms. However, in cluster 3, 4, and 7 (**Table 4**), extracellular region part (GO:0044421), regulation of peptidase activity (GO:0052547), protein activation cascade (GO:0072376) were the most common GO terms.

A total of 2,362 genes (51.2%) were assigned with KEGG annotation. Approximately, 19.64%, 19.17%, 15.29%, and 13.64% of these annotated genes were classified into environmental information processing, genetic information processing, organismal systems, and cellular processes, respectively. The most frequently observed KEGG pathways were metabolic pathways, neuroactive ligand-receptor interaction, cAMP signaling pathway, calcium signaling pathway, and MAPK signaling pathway. Based on a combination of enrichment analysis, KEGG pathway analysis, manual annotation and literature searches,

representative key genes were arranged into five functional categories, including Wnt signaling pathway, Hedgehog signaling pathway, branching genes in morphogenesis, ECM-receptor interaction, cell adhesion molecules (CAMs) (**Table 5**). Members of the Wnt signaling pathway (*wnt1*, *wnt2*, *nfatc1*, *rac2*), Hedgehog signaling pathway (*shh*), and growth factors (*fgf10*, *igf-1*) were identified as DEGs, which might be involved with budding of posterior chamber primordium and progressive development of bi-chambered swimbladder.

Table 4. Summary of GO enrichment analysis of significantly DEGs. Population count is the number of GO term associated genes in the population gene set. Study count is the number of GO term associated genes in the DEGs set. FDR P value < 0.05 was considered as significant GO term.

Table 4

GO ID	GO Term	Population count	Study count	*P* value (FDR)
Cluster 1 & 2 & 9				
GO:0044421	Extracellular region part	15150	26	5.37E-06
GO:0005581	Collagen trimer	2449	7	5.37E-06
GO:0005576	Extracellular region	15150	26	5.37E-06
GO:0031012	Extracellular matrix	2760	18	2.31E-04
GO:0005198	Structural molecule activity	14137	22	2.11E-02
Cluster 3 & 4 & 7				
GO:0044421	Extracellular region part	15150	1366	6.65E-15
GO:0052547	Regulation of peptidase activity	1194	112	5.25E-04
GO:0072376	Protein activation cascade	8109	767	1.63E-03
GO:0005615	Extracellular space	2257	311	2.55E-03
GO:0009897	External side of plasma membrane	3965	394	2.78E-03
GO:0005581	Collagen trimer	2449	211	2.78E-03
GO:0060205	Cytoplasmic vesicle lumen	4304	390	3.44E-03
GO:0031983	Vesicle lumen	5272	500	3.53E-03
GO:0043230	Extracellular organelle	11525	1067	5.19E-03
GO:0044707	Single-multicellular organism process	10716	971	5.59E-03
GO:0032501	Multicellular organismal process	14475	1300	6.77E-03
GO:0044767	Single-organism developmental process	10657	959	7.63E-03
Cluster 5				
GO:0044459	Plasma membrane part	14022	763	2.09E-17
GO:0006811	Ion transport	3745	248	1.28E-10
GO:1990351	Transporter complex	3989	180	1.51E-09
GO:0043235	Receptor complex	3989	180	3.10E-07
GO:0060089	Molecular transducer activity	14137	802	7.56E-07
GO:0007154	Cell communication	12333	668	6.24E-05
GO:0055085	Transmembrane transport	3745	248	1.28E-04
GO:0015849	Organic acid transport	2825	172	1.51E-03
GO:0044449	Contractile fiber part	8974	392	1.78E-03
GO:0044456	Synapse part	15150	865	3.03E-03
GO:0097458	Neuron part	13371	722	3.21E-03
GO:0015711	Organic anion transport	2158	129	4.77E-03
GO:0005509	Calcium ion binding	3462	195	5.14E-03

GO:1901571	Fatty acid derivative transport	2825	172	5.31E-03
GO:0007010	Cytoskeleton organization	2947	103	7.76E-03
Cluster 6				
GO:0044459	Plasma membrane part	14022	571	1.74E-11
GO:0071944	Cell periphery	13371	543	1.74E-11
GO:1990351	Transporter complex	3989	148	5.85E-10
GO:0097458	Neuron part	13371	543	4.00E-09
GO:0055085	Transmembrane transport	3745	190	9.34E-07
GO:0007215	Glutamate receptor signaling pathway	2002	82	1.76E-06
GO:0006811	Ion transport	3745	190	3.76E-06
GO:0022838	Substrate-specific channel activity	850	80	1.65E-05
GO:0030054	Cell junction	15150	619	3.54E-05
GO:0016459	Myosin complex	3275	107	5.83E-04
GO:0099536	Synaptic signaling	1151	78	1.27E-03
GO:0030594	Neurotransmitter receptor activity	832	55	1.58E-03
GO:0032420	Stereocilium	7307	285	1.95E-03
GO:0007610	Behavior	14475	584	2.18E-03
GO:0007267	Cell-cell signaling	9408	401	2.55E-03
Cluster 8				
GO:0007186	G-protein coupled receptor signaling pathway	4202	102	7.38E-05
GO:0060089	Molecular transducer activity	14137	269	7.38E-05
GO:0032501	Multicellular organismal process	14475	268	2.05E-04
GO:0050794	Regulation of cellular process	12476	225	1.73E-03
GO:0004871	Signal transducer activity	14137	269	2.35E-03
GO:0034654	Nucleobase-containing compound biosynthetic process	4985	89	4.42E-03
GO:0019438	Aromatic compound biosynthetic process	5711	99	7.10E-03
GO:0018130	Heterocycle biosynthetic process	5693	99	7.10E-03
GO:0007154	Cell communication	12333	222	7.99E-03

Table 5. Differentially expressed genes in catfish swimbladder involved in Wnt and Hedgehog signaling, branching morphogenesis, ECM-receptor interaction, and cell adhesion.

Table 5

Genes	Channel vs Blue		Channel vs Hybrid		Blue vs Hybrid	
	Fingerling	Adult	Fingerling	Adult	Fingerling	Adult
Wnt signaling pathway						
Protein Wnt-1	**2.66**	2.04	1.04	1.45	-1.62	-0.59
Protein Wnt-2	**2.52**	1.90	1.42	1.47	-1.10	-0.44
Protein Wnt-9b	**2.43**	2.26	2.04	1.98	-0.39	-0.28
Protein Wnt-10b	**4.49**	1.24	2.87	1.18	-1.62	-0.06
Dickkopf-related protein 1	**2.81**	1.06	1.99	0.68	-0.82	-0.39
Frizzled-10-B	**2.53**	1.52	1.35	1.06	-1.18	-0.46
Frizzled-7-A	**-2.35**	-1.62	-0.99	-0.09	1.36	1.53

Adenomatous polyposis coli protein 2	**2.70**	1.82	1.48	1.35	-1.22	-0.47
Axin-1	**2.39**	0.78	0.73	0.05	-1.66	-0.74
Nuclear factor of activated T-cells, cytoplasmic 4	-1.17	**-2.27**	-0.22	-1.38	0.95	0.90
Ras-related C3 botulinum toxin substrate 2	**-2.30**	-1.48	-0.75	-0.75	1.55	0.73
Protein notum homolog	**2.59**	1.30	1.14	1.32	-1.45	0.03
Protein-cysteine N-palmitoyltransferase porcupine	**2.35**	1.91	1.70	1.87	-0.65	-0.04
Secreted frizzled-related protein 5	**2.20**	1.67	1.58	1.45	-0.62	-0.21
Calcium/calmodulin-dependent protein kinase type II	**2.92**	1.24	1.49	1.17	-1.43	-0.07
Pigment epithelium-derived factor	1.54	**4.29**	**2.88**	**3.09**	1.34	-1.19
Transcriptional regulator Myc-2	**-4.10**	**-4.20**	**-3.46**	**-2.95**	0.64	1.25
G1/S-specific cyclin-D2	**-2.71**	**-2.19**	**-4.35**	**-3.05**	-1.64	-0.86
Mitogen-activated protein kinase 8	**-2.24**	-1.75	-1.52	-1.14	0.72	0.60
RuvB-like 1	**-1.91**	-0.95	-0.97	0.31	0.94	1.26
Hedgehog signaling pathway						
Smoothened homolog	**1.91**	**2.68**	**2.30**	1.84	0.39	-0.85
Tiggy-winkle hedgehog protein	**2.45**	1.23	1.65	0.91	-0.81	-0.33
Arrestin-C	**2.64**	1.48	0.53	1.48	-2.12	-0.01
S-arrestin	**2.46**	1.78	1.32	1.98	-1.13	0.19
G-protein coupled receptor 161	**-1.90**	-0.43	-1.07	-0.09	0.83	0.34
Cullin-3	**-2.08**	-1.79	-2.04	-1.40	0.04	0.39
Branching morphogenesis						
Insulin-like growth factor I, adult form	**2.90**	**3.09**	0.81	1.80	-2.08	-1.30
Fibroblast growth factor 10	**3.22**	2.01	1.13	2.07	-2.09	0.06
Mothers against decapentaplegic homolog 4	**-2.45**	-1.96	-2.05	-2.29	0.40	-0.33
Fibroblast growth factor 8b	**2.60**	1.38	0.95	1.25	-1.65	-0.12
Fibroblast growth factor 8	**2.24**	2.17	0.85	1.64	-1.39	-0.53
ECM-receptor interaction						
Collagen alpha-1(I) chain	**4.66**	**5.36**	**5.79**	1.89	1.12	**-3.48**
Collagen alpha-2(I) chain	**5.46**	**5.83**	**5.88**	**2.56**	0.42	**-3.27**
Collagen alpha-2(IV) chain	2.14	**3.58**	0.66	2.13	-1.47	-1.47
Collagen alpha-1(VI) chain	1.62	**2.57**	1.73	0.88	0.11	-1.70
Collagen alpha-2(VI) chain	1.78	**3.03**	2.08	1.44	0.30	-1.58
Collagen alpha-4(VI) chain	**-2.29**	**-2.54**	-0.59	-0.09	1.70	**2.45**
Collagen alpha-6(VI) chain	**2.21**	**2.15**	**3.19**	1.42	0.98	-0.73
Collagen alpha-2(IX) chain	-1.45	**-2.15**	-0.96	**-2.38**	0.49	-0.23
Laminin subunit alpha-1	**2.30**	1.53	1.10	1.42	-1.20	-0.11
Laminin subunit alpha-3	1.31	**2.50**	1.38	2.16	0.08	-0.34
Laminin subunit beta-3	1.71	**2.16**	0.37	0.99	-1.34	-1.17
Laminin subunit beta-4	**2.42**	1.74	0.86	1.36	-1.55	-0.38
Cell adhesion molecules (CAMs)						
Claudin-19	**2.17**	1.66	1.15	1.61	-1.03	-0.05
Claudin-20	**2.52**	**2.90**	1.75	2.21	-0.77	-0.69
Claudin-4	**3.80**	1.32	3.50	0.80	-0.31	-0.53
Cell adhesion molecule 1	**2.19**	1.37	1.43	1.17	-0.76	-0.20
Contactin-1	**2.41**	**2.19**	1.03	1.66	-1.38	-0.53
Contactin-1a	**2.36**	1.89	1.31	1.57	-1.05	-0.33
Contactin-associated protein 1	**2.27**	**2.23**	0.50	1.88	-1.77	-0.35
Contactin-associated protein-like 2	**1.97**	1.63	0.73	1.47	-1.25	-0.15
Neural cell adhesion molecule 1	**3.28**	**4.15**	1.24	0.60	-2.04	**-3.55**
Neural cell adhesion molecule 2	**1.95**	1.67	1.07	1.27	-0.87	-0.40

Figure 3. Heatmap and hierarchical clustering of the DEGs based on log2 normalized counts.

The DEGs are displayed in rows while samples are displayed in columns.

Figure 3

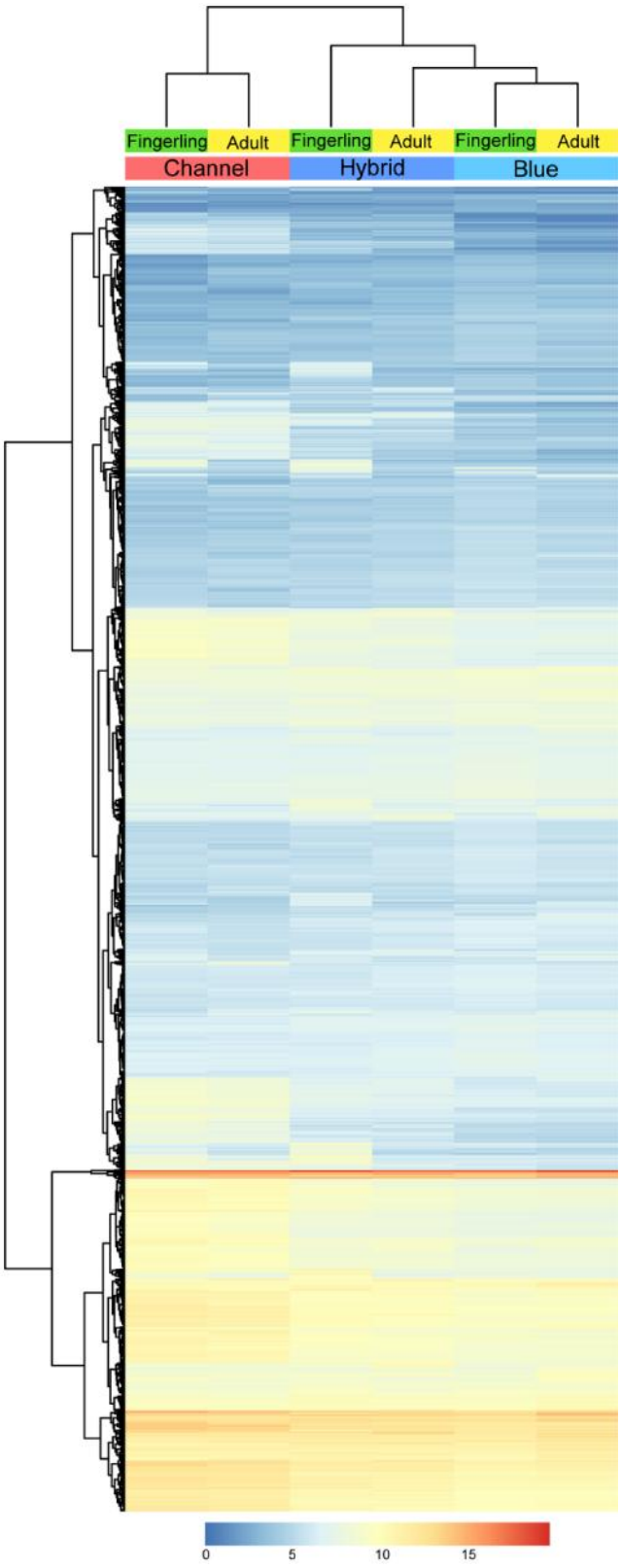

Figure 4. GO term classification of significant DEGs by BLAST2GO on level 2.
Figure 4

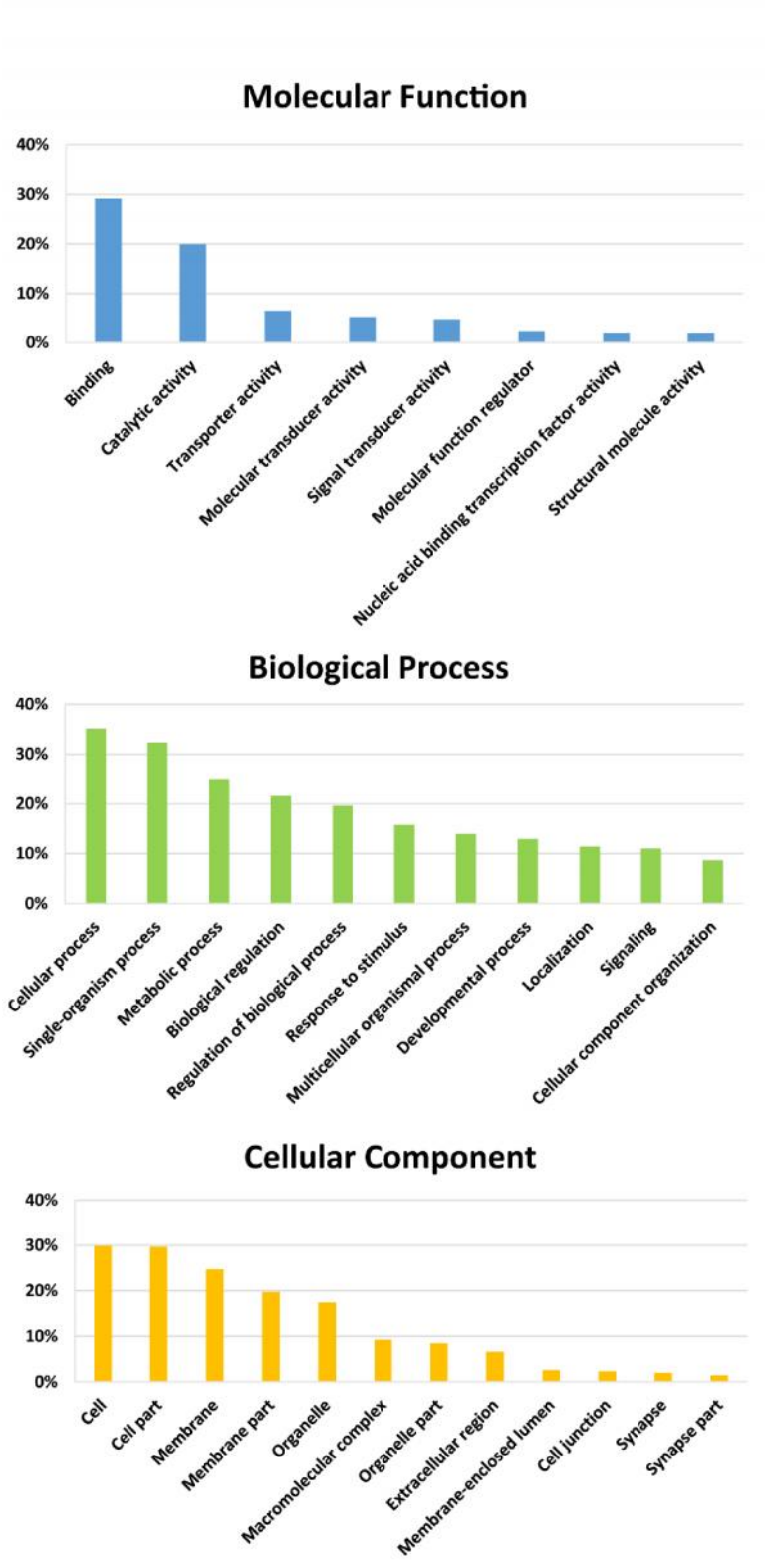

2.4.4 Validation of RNA-seq results by qPCR

To validate the differentially expressed genes identified by RNA-seq analysis, we randomly selected 17 genes for qPCR validation. The remaining 3 replicate pools were preserved as biological replicates for qRT-PCR validation. Melting-curve analysis revealed a single product for tested genes. Fold changes from qPCR were compared with the RNA-seq results, and significant correlations between qPCR and RNA-seq based expression profiles were observed (correlation coefficients of 0.882-0.940), validating the results from RNA-seq analysis (**Figure 5**). The scatter plot between RNA-Seq and qPCR result was in **Figure 6**.

Figure 5. Comparison of relative fold changes between RNA-seq and QPCR results. A: channel catfish vs blue catfish (fingerling group, correlation coefficients 0.892). B: channel catfish vs blue catfish (adult group, correlation coefficients 0.928). C: channel catfish vs C X B hybrid catfish (fingerling group, correlation coefficients 0.882). D: channel catfish vs C X B hybrid catfish (adult group, correlation coefficients 0.918). E: blue catfish vs C X B hybrid catfish (fingerling group, correlation coefficients 0.884). F: blue catfish vs C X B hybrid catfish (adult group, correlation coefficients 0.940).

Figure 5

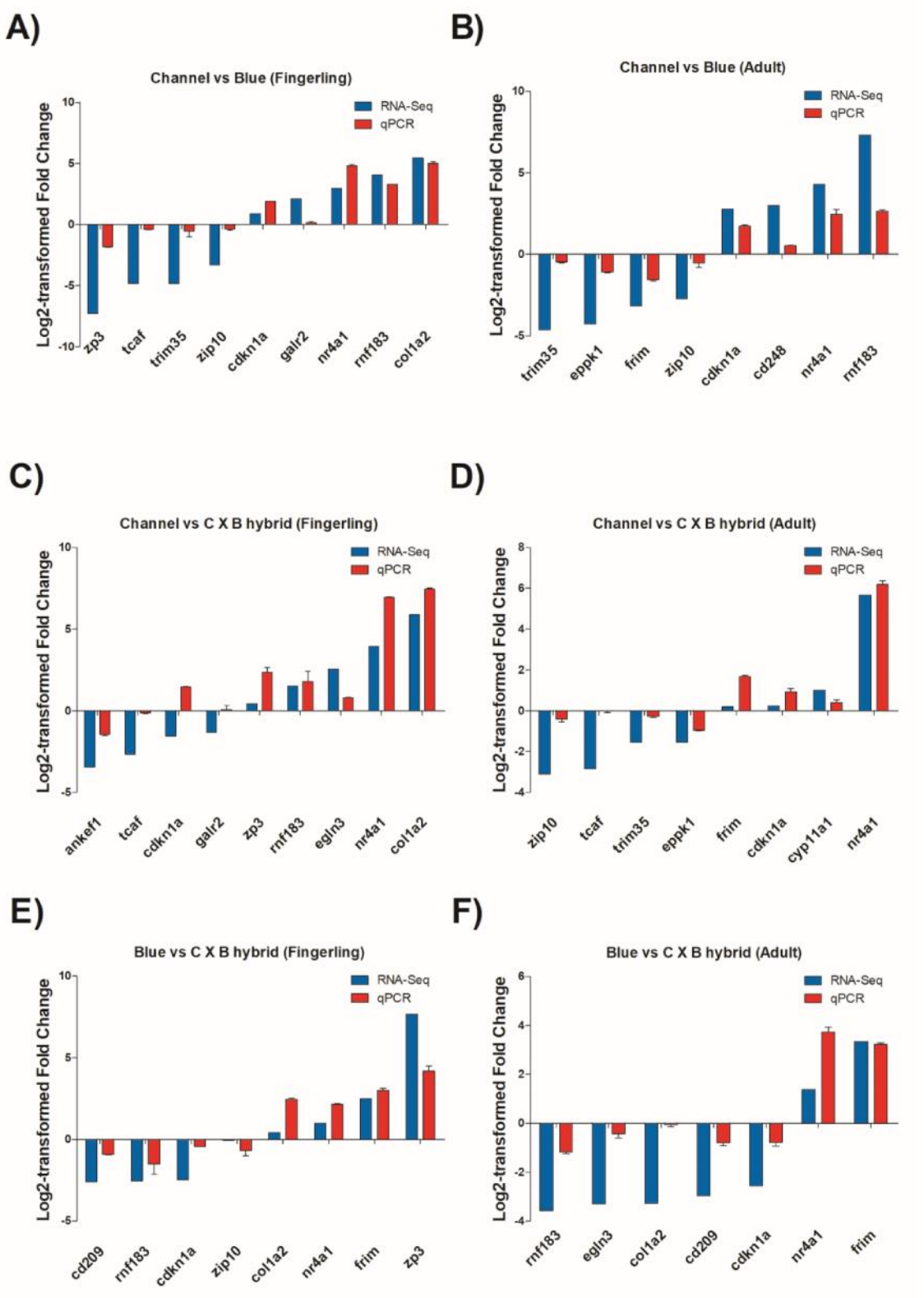
A)
Channel vs Blue (Fingerling)
RNA-Seq
qPCR
Log2-transformed Fold Change
zp3
tcaf
trim35
zip10
cdkn1a
galr2
nr4a1
rnf183
col1a2
B)
Channel vs Blue (Adult)
RNA-Seq
qPCR
Log2-transformed Fold Change
trim35
eppk1
frim
zip10
cdkn1a
cd248
nr4a1
rnf183
C)
Channel vs C X B hybrid (Fingerling)
RNA-Seq
qPCR
Log2-transformed Fold Change
ankef1
tcaf
cdkn1a
galr2
zp3
rnf183
egln3
nr4a1
col1a2
D)
Channel vs C X B hybrid (Adult)
RNA-Seq
qPCR
Log2-transformed Fold Change
zip10
tcaf
trim35
eppk1
frim
cdkn1a
cyp11a1
nr4a1
E)
Blue vs C X B hybrid (Fingerling)
RNA-Seq
qPCR
Log2-transformed Fold Change
cd209
rnf183
cdkn1a
zip10
col1a2
nr4a1
frim
zp3
F)
Blue vs C X B hybrid (Adult)
RNA-Seq
qPCR
Log2-transformed Fold Change
rnf183
egln3
col1a2
cd209
cdkn1a
nr4a1
frim

Figure 6. Scatter plot between RNA-Seq and qPCR result. The positive correlation based on linear model was observed between RNA-Seq and qPCR result: Channel catfish vs Blue catfish (fingerling group, *P*-value=1.21E-03), Channel catfish vs Blue catfish (adult group, *P*-value: 8.92E-04), Channel catfish vs C X B hybrid catfish (fingerling group, *P*-value: 1.63E-03), Channel catfish vs C X B hybrid catfish (adult group, *P*-value: 1.28E-03), Blue catfish vs C X B hybrid catfish (fingerling group, *P*-value: 3.56E-03), Blue catfish vs C X B hybrid catfish (adult group, *P*-value: 1.62E-03).

Figure 6

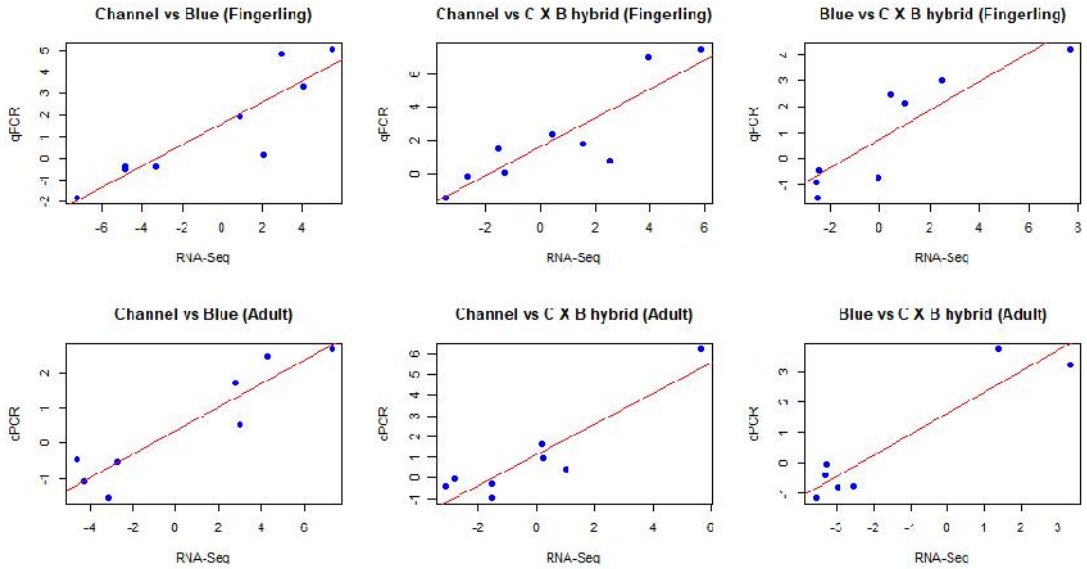

2.5 Discussion

Catfish serve as a good model to investigate the swimbladder morphology, as great variations in morphology of the swimbladder were found among three genetic types of catfish. The great variations in morphology of the swimbladder among three genetic types of catfish might be associated with their hydrostatic function, the variation in the center of gravity, their behavior, and the mode of life (Horn, 1975; Whitehead and Blaxter, 1989). In this study, over

4,000 genes were identified as DEGs by comparing swimbladder transcriptomes of channel catfish, blue catfish and C×B hybrid catfish. Overall, the number of DEGs identified in fingerlings was larger than that in adult fish. The low number of significant DEGs identified between blue and C×B hybrid catfish suggested that the swimbladder transcriptomes are only minimally different between blue and C×B hybrid catfish at both fingerling and adult stages. The heatmap result also supported this assumption (**Figure 3**), which displays the overall expression profiles for swimbladder transcriptomes of channel, blue, and C×B hybrid catfish. Interestingly, the swimbladder of blue catfish was clustered with that of C×B hybrid catfish, whereas the swimbladder of channel catfish itself separates in another cluster. Therefore, the results of hierarchical clustering suggested that the overall expression profiles of swimbladder transcriptomes in C×B hybrid catfish is more similar to those of blue catfish than of channel catfish. One of the explanations might be paternal predominance in C×B hybrid catfish because the blue catfish was used as the paternal parent of the hybrid. Paternal predominance was evident in the shape of swimbladder, more specifically, the swimbladder of C×B hybrid catfish is more similar to that of their male parent (blue catfish) than to their female parent (channel catfish) (Dunham et al., 1982). In addition to the shape of swimbladder, the external appearance and anal fin ray number of hybrids are also more similar to their male parent (Dunham et al., 1982). Other than morphological traits, performance traits, such as growth, morphometric uniformity and susceptibility to capture by seine, are also more influenced by the male parent than the female parent (Dunham et al., 1982).

Enrichment analysis can often provide insights into genes involved in various functions. Here the enrichment analysis, along with annotation and literature searches, allowed

representative key genes to be arranged into five broad categories, including Wnt signaling pathway, Hedgehog signaling pathway, branching genes in morphogenesis, ECM-receptor interaction, and cell adhesion molecules (CAMs) (**Table 5**). Collectively, these categories of genes, and their differential expression, suggested their potential roles in shaping the swimbladder into single- or bi-chambered swimbladders. Putative pathways involved in formation of posterior chamber in catfish swimbladder is illustrated in the context of a diagram (**Figure 7**). The putative functional roles and interaction of these signaling pathways are discussed below.

A number of genes involved in Wnt signaling pathway were significantly differentially expressed in fingerlings. Wnt signaling pathway was demonstrated to be involved both in mammalian lung development (Pongracz and Stockley, 2006) and early development of zebrafish swimbladder (Yin et al., 2011). The conserved role of Wnt signaling in branching morphogenesis between lung and swimbladder have been highlighted in some previous studies (Dean et al., 2005; Yin et al., 2011). For instance, the swimbladder develops into bi-chambered through formation of budding of the anterior chamber in zebrafish (Robertson et al., 2007). The budding of second chamber primordium in zebrafish swimbladder was demonstrated as a simplified form of branching morphogenesis similar to that in mammalian lung (Winata et al., 2009), suggesting roles of Wnt signaling pathway in specification and morphogenesis of the bud of anterior chamber of swimbladder in zebrafish (Yin et al., 2011).

In our study, *wnt1*, *wnt2*, *wnt9b* and *wnt10b* were expressed at higher level in blue catfish than channel catfish with a log-fold-change of 2.66, 2.52, 2.43 and 4.49, respectively. The gene *wnt1* was reported to positively regulate the branching morphogenesis of epithelial ducts during

development of mammary gland (Uyttendaele et al., 1998). Similarly, *wnt2* was highly expressed in microdissected terminal end bud (TEB), which was a putative regulator of branching morphogenesis in the mammary gland (Kouros-Mehr and Werb, 2006). Even though *wnt9b* and *wnt10b* have not been associated with branching morphogenesis in mammalian gland, they are ligands that specifically regulates the canonical Wnt signaling pathway (Many and Brown, 2014; Wend et al., 2012). In the present study, data seemed to indicate that canonical Wnt signaling pathway might be involved in posterior chamber of catfish bi-chambered swimbladder. Canonical Wnt signaling pathway is demonstrated to inhibit branching morphogenesis of the lung and lacrimal gland (Dean et al., 2005). The canonical Wnt pathway causes an accumulation of β-catenin in the cytoplasm and its eventual translocation into the nucleus to act as a transcriptional coactivator of transcription factors (Huelsken and Behrens, 2002). β-catenin would be degraded by a destruction complex, including *axin*, adenomatosis polyposis coli (*apc*), and glycogen synthase kinase 3 (*gsk3*) (MacDonald et al., 2009). *Axin* and *apc* were expressed at higher level in bi-chambered swimbladder than single-chambered swimbladder, which would degrade β-catenin therefore inactivate the canonical Wnt signaling pathway to regulate branching morphogenesis.

Several additional members in Wnt signaling pathway were identified as DEGs among the catfish swimbladder transcriptomes. The activation of *nfatc1* can cause primary defects in branching morphogenesis in kidney (Guo et al., 2015). In the present study, *nfatc4* were expressed at slightly lower levels in blue catfish than in channel catfish, suggesting the potential role of *nfatc4* in inhibiting budding of second chamber primordium in swimbladder. Moreover, the expression of another interesting gene *rac2* was lower in blue catfish than in channel catfish

in fingerlings, with a log fold change of -2.30. The switching of *rac* between active and inactive states promotes turnover of the complex containing E-Cadherin at the cell junction, and maintains the plasticity of the tracheal epithelium to allow branching morphogenesis (Chihara et al., 2003). In addition to these genes, other members in Wnt signaling pathway with crucial roles in morphogenesis of swimbladder were identified as DEGs, such as *dkk1*, frizzled receptors (*fzd7-a*) (Yin et al., 2011). Several regulators of Wnt signaling pathway, including *notum*, *porcn*, *sfrp5*, and *pedf*, were also identified as DEGs (Caricasole et al., 2002; Kakugawa et al., 2015; Kongkham et al., 2010; Park et al., 2011). Taken together, the abundance of members in Wnt signaling pathway identified in our comparative transcriptome analysis suggests the involvement and significance of Wnt signaling pathway in swimbladder morphogenesis.

Smad4, a downstream gene in TGF-beta and BMP signaling pathway, was expressed at lower level in blue catfish (bi-chambered swimbladder) than in channel catfish (single-chambered swimbladder) in fingerlings (**Table 5**). TGF-beta and BMP signaling pathway also play critical roles to drive early embryonic distal lung branching morphogenesis (Warburton et al., 2005). *Smad4* has been demonstrated to negatively regulate embryonic lung branching (Zhao et al., 1998). Zhao et al. have found that abrogation of *smad4* with antisense oligodeoxynucleotide resulted in increased branching morphogenesis (Zhao et al., 1998). Therefore, the high expression of *smad4* might inhibit the budding of second chamber primordium in channel catfish.

A number of members in Hedgehog signaling pathway were identified as differentially expressed genes between single- and bi-swimbladder, including *shhb* and *smo*. Hedgehog

signaling pathway is required for lung development in mammals (Pepicelli et al., 1998) and *Xenopus laevis* (Yin et al., 2010), which is also highlighted in zebrafish swimbladder development (Winata et al., 2009). Hedgehog signaling pathway is required in specification and organization of the three tissue layers in development of zebrafish swimbladder (Winata et al., 2009). In mammalian lung, the mutant of sonic hedgehog (*shh*) failed to branch beyond primary budding, suggesting its involvement in branching morphogenesis in the lung development (Bellusci et al., 1997b; Pepicelli et al., 1998). In zebrafish, mutations in *shha* and *ihha* resulted in prominent reduction of epithelium and deficient differentiation of smooth muscle (Winata et al., 2009). *Smo* was also expressed at higher level in bi-chambered swimbladder than in single-chambered swimbladder in both fingerlings and adults (**Table 5**). As a positive transducer of Hedgehog signaling pathway, *smo* can initiate the signaling cascade, activating transcriptional targets of the Hedgehog signaling pathway (Chuang et al., 2003). The mutation in the Hedgehog co-receptor *smoothened* (*smo*) caused the absence of Hedgehog signaling pathway (Barresi et al., 2000) and missing of epithelium and mesenchymal layer in zebrafish swimbladder (Winata et al., 2009), suggesting that *smo* is essential for swimbladder morphogenesis.

Two important growth factors (*fgf10* and *igf-1*) for lung branching morphogenesis were identified as differentially expressed genes among the catfish transcriptomes. In the present study, *fgf10* was expressed at significantly higher level in blue catfish (bi-chambered swimbladder) than channel catfish (single-chambered swimbladder) with a log fold change of 3.22. Bellusci et al. reported the involvement of the *fgf10* in branching morphogenesis (Bellusci et al., 1997b). In both the developing mammalian lung and *Drosophila* tracheal system, the

fibroblast growth factor (FGF) signaling pathway is required for successive rounds of branching (Metzger and Krasnow, 1999). In a previous study, the expression of the *fgf10* gene was closely associated with key events in branching morphogenesis during early lung development (Bellusci et al., 1997b). *Fgf10* was suggested as an inducer of new bud formation (Bellusci et al., 1997b). Thus, in our study, the high expression levels of *fgf10* might be required for budding of second chamber primordium and posterior chamber formation in fish swimbladder. Hedgehog signaling pathway modulates the expression levels of branching gene *fgf10* (Fernandes-Silva et al., 2017). The expression of *fgf10* is allowed in the growing mesenchymal tip (Fernandes-Silva et al., 2017). However, in the interbud/non-branching regions, Hedgehog signaling pathway is active and represses *fgf10* expression (Fernandes-Silva et al., 2017). Moreover, the expression of another growth factor *igf-1* was higher in blue catfish (bi-chambered swimbladder) and channel catfish (single-chambered swimbladder) in fingerlings and adult fish (**Table 5**). *Igf-1* is essential for terminal end bud formation and ductal morphogenesis during mammary development (Ruan and Kleinberg, 1999). The deficiency of *igf-1* resulted in the reduction of mammary gland branching morphogenesis (Richards et al., 2004), suggesting that *igf-1* is important for mammary branching morphogenesis. The high expression of *igf-1* might be also important for posterior chamber formation in bi-chambered swimbladder.

Many genes associated with extracellular matrix (ECM)-receptor interaction, cell adhesion molecules (CAMs) were identified as DEGs between single-chambered and bi-chambered swimbladder. The ECM, ECM-receptors, ECM-degrading enzymes and their inhibitors are involved in regulation of mouse mammary gland branching morphogenesis (Fata

et al., 2003). The ECM is mainly composed of two types, collagen genes and laminins. In our study, except *col6a4* and *col9a2*, most of these collagen genes (e.g. *col1a1*, *col1a2*, *col4a2*, *col6a1*, *col6a2*, and *col6a6*) and laminins (*lama1*, *lama3*, *itgb3*, *itgb4*) were expressed at relatively higher level in bi-chambered swimbladders (blue catfish and C×B hybrid catfish) than single-chambered swimbladders (channel catfish). In previous studies (refs), both collagen genes and laminins have been reported to play crucial role in branching morphogenesis. For instance, the collagen biosynthesis, extracellular collagen presence, and branching morphogenesis have strong correlations in embryonic lung and salivary gland morphogenesis (Spooner and Faubion, 1980). Additionally, laminin-1 (*lama1*) exert significant role in branching morphogenesis of mouse salivary gland (Hosokawa et al., 1999). Laminin subunit alpha 5 (*lama5*) also has a crucial role for epithelial branching morphogenesis (Kadoya et al., 2003). Moreover, claudin genes (*cldn4*, *cldn19*, and *cldn20*), were expressed at higher level in bi-chambered swimbladder than single-chambered swimbladder. *Cldn4* was expressed at the apico-lateral membrane of epithelial cells in the centre of the branching cords during human salivary gland branching morphogenesis with high intensity (Lourenço et al., 2007).

Branching morphogenesis is involved in many organ development, such as the salivary glands, lungs, pancreas, prostate glands, kidneys, and mammary glands (Noguchi et al., 2006). Many signaling molecules including growth factors and extracellular matrices have been found in previous studies to play crucial roles in branching morphogenesis (Davies, 2002). As discuss above, many members in Wnt and Hedgehog signaling pathways and ECM-receptor interaction with crucial functions in branching morphogenesis were highlighted in our study, suggesting their potential roles in budding of posterior chamber primordium. The conserved elements were

detected between branching morphogenesis in mammary glands and budding of second chamber primordium in bi-chambered swimbladder. The candidate genes and pathways identified in this study will provide molecular evidence of the budding of posterior chamber primordium and formation of posterior chamber in fish species and provide the resources to study the molecular mechanism in single- and bi-chambered swimbladder.

Figure 7. Putative presentation of gene pathways involved in formation of posterior chamber in catfish swimbladder based on RNA-seq expression signatures. The putative diagram includes: 1) The switching of canonical Wnt signaling pathway regulates branching morphogenesis through destruction complex (*axin*, *apc*, *gsk3*). β-catenin would be degraded by the destruction complex to allow branching morphogenesis. 2) The switching of *rac* between active and inactive states allows branching morphogenesis. 3) The downstream gene of TGF-β and BMP signaling pathway, *smad4* negatively regulates branching morphogenesis. 4) *Fgf10* exert potential roles in branching morphogenesis and new bud formation. 5) *Igf-1* exert potential roles in branching morphogenesis and new bud formation. 6) Hedgehog signaling pathway modulates branching morphogenesis via mediating the expression levels of branching morphogenesis related gene, such as *fgf10*.

Figure 7

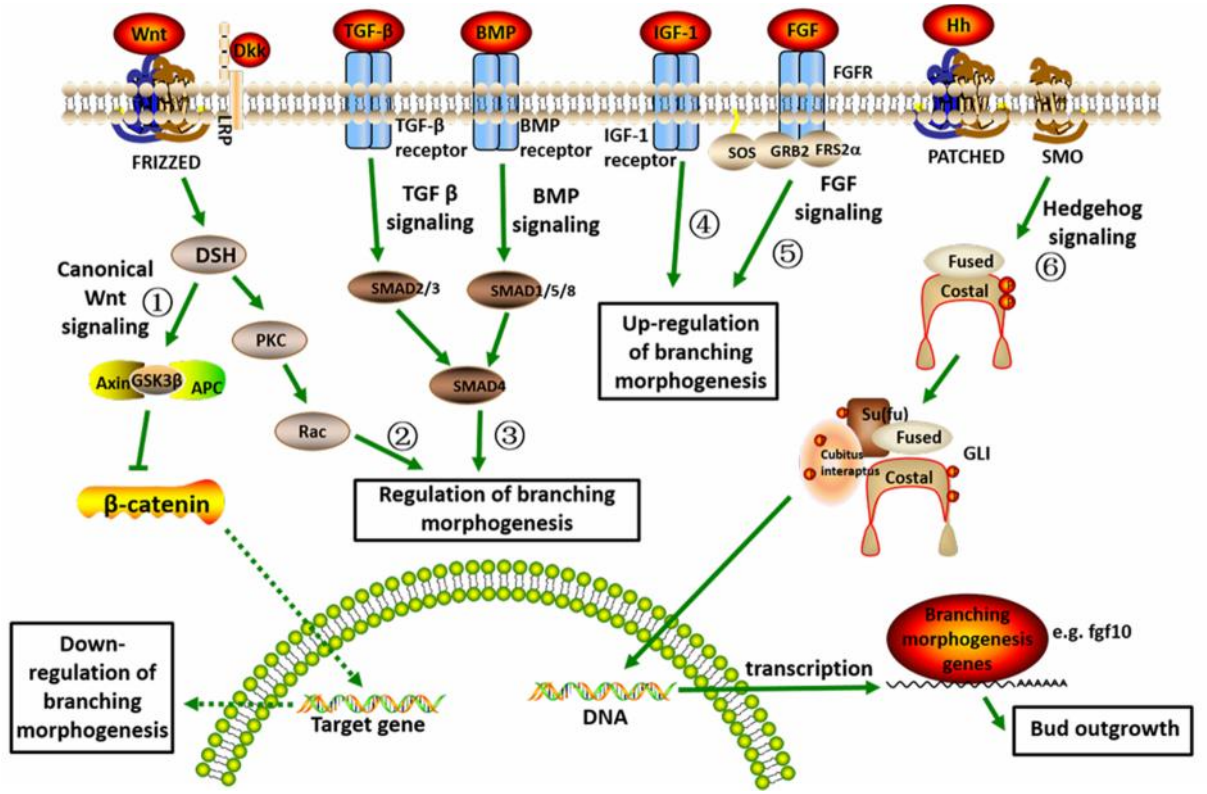
Wnt
Dkk
LRP
FRIZZED
TGF-β
BMP
IGF-1
FGF
FGFR
Hh
TGF-β receptor
BMP receptor
IGF-1 receptor
SOS
GRB2
FRS2α
PATCHED
SMO
TGF β signaling
BMP signaling
FGF signaling
Hedgehog signaling
④
⑤
⑥
DSH
Canonical Wnt signaling ①
SMAD2/3
SMAD1/5/8
Fused
Costal
PKC
Up-regulation of branching morphogenesis
Axin
GSK3β
APC
SMAD4
Su(fu)
Fused
Cubitus interaptus
Costal
GLI
Rac
②
③
β-catenin
Regulation of branching morphogenesis
Down-regulation of branching morphogenesis
Target gene
DNA
transcription
Branching morphogenesis genes
e.g. fgf10
Bud outgrowth

References

Alexander, R., 1966. Physical aspects of swimbladder function. Biol. Rev. 41, 141-176.

Anders, S., Pyl, P.T., Huber, W., 2014. HTSeq–a Python framework to work with high-throughput sequencing data. Bioinformatics, btu638.

Barresi, M., Stickney, H.L., Devoto, S.H., 2000. The zebrafish slow-muscle-omitted gene product is required for Hedgehog signal transduction and the development of slow muscle identity. Development 127, 2189-2199.

Bauer, S., Grossmann, S., Vingron, M., Robinson, P.N., 2008. Ontologizer 2.0—a multifunctional tool for GO term enrichment analysis and data exploration. Bioinformatics 24, 1650-1651.

Bellusci, S., Furuta, Y., Rush, M.G., Henderson, R., Winnier, G., Hogan, B., 1997a. Involvement of Sonic hedgehog (Shh) in mouse embryonic lung growth and morphogenesis. Development 124, 53-63.

Bellusci, S., Grindley, J., Emoto, H., Itoh, N., Hogan, B., 1997b. Fibroblast growth factor 10 (FGF10) and branching morphogenesis in the embryonic mouse lung. Development 124, 4867-4878.

Caricasole, A., Ferraro, T., Rimland, J.M., Terstappen, G.C., 2002. Molecular cloning and initial characterization of the MG61/PORC gene, the human homologue of the Drosophila segment polarity gene Porcupine. Gene 288, 147-157.

Chihara, T., Kato, K., Taniguchi, M., Ng, J., Hayashi, S., 2003. Rac promotes epithelial cell rearrangement during tracheal tubulogenesis in Drosophila. Development 130, 1419-1428.

Chuang, P.-T., Kawcak, T.N., McMahon, A.P., 2003. Feedback control of mammalian

Hedgehog signaling by the Hedgehog-binding protein, Hip1, modulates Fgf signaling during branching morphogenesis of the lung. Genes Dev. 17, 342-347.

Conesa, A., Götz, S., García-Gómez, J.M., Terol, J., Talón, M., Robles, M., 2005. Blast2GO: a universal tool for annotation, visualization and analysis in functional genomics research. Bioinformatics 21, 3674-3676.

Davies, J.A., 2002. Do different branching epithelia use a conserved developmental mechanism? Bioessays 24, 937-948.

Dean, C.H., Miller, L.-A.D., Smith, A.N., Dufort, D., Lang, R.A., Niswander, L.A., 2005. Canonical Wnt signaling negatively regulates branching morphogenesis of the lung and lacrimal gland. Dev. Biol. 286, 270-286.

Dobin, A., Davis, C.A., Schlesinger, F., Drenkow, J., Zaleski, C., Jha, S., Batut, P., Chaisson, M., Gingeras, T.R., 2013. STAR: ultrafast universal RNA-seq aligner. Bioinformatics 29, 15-21.

Dunham, R., Smitherman, R., Brooks, M., Benchakan, M., Chappell, J., 1982. Paternal predominance in reciprocal channel-blue hybrid catfish. Aquaculture 29, 389-396.

Dunham, R.A., Masser, M.P., 2012. Production of hybrid catfish. Southern Regional Aquaculture Center.

Fata, J.E., Werb, Z., Bissell, M.J., 2003. Regulation of mammary gland branching morphogenesis by the extracellular matrix and its remodeling enzymes. Breast Cancer Res. 6, 1-11.

Fernandes-Silva, H., Correia-Pinto, J., Moura, R.S., 2017. Canonical Sonic Hedgehog Signaling in Early Lung Development. J. Dev. Biol. 5, 3.

Finney, J.L., Robertson, G.N., McGee, C.A., Smith, F.M., Croll, R.P., 2006. Structure and autonomic innervation of the swim bladder in the zebrafish (Danio rerio). J. Comp. Neurol. 495, 587-606.

Gregory, D., Waldbieser, G., Bosworth, B., 2004. Cloning and characterization of myogenic regulatory genes in three Ictalurid species. Anim. Genet. 35, 425-430.

Grom, K., 2015. Comparative anatomical study of swimbladder in different species of fish. Scientific Works. Series C. Veterinary Medicine 61, 156-160.

Grossmann, S., Bauer, S., Robinson, P.N., Vingron, M., 2007. Improved detection of overrepresentation of Gene-Ontology annotations with parent–child analysis. Bioinformatics 23, 3024-3031.

Guo, Q., Tripathi, P., Manson, S.R., Austin, P.F., Chen, F., 2015. Transcriptional dysregulation in the ureteric bud causes multicystic dysplastic kidney by branching morphogenesis defect. J. Urol. 193, 1784-1790.

Horn, M.H., 1975. Swim− bladder state and structure in relation to behavior and mode of life in stromateoid fishes. Fish. Bull. 73, 95-109.

Hosokawa, Y., Takahashi, Y., Kadoya, Y., Yamashina, S., Nomizu, M., Yamada, Y., Nogawa, H., 1999. Significant role of laminin-1 in branching morphogenesis of mouse salivary epithelium cultured in basement membrane matrix. Dev. Growth Diffe. 41, 207-216.

Hsia, C.C., Schmitz, A., Lambertz, M., Perry, S.F., Maina, J.N., 2013. Evolution of air breathing: oxygen homeostasis and the transitions from water to land and sky. Compr. Physiol. 3, 849-915.

Huelsken, J., Behrens, J., 2002. The Wnt signalling pathway. J. Cell Sci. 115, 3977-3978.

Kadoya, Y., Mochizuki, M., Nomizu, M., Sorokin, L., Yamashina, S., 2003. Role for laminin-α5 chain LG4 module in epithelial branching morphogenesis. Dev. Biol. 263, 153-164.

Kakugawa, S., Langton, P.F., Zebisch, M., Howell, S.A., Chang, T.-H., Liu, Y., Feizi, T., Bineva, G., O'Reilly, N., Snijders, A.P., Jones, E.Y., Vincent, J.-P., 2015. Notum deacylates Wnt proteins to suppress signalling activity. Nature 519, 187-192.

Kanehisa, M., Sato, Y., Morishima, K., 2016. BlastKOALA and GhostKOALA: KEGG tools for functional characterization of genome and metagenome sequences. J. Mol. Biol. 428, 726-731.

Kongkham, P., Northcott, P., Croul, S., Smith, C., Taylor, M., Rutka, J., 2010. The SFRP family of WNT inhibitors function as novel tumor suppressor genes epigenetically silenced in medulloblastoma. Oncogene 29, 3017-3024.

Kouros-Mehr, H., Werb, Z., 2006. Candidate regulators of mammary branching morphogenesis identified by genome-wide transcript analysis. Dev. Dyn. 235, 3404-3412.

Lechner, W., Ladich, F., 2008. Size matters: diversity in swimbladders and Weberian ossicles affects hearing in catfishes. J. Exp. Biol. 211, 1681-1689.

Liu, Z.J., Liu, S.K., Yao, J., Bao, L.S., Zhang, J.R., Li, Y., Jiang, C., Sun, L.Y., Wang, R.J., Zhang, Y., Zhou, T., Zeng, Q.F., Fu, Q., Gao, S., Li, N., Koren, S., Jiang, Y.L., Zimin, A., Xu, P., Phillippy, A.M., Geng, X., Song, L., Sun, F.Y., Li, C., Wang, X.Z., Chen, A.L., Jin, Y.L., Yuan, Z.H., Yang, Y.J., Tan, S.X., Peatman, E., Lu, J.G., Qin, Z.K., Dunham, R., Li, Z.X., Sonstegard, T., Feng, J.B., Danzmann, R.G., Schroeder, S., Scheffler, B., Duke, M.V., Ballard, L., Kucuktas, H., Kaltenboeck, L., Liu, H.X., Armbruster, J., Xie, Y.J., Kirby, M.L., Tian, Y., Flanagan, Elizabeth M., Mu, W.J., Waldbieser, G.C., 2016. The channel

catfish genome sequence provides insights into the evolution of scale formation in teleosts. Nat. Commun. 7, 11757.

Lourenço, S.V., Coutinho-Camillo, C.M., Buim, M.E., Uyekita, S.H., Soares, F.A., 2007. Human salivary gland branching morphogenesis: morphological localization of claudins and its parallel relation with developmental stages revealed by expression of cytoskeleton and secretion markers. Histochem. Cell Biol. 128, 361-369.

Love, M.I., Huber, W., Anders, S., 2014. Moderated estimation of fold change and dispersion for RNA-seq data with DESeq2. Genome Biol. 15, 550.

MacDonald, B.T., Tamai, K., He, X., 2009. Wnt/β-catenin signaling: components, mechanisms, and diseases. Dev. Cell 17, 9-26.

Many, A.M., Brown, A.M., 2014. Both canonical and non-canonical Wnt signaling independently promote stem cell growth in mammospheres. PloS One 9, e101800.

Marasco, V., Herzyk, P., Robinson, J., Spencer, K.A., 2016. Pre-and Post-Natal Stress Programming: Developmental Exposure to Glucocorticoids Causes Long-Term Brain-Region Specific Changes to Transcriptome in the Precocial Japanese Quail. J. Neuroendocrinol. 28.

Metzger, R.J., Krasnow, M.A., 1999. Genetic control of branching morphogenesis. Science 284, 1635-1639.

Noguchi, Y., Okamoto, A., Kasama, T., Imajoh-Ohmi, S., Karatsu, T., Nogawa, H., 2006. Lysophosphatidic acid cooperates with EGF in inducing branching morphogenesis of embryonic mouse salivary epithelium. Dev. Dyn. 235, 403-410.

Ockendon, N.F., O'Connell, L.A., Bush, S.J., Monzón-Sandoval, J., Barnes, H., Székely, T.,

Hofmann, H.A., Dorus, S., Urrutia, A.O., 2016. Optimization of next-generation sequencing transcriptome annotation for species lacking sequenced genomes. Mol. Ecol. Resour. 16, 446-458.

Okubo, T., Hogan, B.L., 2004. Hyperactive Wnt signaling changes the developmental potential of embryonic lung endoderm. J. Biol. 3, 11.

Owen, R., 1846. Lectures on the Comparative Anatomy and Physiology of the Vertebrate Animals: Delivered at the Royal College of Surgeons of England, in 1844 and 1846. Longman, Brown, Green, and Longmans.

Park, K., Lee, K., Zhang, B., Zhou, T., He, X., Gao, G., Murray, A.R., Ma, J.-x., 2011. Identification of a novel inhibitor of the canonical Wnt pathway. Mol. Cell. Biol. 31, 3038-3051.

Pepicelli, C.V., Lewis, P.M., McMahon, A.P., 1998. Sonic hedgehog regulates branching morphogenesis in the mammalian lung. Curr. Biol. 8, 1083-1086.

Pongracz, J.E., Stockley, R.A., 2006. Wnt signalling in lung development and diseases. Respir. Res. 7, 15.

Richards, R.G., Klotz, D.M., Walker, M.P., DiAugustine, R.P., 2004. Mammary gland branching morphogenesis is diminished in mice with a deficiency of insulin-like growth factor-I (IGF-I), but not in mice with a liver-specific deletion of IGF-I. Endocrinology 145, 3106-3110.

Robertson, G., McGee, C., Dumbarton, T., Croll, R., Smith, F., 2007. Development of the swimbladder and its innervation in the zebrafish, Danio rerio. J. Morphol. 268, 967-985.

Robinson, M.D., McCarthy, D.J., Smyth, G.K., 2010. edgeR: a Bioconductor package for

differential expression analysis of digital gene expression data. Bioinformatics 26, 139-140.

Rozen, S., Skaletsky, H., 1999. Primer3 on the WWW for general users and for biologist programmers. Bioinformatics methods and protocols, 365-386.

Ruan, W., Kleinberg, D.L., 1999. Insulin-Like Growth Factor I Is Essential for Terminal End Bud Formation and Ductal Morphogenesis during Mammary Development 1. Endocrinology 140, 5075-5081.

Shu, W., Jiang, Y.Q., Lu, M.M., Morrisey, E.E., 2002. Wnt7b regulates mesenchymal proliferation and vascular development in the lung. Development 129, 4831-4842.

Spooner, B.S., Faubion, J.M., 1980. Collagen involvement in branching morphogenesis of embryonic lung and salivary gland. Dev. Biol. 77, 84-102.

Trotter, A., Pankhurst, P., Hart, P., 2001. Swim bladder malformation in hatchery-reared striped trumpeter Latris lineata (Latridae). Aquaculture 198, 41-54.

Uyttendaele, H., Soriano, J.V., Montesano, R., Kitajewski, J., 1998. Notch4 and Wnt-1 proteins function to regulate branching morphogenesis of mammary epithelial cells in an opposing fashion. Dev. Biol. 196, 204-217.

Warburton, D., Bellusci, S., De Langhe, S., Del Moral, P.-M., Fleury, V., Mailleux, A., Tefft, D., Unbekandt, M., Wang, K., Shi, W., 2005. Molecular mechanisms of early lung specification and branching morphogenesis. Pediatr. Res. 57, 26R-37R.

Wend, P., Wend, K., Krum, S., Miranda-Carboni, G., 2012. The role of WNT10B in physiology and disease. Acta Physiol. 204, 34-51.

Whitehead, P., Blaxter, J., 1989. Swimbladder form in clupeoid fishes. Zool. J. Linn. Soc. 97,

299-372.

Winata, C.L., Korzh, S., Kondrychyn, I., Zheng, W., Korzh, V., Gong, Z., 2009. Development of zebrafish swimbladder: The requirement of Hedgehog signaling in specification and organization of the three tissue layers. Dev. Biol. 331, 222-236.

Yin, A., Korzh, S., Winata, C.L., Korzh, V., Gong, Z., 2011. Wnt signaling is required for early development of zebrafish swimbladder. PloS One 6, e18431.

Yin, A., Winata, C.L., Korzh, S., Korzh, V., Gong, Z., 2010. Expression of components of Wnt and Hedgehog pathways in different tissue layers during lung development in Xenopus laevis. Gene Expr. Patterns 10, 338-344.

Zeng, Q., Liu, S., Yao, J., Zhang, Y., Yuan, Z., Jiang, C., Chen, A., Fu, Q., Su, B., Dunham, R., Liu, Z., 2016. Transcriptome Display During Testicular Differentiation of Channel Catfish (Ictalurus punctatus) as Revealed by RNA-Seq Analysis. Biol. Reprod. 95, 19.

Zhao, J., Lee, M., Smith, S., Warburton, D., 1998. Abrogation of Smad3 and Smad2 or of Smad4 gene expression positively regulates murine embryonic lung branching morphogenesis in culture. Dev. Biol. 194, 182-195.

Zheng, W., Wang, Z., Collins, J.E., Andrews, R.M., Stemple, D., Gong, Z., 2011. Comparative transcriptome analyses indicate molecular homology of zebrafish swimbladder and mammalian lung. PloS One 6, e24019.

Chapter 3 Comparative transcriptome analysis of the swimbladder reveals expression signatures in response to low oxygen stress in channel catfish, *Ictalurus punctatus*.

3.1 Abstract

Channel catfish is the leading aquaculture species in the US, and one of the reasons for its application in aquaculture is its relatively high tolerance against hypoxia. However, hypoxia can still cause huge economic losses to the catfish industry. Studies on hypoxia tolerance, therefore, are important for aquaculture. Fish swimbladder has been considered as an accessory respiration organ surrounded by a dense capillary countercurrent exchange system. In this regard, we conducted RNA-Seq analysis with swimbladder samples of catfish under hypoxic and normal conditions to determine if swimbladder was responsive to low oxygen treatment, and to reveal genes, their expression patterns and pathways involved in hypoxia responses in catfish. A total of 155 differentially expressed genes (DEGs) were identified from swimbladder of adult catfish, whereas a total of 2,127 DEGs were identified from swimbladder of fingerling catfish, under hypoxic condition as compared to untreated controls. Subsequent pathway analysis revealed that many DEGs under hypoxia were involved in HIF signaling pathway (*nos2*, *eno2*, *camk2d2*, *prkcb*, *cdkn1a*, *eno1*, and *tfrc*), MAPK signaling pathway (voltage-dependent calcium channel subunit genes), PI3K/Akt/mTOR signaling pathway (*itga6*, *g6pc*, and *cdkn1a*), Ras signaling pathway (*efna3* and *ksr2*), and signaling by VEGF (*fn1*, *wasf3*, and *hspb1*) in catfish swimbladder. This study provided insights into regulation of gene expression and their involved gene pathways in catfish swimbladder in response to low oxygen stresses.

3.2 Background

Oxygen is essential for the life of all aerobic organisms. Compared to terrestrial animals, fish have evolved various behavioral and physiological adaptions, enabling them to effectively utilize low levels of dissolved oxygen in aquatic environment. The strategies of behavioral adaptions include reduced spontaneous locomotor activity (Nilsson et al., 1993) and shifting the respiratory mode from strictly water air breathing to surface air breathing (Kramer and McClure, 1982). The physiological adaptions include the changes of metabolic rate and enzymatic activities, and improved ventilation with extremely large gill surface areas (Burggren and Cameron, 1980; Jensen et al., 1993). Hypoxia is frequent for aquaculture fish species, and can adversely affect their performance traits and survival. Catfish is one of the major aquaculture species in the United States. In spite of its strong tolerance to low dissolved oxygen, hypoxia can cause enormous economic losses in catfish industry. In addition to high mortalities, hypoxia can have negatively effects on the immune system, leading to increased susceptibility to infectious diseases (Geng et al., 2014; Kvamme et al., 2013; Welker et al., 2007). In catfish industry, aerators are widely used to overcome the hypoxic conditions, but that dramatically increase the energy costs for production. Therefore, studies on hypoxia tolerance are important for aquaculture as well as for understanding physiology.

To maintain oxygen homeostasis, all aerobic organisms can induce oxygen-regulated genes through a series of oxygen sensing and signal transduction pathways (Wenger, 2000). Under hypoxic conditions, they can trigger a hypoxia response centered on the hypoxia-inducible transcription factors to regulate the expression of hypoxia-inducible genes (Bruick, 2003). A number of studies have been performed to analyze the molecular mechanisms of

hypoxia responses. The predominant hypothesis is that the hypoxia response is at the post-transcriptional level through HIF1-α protein, which is degraded under normal oxygen conditions (Cockman et al., 2000; Maxwell et al., 1999; Ohh et al., 2000; Tanimoto et al., 2000). Exposure to hypoxic conditions, HIF1-α can rapidly accumulates and is responsible for the regulation of a wide variety of hypoxia-induced genes (10). Through binding to hypoxia response elements (HREs) in the promoter and enhancer regions of these HIF1 target genes, HIF1-α activates the transcriptional expression of HIF1 target genes in response to low oxygen stress (Bracken et al., 2003; Nikinmaa and Rees, 2005; Semenza, 1999; Semenza et al., 2002). Examples of these target genes were involved in HIF-1 signaling pathway, MAPK signaling pathway, PI3K-Akt signaling pathway, mTOR signaling pathway, Ras signaling pathway, VEGF signaling pathway, and FoxO signaling pathway (Eijkelenboom and Burgering, 2013; Koong et al., 1994; Lee et al., 2007; Mazure et al., 1997; Risau, 1997; Wang et al., 2017b; Zhong et al., 2017). Even though HIF1-α has been reported to be mostly regulated at the post-transcriptional level (Kietzmann et al., 2016; Semenza, 2000), HIF1-α was also found to be transcriptionally regulated in channel catfish under hypoxic conditions (Geng et al., 2014).

Swimbladder is an internal gas-filled organ in teleosts with an overlying capillary network that contributes to respiration (gas exchange), buoyancy control, pressure reception, sound reception and production (Alexander, 1966; Yang et al., 2018b). Beneath capillary system, swimbladder consists of two layers, tunica externa and tunica interna (Helfman et al., 2009). The tunica externa consists of peritoneal investiture and collagenous layer, while tunica interna contains smooth muscle, fibrous layer, and bladder epithelium (Helfman et al., 2009). In swimbladder, epithelial cells, smooth muscle cells, mesenchymal cells, and gas-gland cells are

main types of cell composition (Prem and Pelster, 2001; Winata et al., 2009). Initially, the cells of swimbladder bud are entirely epithelial cells, which originate from the evagination of the foregut (Yue et al., 2015). During the elongation phase of swimbladder development, there are three tissue layers in fish swimbladder: an epithelial layer (epithelial cells), a mesenchymal layer (mesenchymal cells), and an outer mesothelium (mesenchymal cells) (Finney et al., 2006). The inflation phase of swimbladder development mainly involves inflation of the single-chambered swim bladder (presumptive posterior chamber), inflation of the anterior chamber, and development of the bi-chambered swimbladder (Robertson et al., 2007; Winata et al., 2009). Several developmental regulatory genes (*nkx2.1, foxa2, wnt7b, gata6*) have been reported to be associated with the early development of both tetrapod lungs and zebrafish swimbladders (Cass et al., 2013). In catfish swimbladder, a set of branching morphogenesis-related genes (*wnt1, wnt2, nfatc1, rac2, shh, fgf10, igf-1*) were identified to be involved in formation of the second chamber (Yang et al., 2018a). The swimbladder has been hypothesized as an accessory respiratory organ based on the hints as follows: 1) swimbladder has an overlying rich capillary network for gas exchange, 2) swimbladder is connected with pharynx by the ductus pneumaticus and glottis (Potter, 1927). Here in this study, we performed RNA-Seq analysis of swimbladder in fingerlings and adults of channel catfish under normal and hypoxic conditions in order to identify if the catfish swimbladder is involved in response to low oxygen stress. Here we report the transcriptome and expression patterns and their involved pathways in catfish swimbladder in response to low oxygen stresses.

3.3 Material and methods

3.3.1 Experimental animals and tissue collection

The hypoxia treatment was conducted at Auburn University's Fish Genetics Research Unit using channel catfish. All procedures involving the handling and treatment of fish during this study were approved by the Auburn University Institutional Animal Care and Use Committee (AU-IACUC) prior to the initiation of experiments. Tissue samples were collected after euthanasia. All animal procedures were carried out according to the Guide for the Care and Use of Laboratory Animals and the Animal Welfare Act in the United States. Eighteen channel catfish (*Ictalurus punctatus*) adults (average body mass 1008.40g) and eighteen fingerlings (average body mass 52.32g) were randomly obtained from the Auburn University Fish Genetics Facility and acclimated for one week in two separate aquariums [90×60×30 cm (L×W×H)] with flow-through water prior to challenge.

After acclimation, nine fish of both adult and fingerling were randomly taken to another tank as control groups. The remaining channel catfish adults and fingerlings were used as experimental group. The hypoxia challenge started after another period of two hours for acclimation in the tanks, followed with low oxygen challenge. The samples from the control and the challenge group were taken simultaneously two hours after the start of the hypoxia challenge. Sodium sulfite was used to reduce the dissolved oxygen (DO) levels (Jiang et al., 2011) and measurements were made using a dissolved oxygen meter (YSI Model 58, YSI, Ohio, USA). At the beginning of the experiment, the dissolved oxygen concentration was 9.6 mg/L. Because of the low water temperature and limited numbers of fish in tanks, it was difficult to reduce the DO level to a very low level and finally reduce to a concentration of 4.2 mg/L in 2

h. After 2 h hypoxia challenge, each nine fish of adults and fingerlings were collected both from control and hypoxia treatment tanks and euthanized by tricaine methanesulfonate (MS-222) at a concentration of 0.3mg/L. The entire swimbladders of three fish were dissected, gently washed with cold, sterile PBS (phosphate buffer saline) and pooled together as one replicate. Samples were flash-frozen in liquid nitrogen and stored in -80 freezer until RNA extraction.

3.3.2 RNA extraction, library construction and sequencing

Prior to RNA extraction, samples were removed from the -80 freezer and ground to a fine powder in the presence of liquid nitrogen with sterilized mortar and pestle. Total RNA was extracted from tissue powder using the RNeasy Plus Universal Mini kit (Qiagen, CA, USA) following the manufacturer's protocol. RNA concentration and integrity were measured using a Nanodrop 2000 Spectrophotometer (NanoDrop Technologies, USA). Due to the cost of sequencing, equal amounts of RNA for each group from the three replicates were pooled for RNA-Seq library construction. The remaining replicate pools were preserved as biological replicates for qPCR validation.

RNA-Seq was carried out by the HudsonAlpha Genomics Services Lab (Huntsville, AL, USA) with the total mRNA from swimbladder. The cDNA libraries were prepared using the Illumina TruSeq RNA Sample Preparation Kit (Illumina, CA, USA) according to the TruSeq protocol with modifications to capture total mRNA. The libraries were amplified with 15 cycles of PCR and contained TruSeq indexes within the adaptors, specifically indexes 1-4. Finally, amplified library yields were quantified. After KAPA quantitation and dilution, the libraries were clustered four per lane and sequenced on an Illumina Hiseq v4 instrument with 100 bp

paired-end (PE) reads.

3.3.3 Reads mapping and differential expression analysis

FastQC (http://www.bioinformatics.babraham.ac.uk/projects/fastqc/) was used to assess the quality of sequencing data before and after trimming to make sure high-quality sequences were used in subsequent analysis. Raw reads were trimmed by removing adapter sequences and ambiguous nucleotides using Trimmomatic (version 0.32) (Bolger et al., 2014). Specifically, residual Illumina specific adaptors were clipped from the reads, leading and trailing bases with a Phred score less than 3 were removed and the read trimmed if a sliding window average Phred score over 4 bases was less than 15 (Robledo et al., 2014). Only reads where both pairs had a length greater than 30 bp post-filtering were retained.

The recently assembled channel catfish genome (Liu et al., 2016) was used as a reference for read mapping. The genome assembly included 783 Mb in 34,615 contigs and 9,974 scaffolds, with a contig N50 of 77,200 bp and a scaffold N50 of 7,726,806 bp (Liu et al., 2016). Filtered reads were mapped to the catfish reference genome using STAR alignment software (Dobin et al., 2013), allowing 5% mismatch of the mapped length and restricting the minimum 90% of the bases matched to the genome. HTSeq-count (Anders et al., 2015) was used to extract the read counts from the mapping profiles with the recommended mode. Trimmed mean of M-values (TMM) normalization of expression value was conducted using EdgeR (Robinson et al., 2010) for each group to illustrate differences in the mass composition of the RNA-Seq data. Differential expression between treatment and control samples was calculated using EdgeR and resulting p-values were corrected for false discovery rate (FDR). Differentially expressed genes (DEGs) were defined as showing FDR corrected p-value < 0.05 and fold

change > 2. The DEGs were identified and annotated using Blast2GO with an E-value cutoff of E-6. GO Ontology (GO) annotation analysis was performed using Blast2GO with an E-value cutoff of 1E-6 (Conesa et al., 2005). The annotation result was then categorized with respect to Biological Process, Molecular Function, and Cellular Component at level 2.

3.3.4 Gene Ontology and enrichment analysis

In order to identify overrepresented GO annotations in the DEG set compared to the broader reference assembly, GO analysis and enrichment analysis of significantly expressed GO terms was performed using Ontologizer 2.1 (Bauer et al., 2008) using the Parent-Child-Intersection method with a Benjammini-Hochberg multiple testing correction (Grossmann et al., 2007). Go terms for each gene were compared to the overall catfish reference assembly. The threshold was set as FDR value < 0.05. To identify the overrepresented hypoxia response signaling pathways, we perform pathway analysis via a web server for annotation and enrichment analysis, KOBAS 3.0 (Xie et al., 2011). The threshold was set as FDR-corrected value < 0.05. Gene pathway analysis of significant DEGs was carried out with a cutoff of FDR-corrected value < 0.05 based on GO annotation, KEGG tools (BlastKOALA and GhostKOALA) (Kanehisa et al., 2016) and PANTHER database (Mi et al., 2005), Reactome pathway (Croft et al., 2010), as well as manual literature review.

3.3.5 Experimental validation by quantitative real time qRT-PCR

We randomly selected fifteen genes to validate the RNA-seq results in the present study. The specific primers of all these genes were designed by Primer3 software (Rozen and Skaletsky, 1999) and listed in **Table 6**. The specificity of primers was assessed by aligning

with the channel catfish whole genome database (Liu et al., 2016) using BLASTN with E-value of $1e^{-10}$. Reverse transcription was performed using the qScriptTM cDNA Synthesis Kit (Quanta Bioscience, Gaithersburg, MD). All the cDNA products were then diluted to 250 ng/μL. The qPCR was performed using SYBR Green PCR Master Mix on a CFX96 real-time PCR detection system (Bio-Rad, USA). The cycling conditions of qPCR were denaturation, 95 °C/30 s, 40 cycles of 95 °C/5 s, 60 °C/5 s, and 72 °C/5 s. A no-template control was run on all plates. The *gusb* gene was used as an internal reference gene (Zeng et al., 2016). The melting curve analysis was performed to verify that each primer set amplified a single product. The relative expression was analyzed based on the cycle threshold (Ct) values using BIO-RAD CFX Manager Software.

Table 6. Primers used for qPCR validation.

Table 6

Gene	Gene symbol	Primers
Glucuronidase beta	gusb	F: 5'GGATGGGCGCAAACTCATTC R: 5'ACCAGCTCCTTCATGACGAC
Ferritin, middle subunit	frim	F: 5'GCCTCCTACACCTACACCTC R: 5'AACACCTTTGCTTGACGTCC
Collagen alpha-2(I) chain	col1a2	F: 5'ATGGACGAAAAGGAGAGGCT R: 5'GGACCAGTGTTACCATCAGC
Epiplakin	eppk1	F: 5'CAGTTTACAGCCACCGTGTC R: 5'ACAAGCAGTCTAAGGCCAGT
Probable ATP-dependent RNA helicase DDX5	ddx5	F: 5'ACCTGTTACCAGCCATCGTG R: 5'TTGGGAGCTCCTCCGTAGAT
Egl nine homolog 3	egln3	F: 5'CCTCGGTGAAGCAATTGGTC R: 5'ATGGCTTCGGATCCTCTCTC
Hydrocephalus-inducing protein homolog	hydin	F: 5'CTGGAGGTGAACCCAGTGTC R: 5'TGTTCAAACATGCAGCACCG
Voltage-dependent calcium channel gamma-2 subunit	cacng2	F: 5'GTGTACATCTCTGCGGCACT R: 5'GGAAGAGGTCAGCACGTGAG
Dentin sialophosphoprotein like	dsppl	F: 5'GCTAAAGTTCTCAGTGTGAGCC R: 5'ACCGATGATGGCAGAGGAAC
Tripartite motif-containing protein 35	trim35	F: 5'AGCGGCAGATTAAGGAGGAG

		R: 5'GTCTTCGGCTCTCATCTCCT
TRPM8 channel-associated factor homolog	tcaf	F: 5'GCTTTGCTAGCCATGCCATC R: 5'AACACACTTGCGGAACTCCT
Ankyrin repeat and EF-hand domain-containing protein 1	ankef1	F: 5'GAGCTGCAAATTTACCGGCT R: 5'GGACAAGCACCATGAAGCAT
Apolipoprotein A-I	apoa1	F: 5'ATTACAAGGCACGCCTCACT R: 5'CAGCTCCGCATACTTAGGCT
Zona pellucida sperm-binding protein 4	zp4	F: 5'CTCGTACTACAGTGCTGCCG R: 5'ACCCATTCACCAGAAGGTCC
Serine--pyruvate aminotransferase	agxt	F: 5'GAGAACGCGTGGCTGAAATC R: 5'ACTGAGGATTCTCCGTGTGC
H-2 class I histocompatibility antigen, K-K alpha chain	h2-k1	F: 5'ACACTGCAGTTACACCAGGAAT R: 5'CCTGCCTGATCTGTGTGTTTC

3.4 Results

3.4.1 Sequencing and mapping of short expressed reads

RNA-seq analysis was performed to generate the expressed short reads from the catfish swimbladder samples in control group and hypoxia-treated group, and the results are summarized in **Table 7**. A total of approximately 530 million of 100 bp short reads were generated. The short read sequences of control group were deposited at the NCBI Sequence Read Archive (SRA) with BioProject ID PRJNA400910. The short read sequences of hypoxia group were deposited at the NCBI Sequence Read Archive (SRA) with BioProject ID PRJNA419233. After removing very short reads (length < 30 bp), low-quality sequences (quality score < 20), and ambiguous nucleotides, a total of 470 million clean reads were retained for subsequent analysis, which included 238.8 million short reads and 231.0 million short reads from catfish swimbladder in control group and hypoxia-treated group, respectively (**Table 7**). A total of 84.40% (swimbladder of catfish fingerlings in control group), 78.58% (swimbladder of adult catfish in control group), 77.54% (swimbladder of adult catfish in hypoxia-treated group), and 64.50% (swimbladder of catfish fingerlings in hypoxia-treated

group) of trimmed reads were mapped to channel catfish reference genome assembly.

Table 7. Summary of RNA-seq of swimbladder transcriptomes.

Table 7

Groups	No. of raw reads (million)	Total bases of raw data (Gb)	No. of reads after trim (million)	Average length after trim (bp)	Total bases after trim (Gb)
Control					
Adult	139.59	13.96	123.77	97.41	12.06
Fingerling	128.48	12.85	115.06	95.68	11.01
Subtotal	268.07	26.81	238.83	-	23.07
Hypoxia treatment					
Adult	132.9	13.29	117.71	97.39	11.46
Fingerling	128.86	12.89	113.26	97.10	11.00
Subtotal	261.76	26.18	230.97	-	22.46
Total	529.83	52.98	469.80	-	45.53

As shown in **Figure 8**, there are very large differences between expression profiles of swimbladders of fingerlings and of adults. They were separated by the first principal component (PC1) which accounted for 54% of expression variability. Hypoxia treatment had a large impact on expression profiles, but the differences between expression profiles under hypoxic conditions was second to the age of fish, and they were separated by the second principal component (PC2) which represented 35% of expression variability (**Figure 8**). Much greater differences in expression profiles were observed for fingerlings after hypoxia treatment than for adult catfish, suggesting that fingerlings were more sensitive to the hypoxic stress than adult catfish. As PCA analysis only identified the outliers of the pooled swimbladder samples from each group in this study, the expression signatures of individual fish for each condition was not available for PCA analysis.

Figure 8. Principal component analysis (PCA) of swimbladder transcriptomes in adult and fingerling channel catfish under control and hypoxia treatment.

Figure 8

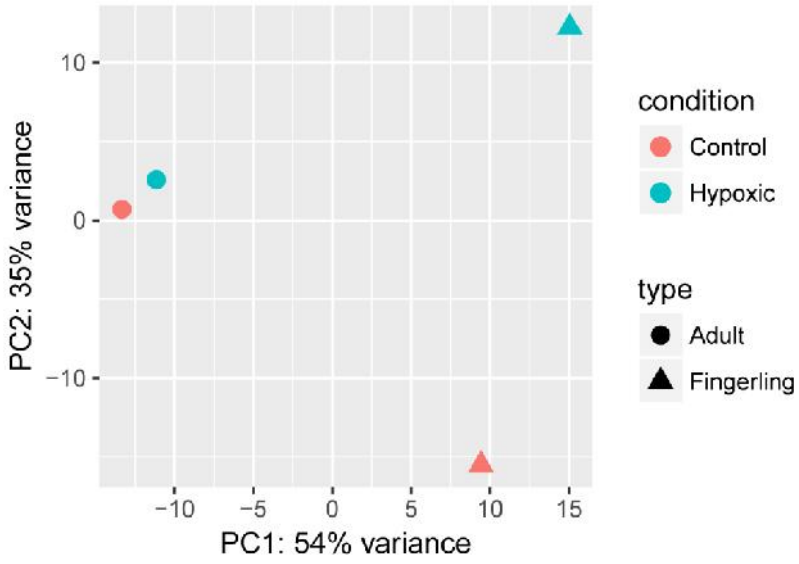

3.4.2 Analysis of differentially expressed genes

In order to identify differentially expressed genes (DEGs) between control and hypoxia-treated catfish swimbladders, pairwise comparisons were performed in catfish fingerlings and adult catfish, respectively. A total of 155 DEGs were identified between control and hypoxia-treated swimbladders of adult catfish, with 77 DEGs up-regulated and 78 DEGs down-regulated in responses to hypoxia treatment (**Table 8**). In contrast, a total of 2,127 DEGs were identified between control and hypoxia-treated swimbladders of catfish fingerlings, with 1,416 DEGs up-regulated and 711 DEGs down-regulated (**Table 8**). Notably, the number of DEGs between control and hypoxia-treated swimbladders of catfish fingerlings was drastically greater than that in adult catfish.

Table 8. Summary of differentially expressed genes in catfish fingerlings and adult catfish

between control and hypoxia-treated group with a cutoff of FDR corrected *P*-value < 0.05 and log-2-fold-change > 2.

Table 8

DEGs	Adult	Fingerling
Up-regulated	77	1,416
Down-regulated	78	711
Total	155	2,127

3.4.3 Analysis of expression signatures, clustering, and go analysis

As shown in **Figure 9**, swimbladder samples of adult catfish in control and hypoxia-treated group were firstly clustered together, and then clustered with that of catfish fingerlings in control group, and finally clustered with that of catfish fingerlings in hypoxia-treated group. Eight clusters of DEGs were identified according to their expression signatures. The identified DEGs between control and hypoxia-treated group were classified according to Gene Ontology (GO) at level 2 (**Figure 10**). In biological processes, cellular process (GO:0009987) and single-organism process (GO:004536899) were the most annotated terms, both taking up more than 25%, respectively. In molecular function category, binding (GO:0005488) and catalytic activity (GO:0003824) were the most two common annotated terms. Under cellular component, cell (GO:0005623), cell part (GO:0044464) and membrane (GO:0016020) were the most common annotation terms. The GO term analysis for each cluster is listed in **Table 9**.

Figure 9. Heatmap display of hierarchical clustering of all differentially expressed genes. The DEGs are displayed in rows while samples are displayed in columns.

Figure 9

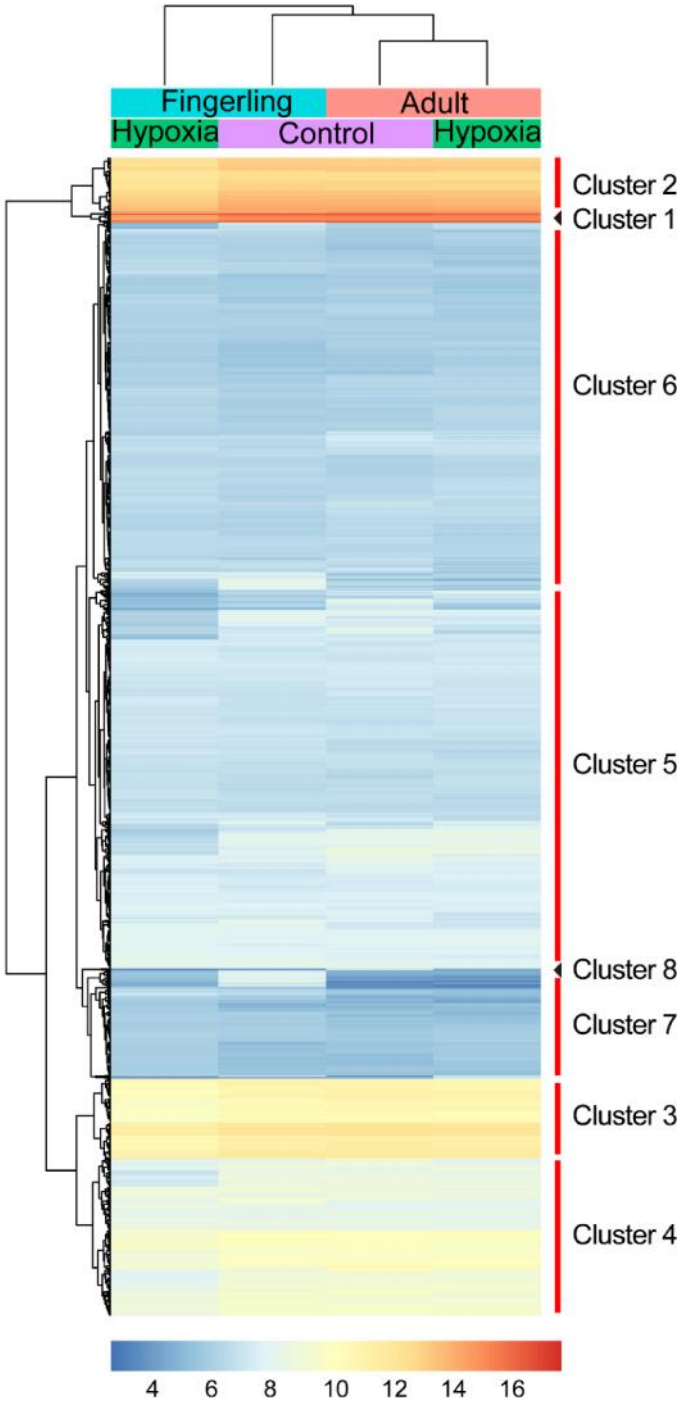

Figure 10. GO term classification of differentially expressed genes in channel catfish swimbladder transcriptomes by BLAST2GO on level 2.

Figure 10

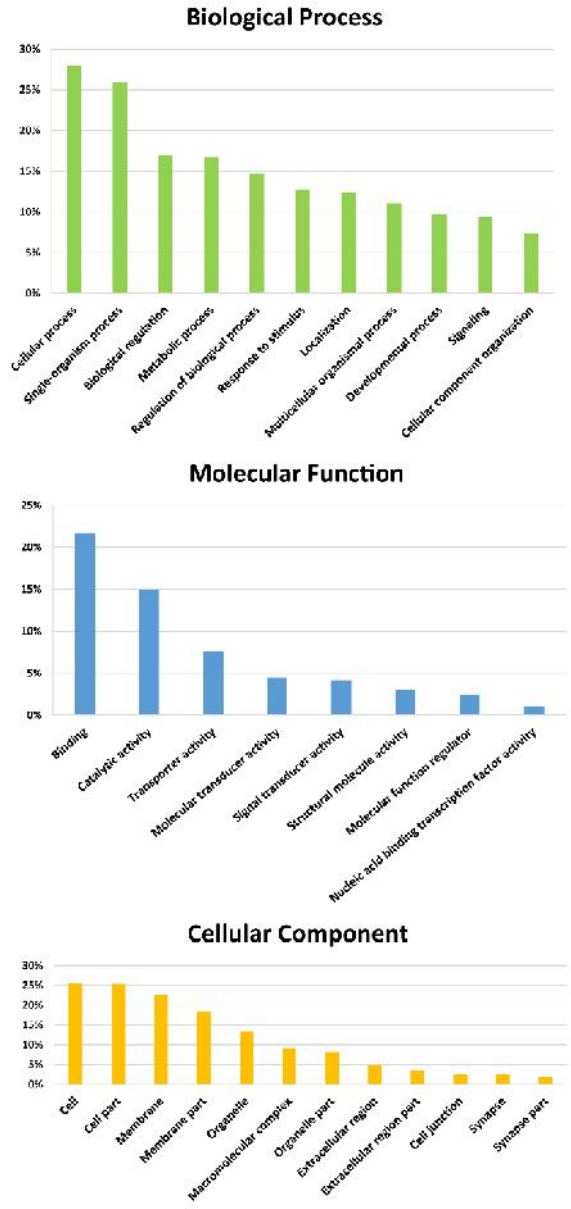

Table 9. Summary of GO enrichment analysis of significantly differentially expressed genes. Population count is the number of GO term associated genes in the population gene set. Study count is the number of GO term associated genes in the differentially expressed gene set. FDR *P* value < 0.05 was considered as significant GO term.

Table 9

GO ID	GO Term	Population count	Study count	*P* value (FDR)
Cluster 1				
GO:0031012	Extracellular matrix	2760	7	1.04E-03
GO:0043062	Extracellular structure organization	9073	4	1.44E-02
Cluster 2				
GO:0005840	Ribosome	8401	67	2.02E-66
GO:0005198	Structural molecule activity	14137	78	2.40E-43
GO:0030529	Intracellular ribonucleoprotein complex	11607	73	2.54E-42
GO:0006412	Translation	6602	53	1.56E-39
GO:0043603	Cellular amide metabolic process	5070	49	2.14E-34
GO:0043604	Amide biosynthetic process	3909	48	4.97E-33
GO:1990904	Ribonucleoprotein complex	3989	58	6.82E-29
GO:1901566	Organonitrogen compound biosynthetic process	5214	51	2.11E-25
GO:0003735	Structural constituent of ribosome	518	46	2.77E-25
GO:1901564	Organonitrogen compound metabolic process	8630	58	3.48E-24
GO:0044391	Ribosomal subunit	8935	67	4.66E-20
GO:0043232	Intracellular non-membrane-bounded organelle	11868	73	1.67E-17
GO:0043228	Non-membrane-bounded organelle	10687	69	2.12E-17
GO:0022626	Cytosolic ribosome	2891	56	2.12E-17
GO:0006518	Peptide metabolic process	1698	49	2.49E-16
GO:0032991	Macromolecular complex	15150	85	6.25E-14
GO:0044445	Cytosolic part	6864	66	1.81E-13
GO:0043043	Peptide biosynthetic process	1204	48	1.54E-12
GO:0019843	Rrna binding	1246	23	1.60E-11
GO:0019538	Protein metabolic process	8468	57	1.36E-09
GO:0044267	Cellular protein metabolic process	7114	54	7.24E-09
GO:0044444	Cytoplasmic part	11607	73	1.96E-07
GO:0003723	RNA binding	3059	24	9.00E-07
GO:0005737	Cytoplasm	11607	73	1.80E-06
GO:0022625	Cytosolic large ribosomal subunit	202	19	2.54E-06
GO:0022613	Ribonucleoprotein complex biogenesis	2217	16	6.49E-06
GO:0030055	Cell-substrate junction	1266	11	9.79E-06

GO:0034660	Ncrna metabolic process	3543	7	1.10E-05
GO:0019083	Viral transcription	2843	5	2.52E-05
GO:0010467	Gene expression	7279	54	4.92E-05
GO:0009058	Biosynthetic process	9019	59	8.03E-05
GO:1901576	Organic substance biosynthetic process	8646	58	8.24E-05
GO:0044249	Cellular biosynthetic process	8283	57	8.24E-05
GO:0034645	Cellular macromolecule biosynthetic process	7439	55	1.25E-04
GO:0009059	Macromolecule biosynthetic process	7937	57	1.87E-04
GO:0044271	Cellular nitrogen compound biosynthetic process	5805	51	2.57E-04
GO:0045047	Protein targeting to ER	467	6	8.97E-04
GO:0031982	Vesicle	9684	27	9.39E-04
GO:0072599	Establishment of protein localization to endoplasmic reticulum	427	5	9.85E-04
GO:0034641	Cellular nitrogen compound metabolic process	8266	57	1.52E-03
GO:0042255	Ribosome assembly	841	12	2.17E-03
GO:0006401	RNA catabolic process	4030	7	2.32E-03
GO:0071826	Ribonucleoprotein complex subunit organization	1325	8	2.58E-03
GO:0006807	Nitrogen compound metabolic process	9019	59	3.09E-03
GO:0070972	Protein localization to endoplasmic reticulum	603	6	3.43E-03
GO:0070161	Anchoring junction	1266	11	4.28E-03
GO:0031012	Extracellular matrix	2760	26	4.80E-03
GO:0010608	Posttranscriptional regulation of gene expression	3226	5	1.28E-02
GO:0006612	Protein targeting to membrane	577	6	1.49E-02
GO:0034470	Ncrna processing	823	7	1.65E-02
GO:0034655	Nucleobase-containing compound catabolic process	4510	9	2.44E-02
GO:0044033	Multi-organism metabolic process	9229	59	2.44E-02
GO:0044421	Extracellular region part	15150	85	3.14E-02
GO:0044183	Protein binding involved in protein folding	6747	22	3.22E-02
GO:0005924	Cell-substrate adherens junction	560	11	3.22E-02
GO:0006450	Regulation of translational fidelity	2677	9	3.53E-02
GO:0044424	Intracellular part	13371	75	4.81E-02
Cluster 3				
GO:0005198	Structural molecule activity	14137	99	5.23E-05
GO:0001968	Fibronectin binding	6747	51	8.85E-05
GO:0043603	Cellular amide metabolic process	5070	30	1.70E-04
GO:0022626	Cytosolic ribosome	2891	29	2.81E-04
GO:0005840	Ribosome	8401	69	2.81E-04
GO:0043604	Amide biosynthetic process	3909	28	2.81E-04
GO:0044445	Cytosolic part	6864	60	3.07E-04

GO:0006412	Translation	6602	47	7.90E-04
GO:0044391	Ribosomal subunit	8935	68	1.23E-03
GO:0005576	Extracellular region	15150	107	1.82E-03
GO:0005509	Calcium ion binding	3462	28	4.18E-03
GO:1901566	Organonitrogen compound biosynthetic process	5214	36	7.59E-03
GO:0002695	Negative regulation of leukocyte activation	652	8	1.14E-02
GO:0050866	Negative regulation of cell activation	3431	28	1.14E-02
GO:0044421	Extracellular region part	15150	107	1.14E-02
GO:0007162	Negative regulation of cell adhesion	3881	30	2.17E-02
GO:0006457	Protein folding	12333	86	2.33E-02
GO:0030036	Actin cytoskeleton organization	1659	13	2.66E-02
GO:0051250	Negative regulation of lymphocyte activation	375	7	3.13E-02
GO:0044444	Cytoplasmic part	11607	76	3.13E-02
GO:0050865	Regulation of cell activation	7957	51	3.87E-02
GO:0032403	Protein complex binding	6796	52	4.32E-02
GO:0045620	Negative regulation of lymphocyte differentiation	261	6	4.67E-02
Cluster 4				
GO:0005576	Extracellular region	15150	211	8.18E-05
GO:0005930	Axoneme	1816	30	1.69E-04
GO:0030286	Dynein complex	1178	13	0.002661426
GO:0044421	Extracellular region part	15150	211	0.003240123
GO:0097014	Ciliary plasm	302	12	0.0090545
GO:0032268	Regulation of cellular protein metabolic process	6175	66	0.0090545
GO:0031982	Vesicle	9684	119	0.010791092
GO:0030031	Cell projection assembly	2599	42	0.015169771
GO:0005577	Fibrinogen complex	4281	84	0.029158885
GO:0033177	Proton-transporting two-sector atpase complex, proton-transporting domain	522	8	0.029158885
GO:0005737	Cytoplasm	11607	144	0.029158885
GO:0044444	Cytoplasmic part	11607	144	0.030552311
GO:0050848	Regulation of calcium-mediated signaling	1245	21	0.031983148
GO:0019932	Second-messenger-mediated signaling	2046	35	0.039452429
GO:0044447	Axoneme part	1344	25	0.039823021
Cluster 5				
GO:0071944	Cell periphery	13371	115	1.47E-05
GO:0005886	Plasma membrane	14080	121	3.25E-05
GO:0044459	Plasma membrane part	14022	120	9.56E-05
GO:0044425	Membrane part	15150	131	1.61E-03
GO:0006811	Ion transport	3745	41	5.04E-03
GO:1990351	Transporter complex	3989	38	7.02E-03
GO:0097458	Neuron part	13371	115	3.42E-02

Cluster 6

GO:0071944	Cell periphery	13371	412	2.49E-19
GO:0044459	Plasma membrane part	14022	437	5.38E-19
GO:0005886	Plasma membrane	14080	437	5.53E-19
GO:1990351	Transporter complex	3989	112	1.42E-15
GO:0042995	Cell projection	13371	412	8.60E-12
GO:0097458	Neuron part	13371	412	3.96E-11
GO:0006811	Ion transport	3745	152	4.01E-11
GO:0005215	Transporter activity	14137	447	6.23E-11
GO:0055085	Transmembrane transport	3745	152	2.58E-10
GO:0098590	Plasma membrane region	7208	282	1.07E-09
GO:0007215	Glutamate receptor signaling pathway	2002	58	3.05E-09
GO:0044425	Membrane part	15150	482	3.13E-09
GO:0034702	Ion channel complex	4258	204	1.52E-08
GO:1902495	Transmembrane transporter complex	5318	241	4.65E-08
GO:0044456	Synapse part	15150	482	8.52E-08
GO:0031226	Intrinsic component of plasma membrane	5841	266	4.72E-07
GO:0042391	Regulation of membrane potential	2672	110	6.10E-07
GO:0005887	Integral component of plasma membrane	5836	266	1.10E-06
GO:0003008	System process	5377	201	1.17E-06
GO:0045202	Synapse	15150	482	1.81E-06
GO:0005509	Calcium ion binding	3462	108	6.14E-06
GO:0099536	Synaptic signaling	1151	67	7.55E-06
GO:0043235	Receptor complex	3989	112	8.45E-06
GO:0098794	Postsynapse	13381	412	1.12E-05
GO:0044297	Cell body	13371	412	1.12E-05
GO:0005231	Excitatory extracellular ligand-gated ion channel activity	737	44	1.20E-05
GO:0044463	Cell projection part	13371	412	1.26E-05
GO:0044708	Single-organism behavior	10647	366	2.51E-05
GO:0044763	Single-organism cellular process	13007	393	3.39E-05
GO:0007610	Behavior	14475	449	3.39E-05
GO:0098878	Neurotransmitter receptor complex	283	26	4.49E-05
GO:0015849	Organic acid transport	2825	103	5.49E-05
GO:0031982	Vesicle	9684	221	6.46E-05
GO:0008066	Glutamate receptor activity	730	44	7.34E-05
GO:0016020	Membrane	15150	482	1.08E-04
GO:0045177	Apical part of cell	13371	412	1.16E-04
GO:0060089	Molecular transducer activity	14137	447	3.39E-04
GO:0030054	Cell junction	15150	482	5.03E-04
GO:0008328	Ionotropic glutamate receptor complex	1240	100	5.35E-04
GO:0099572	Postsynaptic specialization	13514	420	6.34E-04
GO:0022835	Transmitter-gated channel activity	783	47	6.34E-04
GO:0099565	Chemical synaptic transmission, postsynaptic	861	55	6.34E-04

GO:0015711	Organic anion transport	2158	75	8.02E-04
GO:0043292	Contractile fiber	8271	213	1.48E-03
GO:0030594	Neurotransmitter receptor activity	832	51	1.75E-03
GO:0007154	Cell communication	12333	366	2.43E-03
GO:0051179	Localization	14475	449	2.45E-03
GO:0001964	Startle response	1440	67	2.57E-03
GO:0007267	Cell-cell signaling	9408	334	2.68E-03
GO:0022834	Ligand-gated channel activity	960	65	3.88E-03
GO:0044699	Single-organism process	14475	449	3.88E-03
GO:0060004	Reflex	1400	64	4.48E-03
GO:0065008	Regulation of biological quality	8887	267	6.17E-03
GO:1901265	Nucleoside phosphate binding	5015	122	6.31E-03
GO:0044447	Axoneme part	1344	51	8.15E-03
GO:0022857	Transmembrane transporter activity	1154	85	9.85E-03
GO:0044449	Contractile fiber part	8974	221	1.09E-02
GO:1903508	Positive regulation of nucleic acid-templated transcription	2810	45	1.11E-02
GO:0005737	Cytoplasm	11607	297	1.23E-02
GO:0035254	Glutamate receptor binding	1011	33	1.41E-02
GO:0098802	Plasma membrane receptor complex	3887	214	1.51E-02
GO:0072521	Purine-containing compound metabolic process	5495	109	1.51E-02
GO:0035637	Multicellular organismal signaling	7039	259	1.51E-02
GO:0030534	Adult behavior	4977	179	1.57E-02
GO:0030286	Dynein complex	1178	17	1.74E-02
GO:0004871	Signal transducer activity	14137	447	1.74E-02
GO:0015081	Sodium ion transmembrane transporter activity	475	45	1.78E-02
GO:0007611	Learning or memory	4983	179	1.78E-02
GO:2000258	Negative regulation of protein activation cascade	1427	42	1.85E-02
GO:0042577	Lipid phosphatase activity	270	11	2.26E-02
GO:0048878	Chemical homeostasis	1182	45	2.35E-02
GO:1902680	Positive regulation of RNA biosynthetic process	3061	50	2.36E-02
GO:0034762	Regulation of transmembrane transport	2043	109	2.43E-02
GO:0050804	Modulation of synaptic transmission	2491	104	2.43E-02
GO:0001578	Microtubule bundle formation	407	12	2.50E-02
GO:0005929	Cilium	10964	311	2.50E-02
GO:0045893	Positive regulation of transcription, DNA-templated	2946	49	2.54E-02
GO:0001867	Complement activation, lectin pathway	405	10	2.61E-02
GO:0044441	Ciliary part	7030	186	2.66E-02
GO:0023052	Signaling	14475	449	3.02E-02
GO:0033555	Multicellular organismal response to stress	6030	202	3.02E-02

GO:0030551	Cyclic nucleotide binding	2326	78	3.04E-02
GO:0007399	Nervous system development	3698	130	3.12E-02
GO:0032501	Multicellular organismal process	14475	449	3.12E-02
GO:0042165	Neurotransmitter binding	10855	338	3.21E-02
GO:0051604	Protein maturation	6775	147	3.78E-02
GO:0060078	Regulation of postsynaptic membrane potential	328	37	3.78E-02
GO:0010628	Positive regulation of gene expression	4636	80	3.99E-02
GO:0005856	Cytoskeleton	3217	89	3.99E-02
GO:0051402	Neuron apoptotic process	1299	27	3.99E-02
GO:0006836	Neurotransmitter transport	2131	90	4.17E-02
GO:0002209	Behavioral defense response	1148	51	4.72E-02
Cluster 7				
GO:0044459	Plasma membrane part	14022	119	5.87E-07
GO:0005886	Plasma membrane	14080	120	8.88E-06
GO:0071944	Cell periphery	13371	115	1.77E-05
GO:0005215	Transporter activity	14137	121	2.75E-04
GO:0098590	Plasma membrane region	7208	76	2.98E-04
GO:0044425	Membrane part	15150	124	4.77E-04
GO:0042995	Cell projection	13371	115	9.95E-04
GO:0045177	Apical part of cell	13371	115	2.38E-03
GO:0051179	Localization	14475	123	6.51E-03
GO:0044456	Synapse part	15150	124	1.37E-02
GO:0045202	Synapse	15150	124	1.39E-02
GO:0044463	Cell projection part	13371	115	1.43E-02
GO:0032190	Acrosin binding	1364	12	1.77E-02
GO:2000360	Negative regulation of binding of sperm to zona pellucida	3140	28	1.78E-02
GO:0097458	Neuron part	13371	115	1.93E-02
GO:1990351	Transporter complex	3989	22	2.86E-02
GO:2000359	Regulation of binding of sperm to zona pellucida	7898	59	3.12E-02
GO:0072521	Purine-containing compound metabolic process	5495	35	3.41E-02
GO:1904158	Axonemal central apparatus assembly	2017	11	4.58E-02
GO:0007215	Glutamate receptor signaling pathway	2002	15	4.77E-02
GO:0044459	Plasma membrane part	14022	119	5.87E-07

3.4.4 Signaling pathway analysis

In adult catfish, 72 genes were assigned with KEGG annotation. Environmental information processing (37 genes), cellular processes (26 genes), and organismal systems (25 genes) were the top three functional categories for adult catfish. Pathway analysis of DEGs identified between control group and hypoxia-treated group based on PANTHER and KEGG

database was shown in **Table 10**. As show in **Table 11**, representative DEGs of adult catfish were mapped into several pathways such as HIF-1 signaling pathway, MAPK signaling pathway, PI3K-Akt signaling pathway, Ras signaling pathway, signaling by VEGF, FoxO signaling pathway, and chemokine signaling pathway. In catfish fingerlings, a total of 1,095 genes were assigned with KEGG annotation. A total of 460 (42.01%), 372 (33.97%) and 354 (32.33%) annotated genes were classified into environmental information processing, genetic information processing, and organismal systems, respectively. Based on a combination of enrichment analysis, pathway analysis, manual annotation and literature researches, representative DEGs of catfish fingerlings were arranged into eight functional pathways, including HIF-1 signaling pathway, MAPK signaling pathway, PI3K-Akt signaling pathway, mTOR signaling pathway, Ras signaling pathway, signaling by VEGF, FoxO signaling pathway, and chemokine signaling pathway (**Table 12**). Putative pathways involved in low oxygen response in catfish swimbladder is illustrated in the context of a diagram (**Figure 11**).

Table 10. Pathway analysis of differentially expressed genes between control group and hypoxia-treated group based on PANTHER and KEGG database (FDR-corrected P value < 0.05).

Table 10

Term	Database	ID	Input number	Background number	Corrected P-Value
Gastrin-CREB signaling pathway via PKC and MAPK	Reactome	R-HSA-881907	63	421	1.96E-14
MAPK signaling pathway	KEGG	hsa04010	45	255	1.30E-12
VEGFR2 mediated cell proliferation	Reactome	R-HSA-5218921	38	238	1.06E-09
CREB phosphorylation through the activation of Ras	Reactome	R-HSA-442742	15	29	1.38E-09
Prolonged ERK activation events	Reactome	R-HSA-169893	37	233	1.95E-09
VEGFA-VEGFR2 Pathway	Reactome	R-HSA-4420097	43	309	2.69E-09
Signaling to RAS	Reactome	R-HSA-167044	37	237	2.78E-09

SOS-mediated signaling	Reactome	R-HSA-112412	36	226	2.86E-09
SHC1 events in EGFR signaling	Reactome	R-HSA-180336	36	226	2.86E-09
GRB2 events in EGFR signaling	Reactome	R-HSA-179812	36	226	2.86E-09
RAF/MAP kinase cascade	Reactome	R-HSA-5673001	36	226	2.86E-09
MAPK1/MAPK3 signaling	Reactome	R-HSA-5684996	36	231	4.49E-09
Signaling to ERKs	Reactome	R-HSA-187687	37	244	5.02E-09
Signaling by VEGF	Reactome	R-HSA-194138	43	318	5.16E-09
FCERI mediated MAPK activation	Reactome	R-HSA-2871796	37	249	7.93E-09
Signaling by EGFR	Reactome	R-HSA-177929	44	338	9.09E-09
MAPK family signaling cascades	Reactome	R-HSA-5683057	38	269	1.59E-08
IGF1R signaling cascade	Reactome	R-HSA-2428924	38	280	4.02E-08
Signaling by Type 1 Insulin-like Growth Factor 1 Receptor (IGF1R)	Reactome	R-HSA-2404192	38	280	4.02E-08
IRS-related events triggered by IGF1R	Reactome	R-HSA-2428928	38	280	4.02E-08
PI3K-Akt signaling pathway	KEGG	hsa04151	39	342	1.42E-06
MAP2K and MAPK activation	Reactome	R-HSA-5674135	11	39	2.71E-05
Ras signaling pathway	KEGG	hsa04014	24	228	5.94E-04
EGFR interacts with phospholipase C-gamma	Reactome	R-HSA-212718	8	36	1.57E-03
GRB2:SOS provides linkage to MAPK signaling for Integrins	Reactome	R-HSA-354194	4	13	1.41E-02
p130Cas linkage to MAPK signaling for integrins	Reactome	R-HSA-372708	4	14	1.70E-02
PKA activation	Reactome	R-HSA-163615	4	16	2.42E-02
PTK6 Regulates RTKs and Their Effectors AKT1 and DOK1	Reactome	R-HSA-8849469	3	9	3.22E-02
HIF-1 signaling pathway	KEGG	hsa04066	10	103	4.86E-02

Table 11. Representative differentially expressed genes between control and hypoxia-induced group at adult fish stage involved in key molecular pathways.

Table 11

Gene name	Log FC	P value (FDR-corrected)	Signaling pathway
Alpha-enolase (eno1)	-1.22	3.66E-02	HIF-1 signaling pathway
Transferrin receptor protein 1	-1.15	1.59E-02	HIF-1 signaling pathway
Heat shock cognate 71 kDa protein	-1.92	1.19E-06	MAPK signaling pathway
Glucose-6-phosphatase	1.54	4.83E-04	PI3K-Akt signaling pathway
Phospholipase D2	-1.74	1.40E-02	Ras signaling pathway
Phospholipase D2	-1.76	3.10E-04	Ras signaling pathway
Actin, cytoplasmic type 5	-2.40	1.37E-10	Signaling by VEGF
Actin, cytoplasmic 1	-2.16	1.16E-06	Signaling by VEGF
Spectrin beta chain, non-erythrocytic 1	-1.19	9.11E-03	Signaling by VEGF
Glucose-6-phosphatase	1.54	4.83E-04	FoxO signaling pathway

C-C chemokine receptor type 3	1.18	2.88E-02	Chemokine signaling pathway

Table 12. Representative differentially expressed genes between control and hypoxia-induced group at fingerling stage involved in key molecular pathways.

Table 12

Abbreviation	Gene name	Log FC	P value (FDR-corrected)
HIF-1 signaling pathway			
nos2	Nitric oxide synthase, inducible	1.83	2.21E-04
eno2	Gamma-enolase	1.34	1.63E-03
igf1	Insulin-like growth factor I, adult form	1.21	1.73E-02
camk2d2	Calcium/calmodulin-dependent protein kinase type II delta 2 chain	1.16	2.01E-02
prkcb	Protein kinase C beta type	1.03	3.33E-02
cdkn1a	Cyclin-dependent kinase inhibitor 1	-1.03	8.15E-03
MAPK signaling pathway			
cacna1a	Voltage-dependent P/Q-type calcium channel subunit alpha-1A	1.29	2.54E-03
cacna1b	Voltage-dependent N-type calcium channel subunit alpha-1B	1.71	1.94E-05
cacna1d	Voltage-dependent L-type calcium channel subunit alpha-1D	1.25	7.00E-03
cacna1i	Voltage-dependent T-type calcium channel subunit alpha-1I	1.61	1.13E-04
cacna2d3	Voltage-dependent calcium channel subunit alpha-2/delta-3	1.59	2.20E-04
cacnb1	Voltage-dependent L-type calcium channel subunit beta-1	1.54	3.57E-03
cacnb2	Voltage-dependent L-type calcium channel subunit beta-2	1.81	6.87E-04
cacnb4	Voltage-dependent L-type calcium channel subunit beta-4	1.35	4.35E-03
cacng1	Voltage-dependent calcium channel gamma-1 subunit	1.58	8.75E-04
cacng2	Voltage-dependent calcium channel gamma-2 subunit	1.45	3.59E-03
cacng3	Voltage-dependent calcium channel gamma-3 subunit	1.42	4.27E-03
map3k12	Mitogen-activated protein kinase kinase kinase 12	1.43	1.35E-03
taok3	Serine/threonine-protein kinase TAO3	1.42	4.51E-03
ntrk1	High affinity nerve growth factor receptor	1.39	1.25E-03
mapk8ip2	C-Jun-amino-terminal kinase-interacting protein 2	1.23	8.15E-03
rps6ka2	Ribosomal protein S6 kinase alpha-2	1.23	5.23E-03
PI3K-Akt signaling pathway			
itga6	Integrin alpha-6	1.95	2.44E-05
g6pc	Glucose-6-phosphatase	1.14	5.33E-03
cdkn1a	Cyclin-dependent kinase inhibitor 1	-1.03	8.15E-03
fgf13	Fibroblast growth factor 13	1.51	4.02E-04
prlr	Prolactin receptor	1.95	3.81E-06
creb3l3b	Cyclic AMP-responsive element-binding protein 3-like protein 3-B	1.93	2.44E-05
kit	Mast/stem cell growth factor receptor Kit	1.90	6.96E-06
thbs1	Thrombospondin-1	-1.28	5.55E-04

thbs3b	Thrombospondin-3b	1.74	1.80E-04
lama1	Laminin subunit alpha-1	1.56	3.90E-04
lamb4	Laminin subunit beta-4	1.51	1.14E-03
tnr	Tenascin-R	1.33	1.32E-03
ppp2r5b	Serine/threonine-protein phosphatase 2A 56 kDa regulatory subunit beta	1.33	4.09E-03
gng5	Guanine nucleotide-binding protein G(I)/G(S)/G(O) subunit gamma-5	-1.25	5.65E+00
f2r	Proteinase-activated receptor 1	-1.30	7.56E-04
mTOR signaling pathway			
wnt3a	Protein Wnt-3a	1.26	7.23E-03
fzd7-a	Frizzled-7-A	-1.11	4.84E-03
rhoa	Transforming protein RhoA	-1.13	3.05E-03
tiam1	T-lymphoma invasion and metastasis-inducing protein 1	1.43	5.28E-03
Ras signaling pathway			
efna3	Ephrin-A3	1.24	1.44E-02
ksr2	Kinase suppressor of Ras 2	1.82	3.93E-05
pld1	Phospholipase D1	1.46	2.23E-03
syngap1	Ras/Rap GTPase-activating protein SynGAP	1.96	4.04E-05
cam	Calmodulin	-1.08	4.46E-03
grin1	Glutamate receptor ionotropic, NMDA 1	1.77	4.71E-05
grin2b	Glutamate receptor ionotropic, NMDA 2B	1.22	1.01E-02
fgf11	Fibroblast growth factor 11	1.20	1.87E-02
fgf14	Fibroblast growth factor 14	1.32	1.07E-02
Signaling by VEGF			
fn1	Fibronectin	1.25	2.11E-03
wasf3	Wiskott-Aldrich syndrome protein family member 3	1.59	1.59E-03
hspb1	Heat shock protein beta-1	-1.20	1.25E-03
gfra4	GDNF family receptor alpha-4	1.64	2.20E-04
grin2c	Glutamate receptor ionotropic, NMDA 2C	1.71	2.33E-04
grin2d	Glutamate receptor ionotropic, NMDA 2D	1.48	2.77E-03
fga	Fibrinogen alpha chain	-1.54	7.26E-05
fgb	Fibrinogen beta chain	-1.66	1.31E-04
fgg	Fibrinogen gamma chain	-1.85	6.96E-06
jup	Junction plakoglobin	1.35	7.94E-03
sptbn1	Spectrin beta chain, non-erythrocytic 1	1.20	5.45E-03
sptbn4	Spectrin beta chain, non-erythrocytic 4	1.55	1.64E-03
hsp90a.1	Heat shock protein HSP 90-alpha 1	-1.16	2.26E-03
rpl40	Ubiquitin-60S ribosomal protein L40	-1.54	3.06E-05
dlg4	Disks large homolog 4	1.55	7.72E-04
FoxO signaling pathway			
homer1	Homer protein homolog 1	1.10	1.93E-02
grm1	Metabotropic glutamate receptor 1	1.09	3.87E-02
s1pr1	Sphingosine 1-phosphate receptor 1	-1.18	2.24E-03
ccnb3	G2/mitotic-specific cyclin-B3	1.16	2.03E-02
gabarap	Gamma-aminobutyric acid receptor-associated protein	-1.10	4.72E-03

Chemokine signaling pathway			
plcb1	1-phosphatidylinositol 4,5-bisphosphate phosphodiesterase beta-1	1.41	1.51E-03
adcy1	Adenylate cyclase type 1	1.40	1.26E-03
adcy8	Adenylate cyclase type 8	1.37	3.21E-02
grk5	G protein-coupled receptor kinase 5	1.05	5.65E-03

Figure 11. Putative presentation of gene pathways involved in hypoxia responses in catfish swimbladder based on RNA-seq expression signatures.

Figure 11

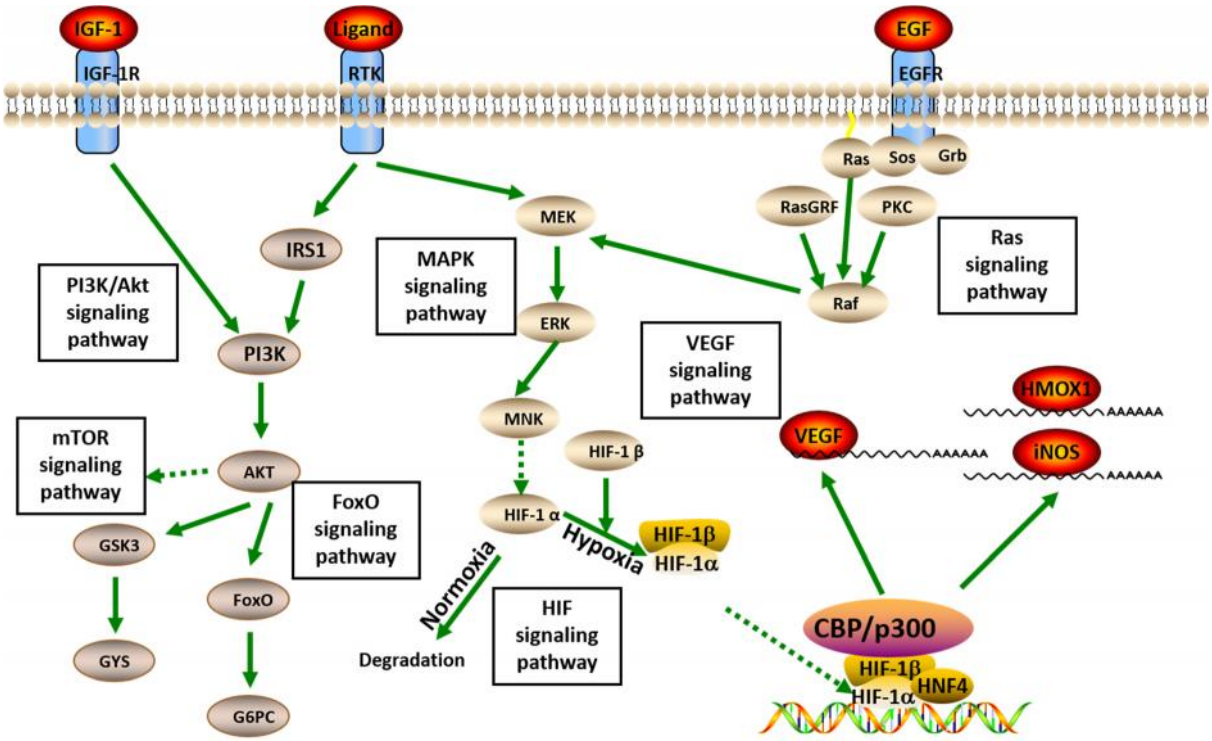

3.4.5 Validation of RNA-Seq results by qRT-PCR

We randomly selected fifteen genes to validate the RNA-seq results in the present study. As shown in **Figure 12**, fold changes from qPCR were compared with the RNA-seq results, and significant correlations between qPCR and RNA-seq based expression profiles were observed. In detail, the correlation coefficient was 0.889 and 0.943 in catfish fingerlings and adult catfish, respectively, reflecting the reliability of RNA-seq for gene expression analysis in

the present study.

Figure 12. Validation of RNA-Seq results using qPCR. A: channel fingerling (CF), fold changes represented gene expression changes in channel fingerling relative to control group, correlation coefficients 0.899. B: channel adult (CA), fold changes represented gene expression changes in channel adult relative to control group, correlation coefficients 0.943.

Figure 12

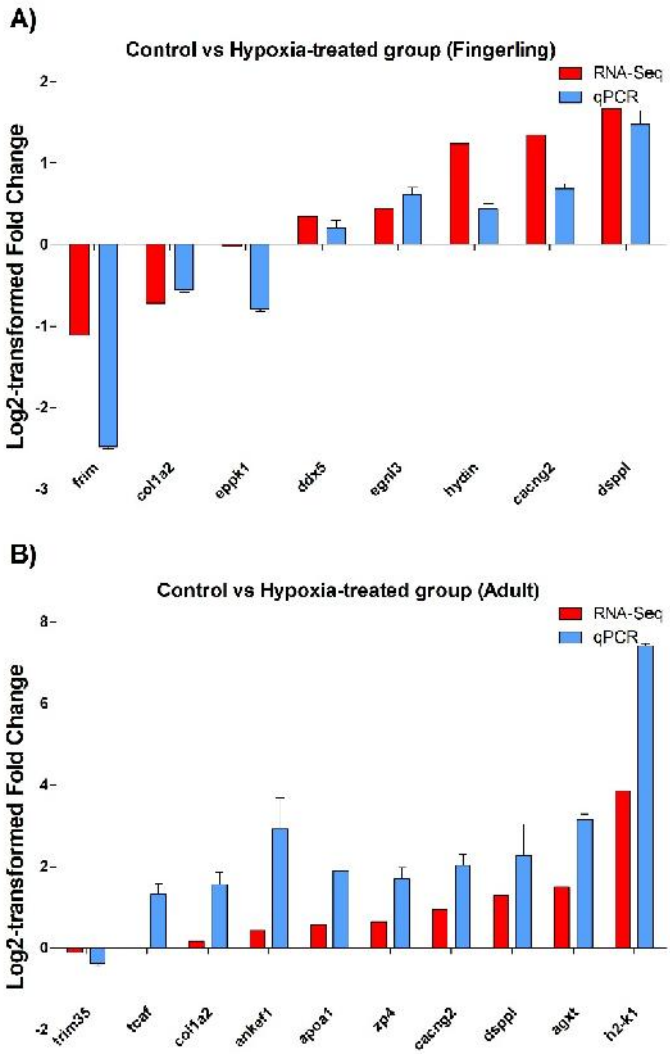

3.5 Discussion

Oxygen is required for aerobic organisms for efficiency of ATP production through the

process of oxidative phosphorylation (Bailey-Serres and Chang, 2005). Exposure to severe hypoxic condition, cell death can be detected if the production of ATP fails to maintain the energy demands for the ionic and osmotic equilibrium (Boutilier and St-Pierre, 2000). Due to the low level of ATP, a series of consequences occur, including depolarization of membrane, uncontrolled calcium entry, cellular swelling, cell hydrolysis, and cell death (Michiels, 2004). As aquatic environment contains low amount of dissolved oxygen, fish species have evolved various strategies to adapt to the environmental conditions. Swimbladder have been hypothesized as an accessory respiratory organ (Owen, 1846). In this study, we performed comparative transcriptome analysis of catfish swimbladder under both hypoxic and normal conditions. Many of the identified DEGs and overrepresented signaling pathways were involved in hypoxia responses and oxygen homeostasis.

In the present study, a total of 155 and 2,127 genes were identified as DEGs in adult fish and fingerlings of catfish after hypoxia treatment, respectively. The amount of up-regulated and down-regulated genes were similar in adult fish, whereas the vast majority of DEGs were up-regulated in fingerlings. Even though it has been reported that the body size has rare effect on the tolerance to low oxygen stresses under hypoxic conditions (Nilsson and Östlund‐Nilsson, 2008), our result of both principal component analysis and hierarchical clustering analysis suggested that catfish fingerlings is more sensitive to the low oxygen stress than adult catfish.

Combined with GO enrichment analysis and literature reviews, representative DEGs between control and hypoxia-treated groups of catfish fingerlings can be divided into several pathways such as HIF-1 signaling pathway, MAPK signaling pathway, PI3K-Akt signaling

pathway, mTOR signaling pathway, Ras signaling pathway, Signaling by VEGF, FoxO signaling pathway, and chemokine signaling pathway. Putative pathways involved in hypoxia responses in catfish swimbladder are illustrated in the context of a diagram (**Figure 11**). The putative functional roles and interaction of these signaling pathways are discussed below.

HIF signaling pathway plays important roles in oxygen homeostasis. The most known member in HIF signaling pathway is hypoxia-inducible factor 1 (HIF-1), which is an important transcriptional activator for hypoxia responses and oxygen homeostasis (Semenza, 2002). In spite of being constantly synthesized, HIF-1α is quickly degraded under normal conditions (34). However, exposure to low oxygen stress, HIF-1α can accumulate and combine with HIF-1β to bind the HRE in the HIF-1 target genes (Kietzmann et al., 2016). The activity of HIF-1 is mediated by the oxygen levels through signal transduction pathways (Semenza, 2002). Many of the HIF-1 target genes are responsible for increased oxygen delivery and adaptive responses to low oxygen stress (Semenza, 2002). In this study, several HIF-1 target genes were identified as differentially expressed genes in catfish swimbladder between control group and hypoxia-treated group, including *nos2*, *eno2*, *camk2d2*, *prkcb*, *cdkn1a*, *eno1*, and *tfrc*. For instance, *nos2* was induced with a fold-change of 3.56 in response to hypoxia treatment. This result is consistent with a previous study, in which hypoxia also induced the expression of *nos2* in pulmonary artery endothelial cells via hypoxia-inducible factor 1 (Palmer et al., 1998). Similarly, another gene (*eno2*) functioned as a glycogenolysis regulator, was up-regulated by HIF-1α in response to hypoxia stress (Colla et al., 2010). In our study, *eno2* was expressed at higher level in hypoxia-treated group than that in control group with a fold-change of 2.53. Furthermore, *igf1* was up-regulated in hypoxia-treated group than that in control group with a

fold-change of 2.31. *Igf1* can induce the expression of HIF-1α by preventing from ubiquitination and degradation (Fukuda et al., 2002) and HIF-1α-mediated glucose transporter 3 (*glut3*) through PI3K/Akt/mTOR signaling pathways (Yu et al., 2012).

MAPK signaling pathway is important for oxygen homeostasis and control of reactive oxygen species (ROS) production (Seifried et al., 2007). In this study, the abundance of members in MAPK signaling pathway were identified as DEGs in catfish swimbladder between hypoxia-treated and control groups. In this study, many voltage-dependent calcium channel subunit genes involved in MAPK signaling pathway were expressed at higher levels in hypoxia-treated group than in control groups. In response to hypoxia, the decreasing of ROS production can cause the activation of voltage-gated calcium channels and an elevation of cytosolic calcium (López-Barneo et al., 2001). The abundance of voltage-dependent calcium channel subunit genes (*cacna1a*, *cacna1d*, *cacna1f*, *cacna1i*, *cacna2d3*, *cacnb1*, *cacnb2*, *cacnb4*, *cacng1*, *cacng2*, *cacng3*) were identified as differentially expressed genes between hypoxia-treated and control group, suggesting that catfish swimbladder might be an important organ in response to hypoxia. In addition, as a critical activator of the MAPK signaling pathway, *map3k12* was induced in responses to hypoxia with a fold-change of 2.69 in our study.

In a genome-wise associate study of hypoxia tolerance in channel catfish, genes within QTL were involved in not only MAPK but also PI3K/AKT/mTOR signaling pathway (Wang et al., 2017b). PI3K/Akt/mTOR signaling pathway was reported to modulate the expression of HIF-1α (Akman et al., 2001). Moreover, PI3K/Akt/mTOR signaling pathway regulates several aspects of cellular functions, including glucose metabolism, vascular homeostasis and angiogenesis (Shiojima and Walsh, 2002). In our study, *itga6* was expressed at a higher level

in hypoxia-treated group than in control group with a fold-change of 3.86. This result is consistent with a previous study, in which *itga6* mRNA increased 2-fold in hypoxia WT cells relative to normoxic WT cells (Brooks et al., 2016). The regulation of *itga6* expression is directly via hypoxia-inducible factors (Brooks et al., 2016). Notably, we found that glucose-6-phosphatase (*g6pc*) was expressed at a higher level in hypoxia-treated group than in control group with a fold-change of 2.91 and 2.20 in catfish fingerlings and adult catfish, respectively. This suggests glycogen synthase activity is relatively active in hypoxia-treated group. *Cdkn1a* was expressed at lower level in hypoxia-treated group than that of control group. In a previous report, HIF-1α may displace C-Myc from the promoter of *cdkn1a* gene, thereby de-repressing its transcription (Koshiji et al., 2004). The abundance of oxygen-regulated genes in PI3K/Akt/mTOR signaling pathway were identified as differentially expressed genes between hypoxia-treated and control groups, suggesting the contribution of PI3K/Akt/mTOR signaling pathway to hypoxia responses.

Ras signaling pathway is required for the hypoxic activity of HIF-1α, in which hypoxia induces HIF-1α via Ras/MAP kinase mediated signaling pathways (Sheta et al., 2001). Ras and MAPK modulate induction of hypoxia response element (HRE) activity via the Ras, MEK1, and HIF-1α (Sheta et al., 2001). The expression of *efna3* was up-regulated in response to hypoxia treatment with a fold-change of 2.36 in adult catfish. Gene expression profiles of normoxic and hypoxia-treated NPC cell lines revealed that *efna3* was an important hypoxia up-regulated gene (Sung et al., 2007). As an angiogenic gene, *efna3* was induced through HIF activation under hypoxic conditions (Khong et al., 2013). Additionally, *ksr2* was induced by hypoxia treatment with a fold-change of 3.53 in swimbladder of adult catfish. *Ksr2* was

reported to positively regulates AMPK activation and promotes glucose and fatty acid metabolism (Costanzo-Garvey et al., 2009).

A set of genes involved in signaling by VEGF were identified as differentially expressed genes between control and hypoxia-treated group. Fibronectin (*fn1*) was induced in response to hypoxia treatment with a fold-change of 2.38. In a previous report, *fn1* was a HIF-1 targeted gene, which was transcriptionally activated by HIF-1 (Lee et al., 2004) and involved in regulation of angiogenesis (White et al., 2004). In addition, *wasf3* was expressed at higher levels in hypoxia-treated group than that of control group with a fold-change of 3.01. *Wasf3* is a HIF-1α-regulated gene, whose expression level increased when exposure to hypoxia conditions (Ghoshal et al., 2012). Further, *hspb1* was expressed at lower level in hypoxia-treated group than that of control group. *Hspb1* plays a key role in regulating angiogenic balance via direct interaction with vascular endothelial growth factor (VEGF) (Lee et al., 2012). Additionally, FoxO signaling pathway have been implicated in metabolism control, cell survival, ROS production, and stress resistance (Kobayashi and Suda, 2012). For instance, the gene expression of several members (*homer1*, *grm1*, *s1pr1*, *ccnb3*, *gabarap*) in FoxO signaling pathway were significantly regulated in hypoxia-treated group in relative to control group. In our study, several genes (*ccr3*, *plcb1*, *adcy1*, *adcy8*, *grk5*) involved in chemokine signaling pathway were also identified as DEGs between control and hypoxia-treated groups. The expression of several CC and CXC chemokine genes from chemokine signaling pathway showed a gene-specific pattern in catfish under hypoxia (Fu et al., 2017a; Fu et al., 2017b; Fu et al., 2017c), suggesting the involvement of chemokine signaling pathway in low oxygen stress.

Swimbladder has been considered as an accessory respiration organ in some fish species surrounded by a dense capillary countercurrent exchange system (Hsia et al., 2013). In this study, we conducted RNA-Seq analysis with swimbladder samples of catfish under hypoxic and normal conditions. A total of 155 DEGs were identified from swimbladders of adult catfish under hypoxic condition as compared with untreated controls, whereas a total of 2,127 DEGs were identified from swimbladders of catfish fingerlings. Pathway analysis revealed that many DEGs under hypoxia were involved in HIF signaling pathway (*nos2*, *eno2*, *camk2d2*, *prkcb*, *cdkn1a*, *eno1*, and *tfrc*), MAPK signaling pathway (voltage-dependent calcium channel subunit genes), PI3K/Akt/mTOR signaling pathway (*itga6*, *g6pc*, and *cdkn1a*), Ras signaling pathway (*efna3* and *ksr2*), and signaling by VEGF (*fn1*, *wasf3*, and *hspb1*) in catfish swimbladder. This study has provided clues for genes and signaling pathways associated with oxygen homeostasis or hypoxia induced process in catfish swimbladder.

References

Akman, H.O., Zhang, H., Siddiqui, M., Solomon, W., Smith, E.L., Batuman, O.A., 2001. Response to hypoxia involves transforming growth factor-β2 and Smad proteins in human endothelial cells. Blood 98, 3324-3331.

Alexander, R., 1966. Physical aspects of swimbladder function. Biol. Rev. 41, 141-176.

Anders, S., Pyl, P.T., Huber, W., 2015. HTSeq—a Python framework to work with high-throughput sequencing data. Bioinformatics 31, 166-169.

Bailey-Serres, J., Chang, R., 2005. Sensing and signalling in response to oxygen deprivation in plants and other organisms. Ann. Bot. 96, 507-518.

Bauer, S., Grossmann, S., Vingron, M., Robinson, P.N., 2008. Ontologizer 2.0—a multifunctional tool for GO term enrichment analysis and data exploration. Bioinformatics 24, 1650-1651.

Bolger, A.M., Lohse, M., Usadel, B., 2014. Trimmomatic: a flexible trimmer for Illumina sequence data. Bioinformatics, btu170.

Boutilier, R., St-Pierre, J., 2000. Surviving hypoxia without really dying. Comp. Biochem. Physiol. A Mol. Integr. Physiol. 126, 481-490.

Bracken, C., Whitelaw, M., Peet, D., 2003. The hypoxia-inducible factors: key transcriptional regulators of hypoxic responses. Cell. Mol. Life Sci. 60, 1376-1393.

Brooks, D.L.P., Schwab, L.P., Krutilina, R., Parke, D.N., Sethuraman, A., Hoogewijs, D., Schörg, A., Gotwald, L., Fan, M., Wenger, R.H., 2016. ITGA6 is directly regulated by hypoxia-inducible factors and enriches for cancer stem cell activity and invasion in metastatic breast cancer models. Mol. Cancer 15, 26.

Bruick, R.K., 2003. Oxygen sensing in the hypoxic response pathway: regulation of the hypoxia-inducible transcription factor. Genes Dev. 17, 2614-2623.

Burggren, W.W., Cameron, J.N., 1980. Anaerobic metabolism, gas exchange, and acid‐base balance during hypoxic exposure in the channel catfish, Ictalurus punctatus. J. Exp. Zool. A Ecol. Genet. Physiol. 213, 405-416.

Cass, A.N., Servetnick, M.D., McCune, A.R., 2013. Expression of a lung developmental cassette in the adult and developing zebrafish swimbladder. Evol. Dev. 15, 119-132.

Cockman, M.E., Masson, N., Mole, D.R., Jaakkola, P., Chang, G.-W., Clifford, S.C., Maher, E.R., Pugh, C.W., Ratcliffe, P.J., Maxwell, P.H., 2000. Hypoxia inducible factor-α binding and ubiquitylation by the von Hippel-Lindau tumor suppressor protein. J Biol. Chem. 275, 25733-25741.

Colla, S., Storti, P., Donofrio, G., Todoerti, K., Bolzoni, M., Lazzaretti, M., Abeltino, M., Ippolito, L., Neri, A., Ribatti, D., Rizzoli, V., Martella, E., Giuliani, N., 2010. Low bone marrow oxygen tension and hypoxia-inducible factor-1 [alpha] overexpression characterize patients with multiple myeloma: role on the transcriptional and proangiogenic profiles of [CD138. sup.+] cells. Leukemia 24, 1967-1971.

Conesa, A., Götz, S., García-Gómez, J.M., Terol, J., Talón, M., Robles, M., 2005. Blast2GO: a universal tool for annotation, visualization and analysis in functional genomics research. Bioinformatics 21, 3674-3676.

Costanzo-Garvey, D.L., Pfluger, P.T., Dougherty, M.K., Stock, J.L., Boehm, M., Chaika, O., Fernandez, M.R., Fisher, K., Kortum, R.L., Hong, E.-G., Jun, J.Y., Ko, H.J., Schreiner, A., Volle, D.J., Treece, T., Swift, A.L., Winer, M., Chen, D., Wu, M., Leon, L.R., Shaw, A.S.,

McNeish, J., Kim, J.K., Morrison, D.K., Tschöp, M.H., Lewis, R.E., 2009. KSR2 is an essential regulator of AMP kinase, energy expenditure, and insulin sensitivity. Cell Metab. 10, 366-378.

Croft, D., O'Kelly, G., Wu, G., Haw, R., Gillespie, M., Matthews, L., Caudy, M., Garapati, P., Gopinath, G., Jassal, B., Jupe, S., Kalatskaya, I., Mahajan, S., May, B., Ndegwa, N., Schmidt, E., Shamovsky, V., Yung, C., Birney, E., Hermjakob, H., D'Eustachio, P., Stein, L., 2010. Reactome: a database of reactions, pathways and biological processes. Nucleic Acids Res. 39, D691-D697.

Dobin, A., Davis, C.A., Schlesinger, F., Drenkow, J., Zaleski, C., Jha, S., Batut, P., Chaisson, M., Gingeras, T.R., 2013. STAR: ultrafast universal RNA-seq aligner. Bioinformatics 29, 15-21.

Eijkelenboom, A., Burgering, B.M., 2013. FOXOs: signalling integrators for homeostasis maintenance. Nature reviews. Mol. Cell. Biol. 14, 83.

Finney, J.L., Robertson, G.N., McGee, C.A., Smith, F.M., Croll, R.P., 2006. Structure and autonomic innervation of the swim bladder in the zebrafish (Danio rerio). J. Comp. Neurol. 495, 587-606.

Fu, Q., Yang, Y., Li, C., Zeng, Q., Zhou, T., Li, N., Liu, Y., Li, Y., Wang, X., Liu, S., Li, D., Liu, Z., 2017a. The chemokinome superfamily: II. The 64 CC chemokines in channel catfish and their involvement in disease and hypoxia responses. Dev. Comp. Immunol. 73, 97-108.

Fu, Q., Yang, Y., Li, C., Zeng, Q., Zhou, T., Li, N., Liu, Y., Liu, S., Liu, Z., 2017b. The CC and CXC chemokine receptors in channel catfish (Ictalurus punctatus) and their involvement

in disease and hypoxia responses. Dev. Comp. Immunol. 77, 241-251.

Fu, Q., Zeng, Q., Li, Y., Yang, Y., Li, C., Liu, S., Zhou, T., Li, N., Yao, J., Jiang, C., Li, D., Liu, Z., 2017c. The chemokinome superfamily in channel catfish: I. CXC subfamily and their involvement in disease defense and hypoxia responses. Fish Shellfish Immunol. 60, 380-390.

Fukuda, R., Hirota, K., Fan, F., Do Jung, Y., Ellis, L.M., Semenza, G.L., 2002. Insulin-like growth factor 1 induces hypoxia-inducible factor 1-mediated vascular endothelial growth factor expression, which is dependent on MAP kinase and phosphatidylinositol 3-kinase signaling in colon cancer cells. J. Biol. Chem. 277, 38205-38211.

Geng, X., Feng, J., Liu, S., Wang, Y., Arias, C., Liu, Z., 2014. Transcriptional regulation of hypoxia inducible factors alpha (HIF-α) and their inhibiting factor (FIH-1) of channel catfish (Ictalurus punctatus) under hypoxia. Comp. Biochem. Physiol. B Biochem. Mol. Biol. 169, 38-50.

Ghoshal, P., Teng, Y., Lesoon, L.A., Cowell, J.K., 2012. HIF1A induces expression of the WASF3 metastasis‐associated gene under hypoxic conditions. Int. J. Cancer 131, E905-E915.

Grossmann, S., Bauer, S., Robinson, P.N., Vingron, M., 2007. Improved detection of overrepresentation of Gene-Ontology annotations with parent–child analysis. Bioinformatics 23, 3024-3031.

Helfman, G., Collette, B.B., Facey, D.E., Bowen, B.W., 2009. The diversity of fishes: biology, evolution, and ecology. John Wiley & Sons.

Hsia, C.C., Schmitz, A., Lambertz, M., Perry, S.F., Maina, J.N., 2013. Evolution of air

breathing: oxygen homeostasis and the transitions from water to land and sky. Compr. Physiol. 3, 849-915.

Jensen, F.B., Nikinmaa, M., Weber, R.E., 1993. Environmental perturbations of oxygen transport in teleost fishes: causes, consequences and compensations, Fish ecophysiology. Springer, 161-179.

Jiang, B., Ren, C., Li, Y., Lu, Y., Li, W., Wu, Y., Gao, Y., Ratcliffe, P.J., Liu, H., Zhang, C., 2011. Sodium sulfite is a potential hypoxia inducer that mimics hypoxic stress in Caenorhabditis elegans. J. Biol. Inorg. Chem. 16, 267-274.

Kanehisa, M., Sato, Y., Morishima, K., 2016. BlastKOALA and GhostKOALA: KEGG tools for functional characterization of genome and metagenome sequences. J. Mol. Biol. 428, 726-731.

Khong, T.L., Thairu, N., Larsen, H., Dawson, P.M., Kiriakidis, S., Paleolog, E.M., 2013. Identification of the angiogenic gene signature induced by EGF and hypoxia in colorectal cancer. BMC Cancer 13, 518.

Kietzmann, T., Mennerich, D., Dimova, E.Y., 2016. Hypoxia-Inducible Factors (HIFs) and phosphorylation: impact on stability, localization, and transactivity. Front. Cell Dev. Biol. 4, 11.

Kobayashi, C.I., Suda, T., 2012. Regulation of reactive oxygen species in stem cells and cancer stem cells. J. Cell. Physiol. 227, 421-430.

Koong, A.C., Chen, E.Y., Mivechi, N.F., Denko, N.C., Stambrook, P., Giaccia, A.J., 1994. Hypoxic activation of nuclear factor-κB is mediated by a Ras and Raf signaling pathway and does not involve MAP kinase (ERK1 or ERK2). Cancer Res. 54, 5273-5279.

Koshiji, M., Kageyama, Y., Pete, E.A., Horikawa, I., Barrett, J.C., Huang, L.E., 2004. HIF‐1α induces cell cycle arrest by functionally counteracting Myc. EMBO J. 23, 1949-1956.

Kramer, D.L., McClure, M., 1982. Aquatic surface respiration, a widespread adaptation to hypoxia in tropical freshwater fishes. Environ. Biol. Fish. 7, 47-55.

Kvamme, B.O., Gadan, K., Finne-Fridell, F., Niklasson, L., Sundh, H., Sundell, K., Taranger, G.L., Evensen, Ø., 2013. Modulation of innate immune responses in Atlantic salmon by chronic hypoxia-induced stress. Fish Shellfish Immunol. 34, 55-65.

López-Barneo, J., Pardal, R., Ortega-Sáenz, P., 2001. Cellular mechanism of oxygen sensing. Annu. Rev. Physiol. 63, 259-287.

Lee, J.-W., Bae, S.-H., Jeong, J.-W., Kim, S.-H., Kim, K.-W., 2004. Hypoxia-inducible factor (HIF-1) α: its protein stability and biological functions. Exp. Mol. Med. 36, 1-12.

Lee, S., Chen, T.T., Barber, C.L., Jordan, M.C., Murdock, J., Desai, S., Ferrara, N., Nagy, A., Roos, K.P., Iruela-Arispe, M.L., 2007. Autocrine VEGF signaling is required for vascular homeostasis. Cell 130, 691-703.

Lee, Y.-J., Lee, H.-J., Choi, S.-h., Jin, Y.B., An, H.J., Kang, J.-H., Yoon, S.S., Lee, Y.-S., 2012. Soluble HSPB1 regulates VEGF-mediated angiogenesis through their direct interaction. Angiogenesis 15, 229-242.

Liu, Z.J., Liu, S.K., Yao, J., Bao, L.S., Zhang, J.R., Li, Y., Jiang, C., Sun, L.Y., Wang, R.J., Zhang, Y., Zhou, T., Zeng, Q.F., Fu, Q., Gao, S., Li, N., Koren, S., Jiang, Y.L., Zimin, A., Xu, P., Phillippy, A.M., Geng, X., Song, L., Sun, F.Y., Li, C., Wang, X.Z., Chen, A.L., Jin, Y.L., Yuan, Z.H., Yang, Y.J., Tan, S.X., Peatman, E., Lu, J.G., Qin, Z.K., Dunham, R., Li, Z.X., Sonstegard, T., Feng, J.B., Danzmann, R.G., Schroeder, S., Scheffler, B., Duke, M.V.,

Ballard, L., Kucuktas, H., Kaltenboeck, L., Liu, H.X., Armbruster, J., Xie, Y.J., Kirby, M.L., Tian, Y., Flanagan, Elizabeth M., Mu, W.J., Waldbieser, G.C., 2016. The channel catfish genome sequence provides insights into the evolution of scale formation in teleosts. Nat. Commun. 7, 11757.

Maxwell, P.H., Wiesener, M.S., Chang, G.-W., Clifford, S.C., Vaux, E.C., Cockman, M.E., Wykoff, C.C., Pugh, C.W., Maher, E.R., Ratcliffe, P.J., 1999. The tumour suppressor protein VHL targets hypoxia-inducible factors for oxygen-dependent proteolysis. Nature 399, 271-275.

Mazure, N.M., Chen, E.Y., Laderoute, K.R., Giaccia, A.J., 1997. Induction of vascular endothelial growth factor by hypoxia is modulated by a phosphatidylinositol 3-kinase/Akt signaling pathway in Ha-ras-transformed cells through a hypoxia inducible factor-1 transcriptional element. Blood 90, 3322-3331.

Mi, H., Lazareva-Ulitsky, B., Loo, R., Kejariwal, A., Vandergriff, J., Rabkin, S., Guo, N., Muruganujan, A., Doremieux, O., Campbell, M.J., Kitano, H., Thomas, P.D., 2005. The PANTHER database of protein families, subfamilies, functions and pathways. Nucleic Acids Res. 33, D284-D288.

Michiels, C., 2004. Physiological and pathological responses to hypoxia. Am. J. Pathol. 164, 1875-1882.

Nikinmaa, M., Rees, B.B., 2005. Oxygen-dependent gene expression in fishes. American Journal of Physiology-Regulatory, Integrative and Comparative Physiology 288, R1079-R1090.

Nilsson, G.E., Östlund‐Nilsson, S., 2008. Does size matter for hypoxia tolerance in fish? Biol.

Rev. 83, 173-189.

Nilsson, G.E., Rosen, P., Johansson, D., 1993. Anoxic depression of spontaneous locomotor activity in crucian carp quantified by a computerized imaging technique. J. Exp. Biol. 180, 153-162.

Ohh, M., Park, C.W., Ivan, M., Hoffman, M.A., Kim, T.-Y., Huang, L.E., Pavletich, N., Chau, V., Kaelin, W.G., 2000. Ubiquitination of hypoxia-inducible factor requires direct binding to the β-domain of the von Hippel–Lindau protein. Nat. Cell Biol. 2, 423-427.

Owen, R., 1846. Lectures on the Comparative Anatomy and Physiology of the Vertebrate Animals: Delivered at the Royal College of Surgeons of England, in 1844 and 1846. Longman, Brown, Green, and Longmans.

Palmer, L.A., Semenza, G.L., Stoler, M.H., Johns, R.A., 1998. Hypoxia induces type II NOS gene expression in pulmonary artery endothelial cells via HIF-1. Am. J. Physiol. Lung Cell. Mol. Physiol. 274, L212-L219.

Potter, G.E., 1927. Respiratory function of the swim bladder in Lepidosteus. J. Exp. Zool. A Ecol. Genet. Physiol. 49, 45-67.

Prem, C., Pelster, B., 2001. Swimbladder gas gland cells cultured on permeable supports regain their characteristic polarity. J. Exp. Biol. 204, 4023-4029.

Risau, W., 1997. Mechanisms of angiogenesis. Nature 386, 671.

Robertson, G., McGee, C., Dumbarton, T., Croll, R., Smith, F., 2007. Development of the swimbladder and its innervation in the zebrafish, Danio rerio. J. Morphol. 268, 967-985.

Robinson, M.D., McCarthy, D.J., Smyth, G.K., 2010. edgeR: a Bioconductor package for differential expression analysis of digital gene expression data. Bioinformatics 26, 139-

140.

Robledo, D., Ronza, P., Harrison, P.W., Losada, A.P., Bermúdez, R., Pardo, B.G., Redondo, M.J., Sitjà-Bobadilla, A., Quiroga, M.I., Martínez, P., 2014. RNA-seq analysis reveals significant transcriptome changes in turbot (Scophthalmus maximus) suffering severe enteromyxosis. BMC Genomics 15, 1149.

Rozen, S., Skaletsky, H., 1999. Primer3 on the WWW for general users and for biologist programmers. Bioinformatics methods and protocols, 365-386.

Seifried, H.E., Anderson, D.E., Fisher, E.I., Milner, J.A., 2007. A review of the interaction among dietary antioxidants and reactive oxygen species. J. Nutr. Biochem. 18, 567-579.

Semenza, G.L., 1999. Regulation of mammalian O2 homeostasis by hypoxia-inducible factor 1. Annu. Rev. Cell Dev. Biol. 15, 551-578.

Semenza, G.L., 2000. HIF-1: mediator of physiological and pathophysiological responses to hypoxia. J. Appl. Physiol. 88, 1474-1480.

Semenza, G.L., 2002. Signal transduction to hypoxia-inducible factor 1. Biochem. Pharmacol. 64, 993-998.

Semenza, G.L., Agani, F., Feldser, D., Lyer, N., Kotch, L., Laughner, E., Yu, A., 2002. Hypoxia, HIF-1, and the pathophysiologi of common human diseases, Oxygen Sensing. Springer, 123-130.

Sheta, E.A., Trout, H., Gildea, J.J., Harding, M.A., Theodorescu, D., 2001. Cell density mediated pericellular hypoxia leads to induction of HIF-1 [alpha] via nitric oxide and Ras/MAP kinase mediated signaling pathways. Oncogene 20, 7624.

Shiojima, I., Walsh, K., 2002. Role of Akt signaling in vascular homeostasis and angiogenesis.

Circ. Res. 90, 1243-1250.

Sung, F.L., Hui, E.P., Tao, Q., Li, H., Tsui, N.B., Lo, Y.D., Ma, B.B., To, K.F., Harris, A.L., Chan, A.T., 2007. Genome-wide expression analysis using microarray identified complex signaling pathways modulated by hypoxia in nasopharyngeal carcinoma. Cancer Lett. 253, 74-88.

Tanimoto, K., Makino, Y., Pereira, T., Poellinger, L., 2000. Mechanism of regulation of the hypoxia‐inducible factor‐1α by the von Hippel‐Lindau tumor suppressor protein. EMBO J. 19, 4298-4309.

Wang, X., Liu, S., Jiang, C., Geng, X., Zhou, T., Li, N., Bao, L., Li, Y., Yao, J., Yang, Y., Zhong, X., Jin, Y., Dunham, R., Liu, Z., 2017. Multiple across-strain and within-strain QTLs suggest highly complex genetic architecture for hypoxia tolerance in channel catfish. Mol. Genet. Genomics 292, 63-76.

Welker, T.L., Mcnulty, S.T., Klesius, P.H., 2007. Effect of sublethal hypoxia on the immune response and susceptibility of channel catfish, Ictalurus punctatus, to enteric septicemia. J. World Aquac. Soc. 38, 12-23.

Wenger, R.H., 2000. Mammalian oxygen sensing, signalling and gene regulation. J. Exp. Biol. 203, 1253-1263.

White, J.R., Harris, R.A., Lee, S.R., Craigon, M.H., Binley, K., Price, T., Beard, G.L., Mundy, C.R., Naylor, S., 2004. Genetic amplification of the transcriptional response to hypoxia as a novel means of identifying regulators of angiogenesis. Genomics 83, 1-8.

Winata, C.L., Korzh, S., Kondrychyn, I., Zheng, W., Korzh, V., Gong, Z., 2009. Development of zebrafish swimbladder: The requirement of Hedgehog signaling in specification and

organization of the three tissue layers. Dev. Biol. 331, 222-236.

Xie, C., Mao, X., Huang, J., Ding, Y., Wu, J., Dong, S., Kong, L., Gao, G., Li, C.-Y., Wei, L., 2011. KOBAS 2.0: a web server for annotation and identification of enriched pathways and diseases. Nucleic Acids Res. 39, W316-W322.

Yang, Y., Fu, Q., Liu, Y., Wang, X., Dunham, R., Liu, S., Bao, L., Zeng, Q., Zhou, T., Li, N., Qin, Z., Jiang, C., Gao, D., Liu, Z., 2018a. Comparative transcriptome analysis reveals conserved branching morphogenesis related genes involved in chamber formation of catfish swimbladder. Physiol. Genomics 50, 67-76.

Yang, Y., Wang, X., Liu, Y., Fu, Q., Tian, C., Wu, C., Shi, H., Yuan, Z., Tan, S., Liu, S., 2018b. Transcriptome analysis reveals enrichment of genes associated with auditory system in swimbladder of channel catfish. Comp. Biochem. Physiol. Part D Genomics Proteomics 27, 30-39.

Yu, J., Li, J., Zhang, S., Xu, X., Zheng, M., Jiang, G., Li, F., 2012. IGF-1 induces hypoxia-inducible factor 1α-mediated GLUT3 expression through PI3K/Akt/mTOR dependent pathways in PC12 cells. Brain Res. 1430, 18-24.

Yue, M.S., Peterson, R.E., Heideman, W., 2015. Dioxin inhibition of swim bladder development in zebrafish: is it secondary to heart failure? Aquat. Toxicol. 162, 10-17.

Zeng, Q., Liu, S., Yao, J., Zhang, Y., Yuan, Z., Jiang, C., Chen, A., Fu, Q., Su, B., Dunham, R., Liu, Z., 2016. Transcriptome Display During Testicular Differentiation of Channel Catfish (Ictalurus punctatus) as Revealed by RNA-Seq Analysis. Biol. Reprod. 95, 19.

Zhong, X., Wang, X., Zhou, T., Jin, Y., Tan, S., Jiang, C., Geng, X., Li, N., Shi, H., Zeng, Q., Yang, Y., Yuan, Z., Bao, L., Liu, S., Tian, C., Peatman, E., Li, Q., Liu, Z., 2017. Genome-

wide association study reveals multiple novel QTL associated with low oxygen tolerance in hybrid catfish. Mar. Biotechnol. 19, 379-390.